LEACHATE PLUME DISCHARGING TO A POND

LANDFILL LEACHATE-AFFECTED GROUNDWATER DISCHARGING TO A POND

By TAMMY HUA, B.Sc.

A Thesis Submitted to the School of Graduate Studies in Partial Fulfillment of the Requirements for the Degree Masters of Science

McMaster University MASTER OF SCIENCE (2021) Hamilton, Ontario (Earth and Environmental Science)

TITLE: Landfill Leachate-Affected Groundwater Discharging to a Pond AUTHOR: Tammy Hua, B.Sc. (McMaster University) SUPERVISORS: Professor J.E. Smith and J.W. Roy NUMBER OF PAGES: XV, 161

Lay Abstract (max 150)

Groundwater contaminated by historic landfills, closed and typically without liners or leachate-collection systems, can potentially discharge to surrounding surface waters, threatening their ecological communities. The objective of this study was to better understand the ecological risk posed by a historic landfill plume discharging to a nearby pond, and how this might vary spatially and temporally. The study site contained an artificial pond 40m west of a historic sanitation landfill and was monitored for contaminant concentrations and contaminant discharge for ~1 year. Elevated concentrations of leachate contaminants were relatively steady within the sediments (endobenthic zone) and similar across the contaminant discharge area but varied substantially in space and time (higher at night, after events, in the winter) at the pond bed (epibenthic zone), while the patterns differed by contaminant in the surface water above (pelagic zone). These findings can provide insights into improved monitoring and protection of ecosystems at landfill sites.

Abstract (max 300)

Groundwater contaminated by leachate from historic landfills, closed and typically without liners or leachate-collection systems, can potentially discharge to surrounding surface waters and impair their ecological communities. However, few studies have focused on emerging contaminants (e.g., per- and poly-fluoroalkyl substances (PFAS)), inputs to non-flowing water bodies, and exposure across the various ecological zones. The objective of this study was to better understand the ecological risk posed by a historic landfill plume discharging to a nearby pond, and how the pond's ecosystem may be affected by potential spatio-temporal variability in contaminant concentrations and contaminant discharge. The site contained an artificial pond 40m west of a historic sanitation landfill and was monitored for ~1 year. Seasonal samples of shallow groundwater analyzed for standard chemistry plus artificial sweeteners and PFAS revealed a large and seasonally stable plume footprint in the pond and relatively constant exposure to the endobenthic zone (within sediments), with some constituents at potentially toxic concentrations. Elevated electrical conductivity measured just above (~1 cm) the sediment bed indicated exposure to the epibenthic zone, with greater exposure associated with higher groundwater fluxes at night, after rain and melt events, and in winter. It is speculated that terrestrial evapotranspiration and pond evaporation play a role in these temporal patterns. Estimated contaminant mass fluxes into the pond using contaminant and temperature-based flux data showed spatial variability within the plume footprint and seasonal patterns. Concentrations in the pond water showed exposure to pelagic organisms was consistent for chloride and saccharin (and likely PFAS), but

varied seasonally for nitrate and ammonium, with all at lower concentrations compared to the endobenthic and epibenthic zones. This study revealed significant and variable ecological exposure from a landfill leachate plume discharging to a pond and provides guidance to landfill operators on improved monitoring protocols for such sites.

Acknowledgements

I would like to acknowledge my two co-supervisors, James Smith, and James Roy. James Smith provided me with so much emotional support, and James Roy was very patient as he guided me through this research thesis. Special thanks to field and laboratory support from Pam Collins, Grant Hodgins, Sue Brown, Amila De Silva, Greg Bickerton, Lee Grapentine, Shannon James, and Ross MacKay. Additional thanks to the landfill operators for providing access to the site. My two lab mates, Victoria and Claire have become my two pillars throughout this master's program, and I am so lucky to have made wonderful lifelong friends. I would like to acknowledge Marvick for being my anchor and believing in me. Special thanks to my parents for supporting me through my educational career, and for giving me the love and support I needed all these years. Thank you to McMaster University for giving me this opportunity.

Table of Contents

List of Figures

List of Tables

List of all Abbreviations and Symbols

BTEX benzene, toluene, ethylbenzene, xylene
°C degrees Celsius
CEC contaminants of emerging concern
Cl Chloride
DOC Dissolved Organic Carbon
EC electrical conductivity
ET evapotranspiration
Fe iron
FOSA Perfluorooctanesulfonamide
mg/L milligram per litre
Mn manganese
NH_4 ammonium N
ng/L nanogram per litre
SAC saccharin
TKN Total Kjeldahl Nitrogen
µS/cm microSiemens per centimetre
µg/L microgram per litre
PFAS per-and polyfluoroakyl substances
PFBA Perfluorobutanoic acid
PFPeA Perfluoropentanoic acid
PFHxA Perfluorohexanoic acid
PFHpA Perfluoroheptanoic acid
PFOA Perfluorooctanoic acid
PFNA Perfluorononanoic acid
PFDA Perfluorodecanoic acid
PFUnA Perfluoroundecanoic acid
PFDoDA Perfluorododecanoic acid
PFTriDA Perfluorotridecanoic acid
PFTeDA Perfluorotetradecanoic acid
PFBS Perfluorobutanesulfonate
PFHxS Perfluorohexanesulfonate
PFOS Perfluorooctanesulfonate
PFDS Perfluorodecanesulfonate
PFECHS Perfloroethylcyclohexane sulfonate
PFSA perfluoroalkyl sulfonic acids
PFCA perfluoroalkyl carboxylic acids
WQGs Water Quality Guidelines

Declaration of Academic Achievement

I am the sole author of this thesis. I conducted fieldwork under the supervision of James W. Roy from Environment and Climate Change Canada, with the assistance of Victoria Propp, Grant Hodgins, Lee Grapentine, Ross MacKay, and Shannon James. I managed and assessed the field data and lab analytical data provided by various labs and associated scientists, Pamela Collins, Amila De Silva, Christine Spencer, and Susan Brown. I interpreted all the data and wrote all the thesis content about the field and lab results under the supervision of James E. Smith, and James W. Roy.

1.0 Introduction

1.1 General Background

Landfill leachate is water, usually from infiltrated precipitation but it can also come directly from the waste itself, that has percolated through landfill waste and dissolved various contaminants. Typical landfill leachate will contain dissolved organic matter, inorganic macro components (nutrients and major ions), and heavy metals (Christensen et al., 2001). Although groundwater can also contain these constituents, in landfill leachate the concentrations are typically elevated compared to groundwater concentrations in most shallow aquifers. It has been long established that most landfills also contain organic pollutants (often xenobiotic compounds) like pesticides and petroleum compounds (e.g., benzene, toluene, ethylbenzene and, xylene (BTEX)). In addition to these common contaminants, there are also contaminants of emerging concern (CECs), which are contaminants that were deemed safe in the past or have recently been detected in the environment and have the potential for detrimental impacts to human health or the environment (Stuart et al., 2012). Of recent concern are per- and polyfluoroalkyl substances (PFAS) because they are potentially harmful, persistent, and mobile compounds. Additionally, there is limited information on PFAS. PFAS have been found in both modern (Hamid et al., 2019) and old (Hepburn et al., 2019; Propp et al., 2021) landfills.

Most contemporary landfills have liners composed of impermeable material such as clay or engineered geotextile, as well as leachate collection systems which isolate the

leachate until it is disposed of or treated. These systems do fail on occasion and can result in leakage into the surrounding groundwater. Older landfills and dumps, especially those closed for several decades (termed historic here, for those closed > 25 years) often do not have leachate collection systems or engineered liners, and therefore are more likely to leak leachate and contaminate surrounding groundwater (South Australia EPA, 2019). Landfills located above a hydraulically conductive aquifer are especially prone to contamination and off-site transport via a groundwater plume. This raises health concerns since leachate can migrate to drinking water wells and negatively impact human health. Moreover, there is a concern for the wellbeing of aquatic ecosystems because leachate-impacted groundwater can discharge into surface waters and can potentially damage aquatic ecosystems.

Past research has revealed the complex fate and transport of landfill groundwater plumes, and their contaminants (e.g., Barker, 1987). Due to the heterogeneous nature of groundwater flow and solute transport, it can be difficult to fully identify the spatial distribution of contaminant concentrations within a leachate plume (Barker, 1984). Processes can get particularly complex when looking into point source contaminant plumes discharging to surface waters (Conant et al., 2004; Conant et al., 2019). Several studies have investigated the discharge of a landfill plume to a surface water body and revealed some of this complexity (Table 1). Particularly, Milosevic et al. (2012) and Thomsen et al. (2012) revealed substantial spatial variability due to source composition, attenuation processes, and heterogeneous groundwater flow systems. These two studies also have shown that there can be temporal variability in the plume composition,

concentration, and extent due to the different environments during each season. More specifically, there can be more precipitation infiltration resulting in the migration of the plume extent during rainy seasons.

Considering these past studies, there are several topics or conditions that have received limited attention to date (Table 1). For example, there has been only one study looking into landfill plumes entering a non-flowing water body, such as a ponded wetland (Table 1). A pond has the potential for very different ecological impacts compared to streams or lakeshores. For example, given a pond's shallower depth compared to a lake, there is no lake stratification for thermal mixing. Furthermore, a stream is flowing and turbulent and therefore has more mixing than a pond. Lorah et al. (2009) investigated a ponded-wetland (like a pond) and influence from the nearby unlined historical landfill. All in all, it is important to better understand the spatio-temporal variation associated with the leachate-affected groundwater plume discharging into the pond.

Table 1.1: Compilation of studies assessing landfill leachate impacts on surface waters

Study	Surface Water	Summary
Coakley (1989)	lake	Investigated 230 waste disposal sites near the Great Lakes in Ontario
Borden and Yanoschak (1990)	stream	Monitoring program assessed impacts of municipal sanitary landfills near large streams
Douglass and Borden (1992)	stream	Assessed impact of a historic landfill on nearby creek during dry versus wet periods
Dickman and Rygiel (1998)	stream	Assessed impacts of a landfill on an escarpment near a creek and the invertebrate community
Atekwana and Krishnamurthy (2004)	stream	Used heavy isotopes to assess potential impacts of landfill leachate on a nearby stream
Parisio et al. (2006)	spring	Investigated iron deposits at groundwater discharge zones in mineral springs
Lorah et al. (2009)	wetland	Assessed impacts on ponded wetland nearby an unlined historic landfill
Yusof et al. (2009)	river	Studied discharging treated and untreated leachate influence on river water concentrations
Ford et al. (2011)	cove	Delineated leachate discharge from historic unlined landfill to a contaminant cove
Maqbool et al. (2011)	stream	Studied impact of an open solid waste dump along a stream in Pakistan
Milosevic et al. (2012)	stream	Studied impacts of Risby Landfill on nearby Risby Stream
Thomsen et al. (2012)	stream	Studied impacts of Risby Landfill on nearby Risby Stream
Gooddy et al. (2014)	river	Investigated impacts of industrial landfills dumped on peri-urban floodplain
Fitzgerald et al. (2015)	stream	Tested for groundwater inputs of nutrients in urban stream beside landfill
Stefania et al. (2019)	stream	Identified groundwater pollution near an old and modern landfill downstream
Ancic et al. (2020)	stream	Analyzed leachate and groundwater samples at a landfill site and upstream/downstream during different seasons

In addition, there are not many studies that focus on cold climates experiencing freezing winters. Also, within these surface waters, there is not much investigation into potential impacts to the different aquatic ecological zones, specifically the benthic and pelagic zones. The endobenthic zone is below the sediment interface, and where organisms that burrow in the sediment reside. The epibenthic zone is right above the sediment interface, and finally, the pelagic zone is the area within the water column. And finally, there is also limited knowledge when assessing emerging contaminants like PFAS within landfill leachate discharging into surface waters. With more research on PFAS fate and transport, they can potentially be used as tracers for landfill leachate, especially being known as a "forever" chemical. However, PFAS analysis is pricier, and therefore more research could lead to determining which other constituents are potential proxies.

Improved understanding of landfill plume behaviour discharging into a pond, and emerging contaminants within said plume is required for more optimal protection and management at landfill sites. Additional research can provide guidance on assessing environmental impacts and monitoring protocols for those managing historic and modern landfills. Typically, landfill operators and environmental consultants sample groundwater wells located within the landfill and hydraulically downgradient to monitor contamination levels to abide by regulations and contaminant guidelines. Additionally, they will sample nearby surface waters to monitor ecosystem impacts, and it is common to conduct grab samples of the surface water without addressing the endobenthic or epibenthic zones. Furthermore, sampling of surface water and discharging groundwater at night or during the winter season are rarely done. The winter season has conditions which

are much harsher for field sampling campaigns. There is a possibility that these monitoring protocols could be missing the times or locations where contaminants are largely impacting the aquatic ecosystems at nearby surface water bodies.

1.2. Objectives and Approach

This study's objective is to better understand the ecological risk posed by a historic landfill plume discharging to a nearby pond, and how the pond's ecosystem may be affected by potential spatial and temporal variability in contaminant concentrations and contaminant discharge. A key contaminant of interest here is PFAS. While it presents an ecological risk, there is little information on groundwater inputs of PFAS to surface waters. The evaluation of potential ecological impacts will focus on three parts of the pond community - the endobenthic, epibenthic and pelagic zones, as well as downstream ecosystems. The study will consist of detailed hydrogeology and contaminant assessment at an artificial pond beside a closed landfill (location "HB" for privacy purposes) performed over one year to encompass all the seasons. This pond is known to be impacted by a landfill plume based on annual reports from landfill site operators to fulfill provincial regulations requirements (WSP, 2018). Landfill leachate impacts were also confirmed by a previous landfill survey (Propp et al., 2021) conducted in 2018 as part of the broader landfill project to which this MSc project also belongs. They collected a sample from discharging groundwater at the edge of the pond and found elevated concentrations of common landfill leachate constituents and a total PFAS concentration (17 compounds) of 1517 ng/L.

As part of this study, various hydrological measurements were made to evaluate the nature of shallow groundwater flow into the pond. For instance, pressure transducers were installed in piezometers in and around the pond to monitor water levels over time. Temperature depth data were collected within the subsurface by iButtons installed in iron rods. With the resulting temperature depth profiles, the groundwater flux across the pond bed was determined. Outlet stream discharge was measured periodically over the year to determine seasonal patterns in water exiting the pond. Much of these measurements were made continually to capture hydrologic patterns at a variety of temporal scales, such as daily, seasonal and event based. These daily, seasonal, and event-based patterns may influence the contaminant transport and exposure patterns.

Data on the leachate plume contaminants were obtained by collecting shallow groundwater samples, along with field parameter measurements, at transects along the east bank and across the pond, as well as occasional groundwater seep samples. These samples were analyzed for the presence and the concentrations of common and emerging contaminants. The constituents analyzed included ammonium, artificial sweeteners (AS), soluble reactive phosphorus (SRP), various anions and dissolved cations-metals, and PFAS. Saccharin, a common artificial sweetener, was used as a CEC tracer to extrapolate upon the limited PFAS measurements. Other key leachate tracers of focus were ammonium, electrical conductivity, and chloride. The groundwater flux combined with the groundwater contaminant concentrations provided information on the contaminant flux discharging into the pond. In addition, continuous measurements of electrical conductivity at the sediment interface within the pond provided a measure of salt ions

entering the pond. Finally, the discharge at the outlet stream was used with contaminant concentrations to determine contaminant mass discharge to a receiving creek.

Using this multi-method approach, contaminant exposure and thus potential ecological risk to various parts of the aquatic ecosystem were assessed. The shallow groundwater contaminant concentrations targeted the conditions experienced by the endobenthic organisms. Meanwhile, the electrical conductivity measured at the sediment bed and calculated contaminant fluxes revealed potential conditions experienced by epibenthic organisms. Finally, pond and outlet surface water concentrations and mass discharge revealed conditions experienced by the pelagic organisms in the pond and organisms downstream. This study was part of a broader investigation of the threat posed by groundwater contaminated by landfill leachate discharging to surface waters. It started off with a leachate survey for CECs in historic landfills (Propp et al., 2021). Followed by detailed site investigations assessing the presence of various contaminants and exposure zones in two different receiving surface water bodies, this study with a pond and another for a stream. Finally, ecotoxicology assessments at both sites, involving endobenthic community assessment and in situ caging toxicity tests, are still in progress. This study's results will provide guidance on sampling and monitoring protocols, particularly for landfill operators and those investigating contaminant plumes entering a non-flowing surface water body. This study will also provide insights into risks posed by contaminant exposure in different parts of the ecosystem. Finally, this study will improve understanding of how historic landfills may contribute to potential threats posed by PFAS and other emerging contaminants.

2.0 Literature Review

2.1 Landfill Leachate

Landfills are a common method of waste disposal. There are various types of wastes that can be disposed of such as municipal solid waste (i.e., typical domestic garbage), industrial waste, or hazardous waste. Municipal solid waste is often compacted and buried with soil daily. Infiltration of precipitation or water from waste itself can percolate through landfill waste and dissolve contaminants producing landfill leachate. In the past, landfills were placed anywhere without much regard, and over the years, more design and regulations were introduced (Lisk, 1991).

Modern landfills are engineered with liners meant to isolate the potentially harmful waste from groundwater and air. For example, a modern municipal landfill can use a clay liner or synthetic liner, usually plastic, to isolate the waste (Youcai, 2018). The clay layer slows down the migration of the leachate, potentially allowing microbiological degradation of susceptible compounds to occur (Youcai, 2018). Modern landfills typically also have leachate collection systems, which are engineering infrastructure built within the landfill to catch leachate from the landfill so that it can be removed and then contained or treated (on-site or sent to wastewater treatment plants). These systems are meant to prevent harmful contaminants from entering the environment and harming the organisms within it, including humans. And still, these landfills may leak and contaminate surrounding groundwater (e.g., Stefania et al. (2019)).

Older landfills are of concern since they may not have liners or leachate collection systems in place to catch the potentially harmful leachate that would then enter the

environment through the groundwater flow regime. Many closed landfills also require long-term monitoring as these landfills will continue to generate leachate that can potentially leak. Closed historic landfills sometimes do not even have monitoring programs because they are either forgotten or not captured under regulations.

Depending on what was disposed at the landfill site, the leachate contaminant concentrations will vary. This becomes even more complicated when considering the degradation and transformations into end products of said contaminants. Typically landfill leachate composition include cations, nitrogen, volatile organic compounds, chlorides, sulfates, heavy metals, and trace metals. Groundwater can contain small amounts of some of these constituents but often at trace amounts, and therefore leachate indicators help determine the difference. Leachate indicators are persistent (within the plume at least), and mobile constituents that help diagnose landfill leachate plumes from other potential sources. Major leachate tracers include ammonium, and chloride and, a more recently applied leachate indicator, saccharin.

Additionally, Harrad et al. (2019) compared leachate concentrations between unlined, mixed, and lined landfills. They describe mixed landfills as previously unlined landfills fit with new HDPE liners. Intuitively, leachate concentrations were greatest with lined, moderate with mixed, and lowest with unlined landfills. This is due to dilution factors and the age of the landfill. It is also likely due to the times in which various contaminants were introduced. The leachate concentrations were also probably lowest at the unlined landfills because the leachate plume was migrating downgradient. Their results raise concerns for unlined landfills who do not treat their leachate.

Kjeldsen and Christophersen (2001) investigated typical compositions of leachate coming from 106 old landfills. They found that newer sanitary landfills will have different compositions to older municipal landfills. This is partly because of the different waste disposed of at each, and partly because of the age difference. However, it is difficult to quantify because of attenuation processes (Kjeldsen and Christophersen, 2001). The association with landfill age is related to the common phases of leachate decomposition, which include aerobic, anaerobic acid, initial methanogenesis, and stable methanogenesis (Kjeldsen et al. 2002). New landfill leachate will start off in the aerobic phase, and typically, older landfill leachate will be in the methanogenic phase (Kjeldsen et al. (2002). Within each of these stages, there will be different levels of oxygen, water, pH, BOD, COD, and biodegradable constituents.

Landfill leachate can also change seasonally. Ančić et al. (2020) analyzed leachate up and downstream a landfill over different seasons. Their results showed cytotoxic, pro-oxidative, and mutagenic effects from leachate exposure. They found that toxicity increased in dry and warm periods because of the increased degradation rate and therefore different chemicals (degradation products) were found in the leachate. Fortunately, the concentration levels were not high enough to present a toxicological threat.

Cozzarelli et al. (2011) looked at landfill leachate plumes and their biogeochemical evolution as they migrated away from the site. As expected, there is immense temporal and spatial variability which largely depends on the redox conditions within the plume. These important redox conditions are controlled by the aquifers

hydrogeologic framework and the composition of the leachate. Therefore, understanding redox conditions will help determine the attenuation processes and therefore the fate of the contaminants within the leachate plume. Generally, the redox conditions are mostly anaerobic near the landfill and become more aerobic towards the outskirts of the leachate plume (Bjerg et al., 2011). Furthermore, among the literature, there is a consensus that leachate plumes are narrow and never extend past the width of the landfill (Christensen et al., 2001). However, Christensen et al. (2001) also mention that very few studies fully document leachate plumes that are not in sandy aquifers.

2.2 Contaminants of Emerging Concern in Landfills

Contaminants of Emerging Concern (CECs) is a term used for compounds in the environment that have not previously been of concern, only now detected over detection limits, or simply not looked at before, and has the potential to cause detrimental effects to ecology or human health (Stuart et al., 2012). Categories or types of CECS include pesticides (particularly new types of pesticides), pharmaceuticals, personal care products, industrial additives, and byproducts, food additives, water treatment byproducts, flame/fire retardants, surfactants, hormones and sterols, ionic liquids, and “life-style compounds” (Stuart et al., 2012). Life-style compounds are compounds such as caffeine, nicotine, and cotinine (Stuart et al., 2012). These CECs are generally not yet regulated or have loose regulations due to lack of research and knowledge. Some challenges with regulating CECs are that there needs to be a better understanding of their fate and transport within the environment, as well as mode of toxicity. One of the other challenges

is lack of analytical ability. However as analytical techniques improve, more previously undetected CECs can be monitored (Stuart et al., 2012).

Key sources of CECs include wastewater treatment effluent, landfill leachate, leaking storage tanks, storm water, agriculture, and industrial practices. Particularly with wastewater treatment plants, the CECs are untreated due to lack of infrastructure catered to the new contaminants (Stuart et al., 2012). One of the ways CECs enter the water cycle is through landfill leachate and can eventually enter the public water supply system. Studies have shown that landfills can contain a large variety of CECs. For example, Masoner et al. (2020) looked at 19 landfills across the United States and tested for 129 CECs, most of which were pharmaceuticals, industrial chemicals, household chemicals, steroids, and plant/animal sterols. Bisphenol-A, cotinine, and N, N-Diethyl-meta-toluamide (DEET) were the most ubiquitous. Other CECs not mentioned include polycyclic aromatic hydrocarbons (PAHs), and pesticides (Masoner et al., 2019). Buszka et al. (2009) sampled groundwater from a well downgradient from a landfill to determine concentrations of wastewater indicators and pharmaceutical compounds. They found various compounds including pharmaceuticals that indicate that those compounds were disposed of in the landfill. They emphasized the importance of testing for these compounds to build up a database of their potential occurrence and persistence in the environment, especially if they are harmful to human health. This database will be useful to future studies that also look at the similar contaminants.

A group of CECs of particular interest are per- and poly-fluoroalkylated substances (PFAS). PFAS are a group of synthetic chemicals containing over 5000

different types that tend to persist in the environment and accumulate in the human body (Hamid et al., 2019). PFAS are synthetic organofluorine compounds with fluorine atoms attached to an alkyl chain containing at least one perfluoroalkyl moiety (C_nF_{2n+1-}). PFAS have been deemed as the "forever" chemicals because many of them are resistant to degradation. There are many different types of PFAS and uses for these compounds as it makes manufactured products resistant to grease, oil, water, and heat. Some products include textiles, paper, non-stick cookware, carpets, cleaning agents, electronics, and fire-fighting foams (Hamid et al., 2019). PFAS can enter the environment as a by-product of their precursors. For example, fluorotelomer alcohol (FTOH), fluorotelomer carboxylic acid (FTCA), fluorotelomer unsaturated carboxylic acids (FTUCA) are precursors of perfluoroalkyl acids (PFAA). More specifically, FTOHs are in raw materials of fluorotelomer polymers, which are used in textiles, papers etc.

As mentioned before, PFAS can present human health risk. For example, Gyllenhammar et al. (2019) investigated the health risks associated with PFAAs in children through drinking water. Specifically, they tested the children's serum for PFAAs. As expected, children had an increased concentration of PFAAs which had accumulated over time. It was found that contaminated drinking water is a significant source, especially for younger children. Long term studies will be needed to determine long term effects of exposure to PFAAs. PFAS is known to have slow elimination rates in organisms as well, and therefore bioaccumulates (Hamid et al., 2019). Although PFAS tends to accumulate in larger mammals, it is not confirmed that there is no impact on smaller organisms.

Perfluorooctane sulfonate (PFOS) and perfluorooctanoic acid (PFOA) (along with other PFAAs) are most detected in the environment. PFOA and PFOS are considered long-chain PFAS. Long-chain PFAS are PFAS which contain 6 or more carbons and 7 or more carbons (for perfluoroalkyl sulfonic acids (PFSA) and perfluoroalkyl carboxylic acids (PFCA), respectively). After numerous studies depicted the widespread and harmful effects of PFAS, the manufacture of PFOS and PFOA have been restricted under Stockholm Convention and placed on the Toxic Substances List in Canada. Although some longer chained PFAS get banned, smaller chained types are being used as an alternative. However, the short-chained types have shown to be more mobile than their banned counterparts (Brandsma et al., 2019). All in all, the switch to short chained alternatives may not be a solution as the new contaminants are accumulating in different environmental reservoirs (Brandsma et al., 2019).

PFAS is particularly difficult to analyze due to its novel nature and the vast variety of compounds. D'Agostino and Mabury (2017) analyzed various PFAS and highlighted the limitations with total organofluorine combustion-ion chromatography. It was revealed that 36% to 99.7% of the total organofluorine was not measured. Consequently, total PFAS is not representative of the actual total PFAS within water samples.

There has been much concern over the possibility of cross contamination while collecting samples for PFAS analysis. However, newer studies have found that typical precautions are enough to avoid contamination. Rodowa et al. (2020) demonstrated the implausibility of contaminating samples for PFAS analysis (false positives) and found

that most field sampling materials did not have enough to reach the Environmental Protection Agency (EPA) health advisory limit (70ng/L for a 1L sample). Those that do have quantifiable PFAS concentrations have no plausible pathway to contaminate the sample. In other words, materials that potentially do not encounter the sample do not have cause for concern. However, the materials that do come in direct contact may have a plausible pathway to impact PFAS levels but have low risk. Therefore, restricting materials can increase the difficulty of sampling and it is recommended to document and quantify their risk. This is especially important when testing for trace concentrations.

The most contaminated groundwater sites for PFAS have been linked to firefighting foams. Milley et al. (2018) conducted a Canada wide study investigating the contamination PFAS at airports. By using public resources, they were able to predict how many airports potentially impacted their nearby surface waters. They concluded that 152 to 420 airports across Canada have potential contamination of PFAS. They used information regarding the use of PFAS (firefighting training), storage of PFAS, surficial geology, and proximity to surface waters to determine this claim.

One of the other ways PFAS enters the water system is by leachate from landfills with PFAS containing products. Some products disposed of include cookware, pizza boxes, stain/water repellent items. Hamid et al. (2018) conducted a critical review of literature to summarize the role of PFAS in landfills. Generally, short chain PFAAs were most abundant due to their greater mobility, and production in the industry.

There are few reports of PFAS from groundwater impacting an aquatic ecosystem. However, Briggs et al. (2020) found out that groundwater discharge from

hillslopes diluted PFAS concentrations. They applied heat tracing methods to determine zones of discharge at a recharging stream. Higher concentrations of PFAS were found from flow paths originating from regional groundwater (not the hillslopes), increasing PFAs concentrations going downstream.

2.3 Tracers of Landfill Leachate

An ideal tracer should have low background levels, be conservative (i.e., non-reactive as much as possible), and have low detection limits. The most common tracers of landfill leachate in groundwater are chloride and ammonium. Using chloride as a landfill tracer can be challenging due to its widespread use as road salts in colder climates, and therefore can have multiple point sources. Ammonium is a leachate indicator because of the high levels of organics within the waste disposed of at a landfill site and is known to persist within the landfill (Christensen et al., 2001). Christensen et al. (2001) claim that in landfill leachate the concentration of chloride is typically 150-4500 mg/L while the concentration of ammonium is 50-2200 mg/L. These are elevated concentrations compared to amounts normally found in shallow groundwater.

Oftentimes, emerging contaminants are sampled along with more common constituents such as ammonium to help better understand the transport of said contaminants. It is also useful to find contaminants that correlate with these emerging contaminants since the analysis of these contaminants are oftentimes pricier due to their novel nature. It is especially more difficult for PFAS since there are many types and some analyses do not cover all of them. Hepburn et al. (2019) investigated legacy (historic) landfills acting as a point source for PFAS, which again is a poorly constrained

contaminant. Concentrations of various PFAS forms were detected and most correlated with common leachate constituents such as ammonium and methane. This leads to possible use of these PFAS as a conservative tracer. This is because they are sourced from landfill leachate and can help distinguish from other sources. PFAS is also highly mobile and persistent which is bad in terms of health impacts, but ideal as a tracer. Hepburn et al. (2019) provides a framework for assessing PFAS impacts on groundwater from legacy landfill. Where if PFOA concentration divided by total PFAA concentration is greater or equal to 10%, the impact is likely due to a legacy landfill. However, this system did not hold up for the 20 historic landfills surveyed by Propp et al. (2021). Additionally, Li et al. (2012) investigated two synthetic compounds PBDEs, and PFCs which are used in a variety of products. Due to their highly persistent nature and toxic effects on human health, they both pose a risk. Li et al. (2012) conducted a review of various studies from different landfill leachate plumes to better understand how these compounds behave. They also explored possible correlations between these compounds and their precursors. They found that all the 24 landfills studied detected these compounds, and that the degradation products are the major source for these contaminants of emerging concern.

Another important group of CECs for landfills are artificial sweeteners (AS), as these have been touted as useful tracers in landfills (Roy et al., 2014). AS are a sugar substitute that is added to sweeten foods without adding more calories, also used with personal care products, drugs, etc. Four common AS assessed in the environment are acesulfame, sucralose, cyclamate, and saccharin. Saccharin was most predominant in a

stream adjacent to an old landfill site (Roy et al., 2014). This makes sense since saccharin is the oldest artificial sweetener and became popular around the 1960s and 1970s. Therefore, even though acesulfame is a more ideal tracer (conservative), it was only introduced in the early 1990s and not as useful when studying older landfills. However, detection of acesulfame and sucralose can indicate contamination by modern wastewater in studies targeting old landfills (Propp et al. 2021).

Stolte et al. (2013) investigated potential ecotoxicity of artificial sweeteners as an emerging contaminant. All four artificial sweeteners are widely distributed with no firm research regarding their ecotoxicity on a large scale. Luo et al. (2019) looked at the distribution of artificial sweeteners in the environment and found high correlation to consumption patterns and removal efficiency at associated wastewater treatment plants. Subsequently, surface water, groundwater, and drinking water also have concentrations of artificial sweeteners although not as high as wastewater treatment plant influent. The laboratory results from Stotle et al. (2013) on algae, water fleas, and duckweed demonstrated that artificial sweeteners present low potential risk to these organisms. However, the researchers suggest that further research be conducted and that regulations for food additives are necessary.

Some analysis for AS also analyze sulfamate, an anion of sulfamic acid that has been detected in environmental waters. It is a product of oxidation of cyclamate by ozone. Similarly, sulfamate was detected as an oxidation product of acesulfame. A study by Van Stempvoort et al. (2019) found that sulfamate has many sources, including precipitation making it a less than ideal tracer for wastewater. They found that the lowest

concentrations were in groundwater samples with reducing conditions and could cause the degradation of sulfamate.

2.4 Groundwater - Pond Interactions

The interaction between groundwater and surface water can be influenced by several factors. Winter et al. (1998) describes the interaction between a lake and groundwater which is similar conceptually to a pond. However, a pond is without wave action due its smaller size. Oftentimes, the water level is less variable compared to streams but not always and evaporation has a greater effect due to the greater surface area and lack of shade. There are three different types of interactions between a pond and the aquifer. A pond can be gaining which means there is groundwater inflow from the surrounding aquifer. A pond can also be losing which means the pond surface water seeps into the aquifer. Finally, a pond can be flow-through which means there is both gaining and losing occurring (Winter et al., 1998).

Walter et al. (2002) simulated a pond-aquifer interaction under natural and stressed conditions at a kettle pond. In their report, they discuss the conceptual model of pond-aquifer interactions, and variables that affect these interactions. A pond will interact with a surrounding aquifer depending on the size of the pond and the thickness of the aquifer. Typically, water discharges in upgradient areas and recharges in downgradient areas. A greater horizontal hydraulic conductivity of the aquifer sediment will mean less groundwater discharging into the pond. Under homogeneous conditions, the hydraulic gradients will decrease exponentially with distance away from the shore, therefore the highest hydraulic gradients are found along the shore of the pond and where the greatest

inflow and outflow of water will occur. Permeability of the aquifer or pond bottom sediment will also influence the rate of recharge or discharge where a highly permeable sediment will result in greater rate of groundwater movement. There will also be outlets and inlets at a pond in most cases, and therefore the pond water level will depend on the outlet, inlet, precipitation, and net groundwater exchange. These are factors affecting the interaction between the pond and the associated aquifer. There are also other external factors that play a role in the interactions between pond and groundwater. For example, topological, hydrological, anthropogenic, and ecological factors. Ecological factors can include surrounding vegetation causing drops in water level because of evapotranspiration. Anthropogenic factors can include land management, land use, and dams. Hayashi (2004) found that evapotranspiration is also a natural factor that can affect groundwater-surface water interactions. Evapotranspiration of plants surrounding a surface water body can affect the groundwater discharging into the pond. Therefore, there are diurnal patterns in surface water bodies as plants will uptake groundwater during the day and pause at night.

Due to the lack of surface water movement and circulation in a pond (compared to a stream) there are greater organic deposits at the pond bed, therefore affecting the types of biogeochemical exchanges (Winter et al., 1988). Some common types of biogeochemical reactions include acid-base reactions, sorption and ion exchange, precipitation, and dissolution of minerals, oxidation-reductions reactions, biodegradation, and dissolution and exsolution of gases (Winter et al., 1988).

The interaction between a pond and its aquifer is not limited to whether the groundwater is discharging or being recharged (Conant et al., 2019). There is a more complicated relationship at the pond and groundwater interface, also known as the transition zone. The transition zone is defined by Conant et al. (2019) “as a three-dimensional volume beneath and adjacent to surface water bodies where groundwater-surface water interactions occur and conditions transition from groundwater dominated system to a surface water dominated system.”. This zone is significantly different from the surface water and groundwater zones individually because of various processes. For example, the biogeochemistry (i.e., redox reactions) of the transition zone is significantly different. Conditions will vary spatially across the pond bottom because of the varying hydraulic gradients. The spatial heterogeneity is because biogeochemical processes are controlled by advection or diffusion/dispersion processes. Different biogeochemical zones also vary temporally as different times of the day or season changes the ecological and hydrologic conditions.

2.5 Temperature-based Groundwater Flux Calculations

Groundwater can influence the typical temperature profile in the earth. Naturally, the earth has a small upward thermal gradient which can be affected by moving water. Stallman (1963) formulated an analytical relationship between the transfer of heat and water in the earth which allowed the calculation of groundwater movement using temperature measurements. Bredehoeft and Papadopulos (1965) presented a solution of this relationship in steady state conditions, because groundwater movement causes temperature variations within the earth. This analytical solution is a type-curve method

used to describe vertical (1-dimensional) steady-state flow of groundwater and transfer of heat through an isotropic, homogenous, and fully saturated semi-infinite layer. The type curve shows that no flow conditions (heat transfer by conduction only) the thermal gradient is linear with depth. Groundwater flow causes heat transfer by convection with the water, causing the temperature profile to be non-linear. The temperature curve is convex or concave up depending on the direction of water movement (recharging or discharging, respectively), and the curvature increases with groundwater velocity. This solution is useful to hydrogeologists as it is possible to calculate the rate of groundwater movement using temperature measurements within the earth. This is especially useful for groundwater and surface water interactions as the recharge and discharge of groundwater can be measured at surface water bodies.

Shan and Bodvarsson (2004) produced an analytical solution for 1D steady heat transfer through a multilayered system to provide estimated percolation rates. They based their solution off Bredehoeft and Papadopulos. Their assumptions are that each layer is homogeneous, and has a constant thermal diffusivity, that the heat/mass flow is 1D and perpendicular to the surface, and constant.

FLUX-LM by Kurylyk et al. (2017) is an analytical solution and spreadsheet model that requires temperature depth measurements, layer thickness (from 1 to 3 layers), and thermal conductivity of the layers to calculate the vertical groundwater flux based on the solutions of Shan and Bodvarsson (2004) and Bredehoeft and Papadopulos (1965). FLUX-LM is useful to hydrogeologists who can then use heat as a groundwater tracer. This is useful since heat is ubiquitous. For application to groundwater interactions with

surface waters, this model is best used at discharge zones where there is minimal or no diurnal influence because downward conduction would be impeded by upward advection. To account for the diurnal influence, the sensors can be installed deep below the influence of diurnal fluctuations (typically 50 cm). For FLUX-LM, the user supplies the temperature depth profiles, as well as the layer properties from which the excel solver will calculate a theoretical temperature depth profile by "guessing" the groundwater flux. The solver then finds the optimal flux value by minimizing root mean square error (RMSE) between the calculated and measured temperature depth profiles. Oftentimes the sediment layer properties are not known or measured. However, these can be estimated based on sediment property tables in the literature. For example, Lapham (1989) provided a table outlining a range of values for thermal conductivity of saturated fine- and coarse-grained sediment.

2.6 Groundwater Contaminants from Landfills Affecting Surface Waters

Contaminants in groundwater that discharges to a surface water body have the potential to cause harm to its aquatic and surrounding terrestrial ecosystems, as well as impair the quality of the surface water and potentially pose a threat to human health. For point sources of contaminants, like landfills, studies of the contaminant plumes reaching surface waters have largely occurred in the past two decades. Conant et al. (2004) was one of the first studies to investigate the impacts. They investigated a PCE plume entering a streambed. Simply sampling only, the surface water or only the groundwater was a gross misinterpretation of the plume discharging into the river. They found that the transition zone had high heterogeneities in plume composition, concentration, and

distribution. Therefore, it is important to obtain data from both surface water and groundwater to capture heterogeneity in the plume. Years later, Conant et al. (2019) created a framework to help conceptualize the ground-surface water interactions by describing the flow, biogeochemical, and biological patterns of all types of settings. In turn, this conceptual model will help identify potential impacts and issues on water quantity, quality, and associated ecosystems.

There have been several studies focused on landfill plumes reaching various types of surface water bodies (Table 1.1). Some examples of such studies include Thomsen et al. (2012) who conducted a screening as part of a risk assessment of an old landfill above clay till settings in Central Zealand, Denmark. They used historical investigation, and contaminant mass balance to estimate contaminant mass discharge into the stream. Chloride was used as a tracer, and dissolved organic carbon was used for indication of oxygen depletion, and ammonium was used as a toxicity indicator. Their results showed substantial spatial variability in contaminant concentrations due to the heterogeneous geology which will affect attenuation processes. More specifically, various attenuation processes occurred during the transport of the leachate, and therefore results showed high variability in leachate indicators, redox parameters, and xenobiotic organic compounds due to complex geology. The source composition will also influence the contaminant concentrations as waste is not disposed of at the same time at the landfill. At the same landfill, Milosevic et al. (2012) determined direct toxicity effects and indirect oxygen depletion risks from landfill leachate to associated ecology. They used streambed temperature gradients and seepage meters to determine groundwater flux. They also

sampled groundwater at “hot spots” for a variety of compounds. Interestingly, surface water concentrations were similar to groundwater concentrations during dry periods. This was due to low water levels and therefore less dilution influencing contaminant concentrations in the stream. Similarly, Fitzgerald et al. (2015) suggested that ammonium levels were elevated in a receiving stream due to inputs of groundwater affected by several nearby landfills.

The high heterogeneity of groundwater and surface water interactions is not limited to spatial processes but also temporal. Lorah et al. (2009) looked at leachate plume in a swamp and its biochemical interactions that cause attenuation. They studied particularly groundwater and surface water interactions. The wetland-groundwater interactions changed during wet and dry conditions, discharging and discharging/recharging periods, respectively. Dry conditions (low water table) showed lower levels of ammonium in the slough due to vertically upward discharge only in the middle of the slough and attenuation by dispersion and dilution. During wet seasons there were high concentrations of ammonium and other leachate constituents that travelled further downgradient, and primarily attenuated through sorption. Therefore, seasonality seems to play an important role during groundwater and surface water interactions.

Few studies report on the impacts of groundwater contaminants entering a surface water body on aquatic ecosystems, especially related to landfills. However, Dickman and Rygiel (1998) found that after 15 years of exposure to a discharging leachate plume, the species within the study stream had changed to more pollutant tolerant species as the more sensitive species were presumably wiped out. Another example, but not related to

landfills, is the study of Roy et al. (2018), who investigated impacts on benthic ecosystems in an urban stream receiving groundwater from a contaminant plume containing volatile organic compounds (VOCs). They found that there was a reduced abundance and richness of taxa in zones of high contaminant concentrations. Essentially, the contaminant plume potentially altered the benthic community structure within the urban stream. However, due to the complexity of groundwater-surface water interactions the cause could not conclusively be attributed to a single factor.

3.0 Field Site

The closed landfill site is approximately 40.5 hectares and is bounded by agricultural land to the east and west, and by swampy lands to the north and south. This former unlined sanitation landfill was in operation from 1970 to 1986 and received domestic, commercial, and non-hazardous industrial solid waste. In July 1986, the landfill ceased operations and subsequently was capped and seeded. No landfill leachate collection or containment system has been installed to date.

The landfill itself is approximately 280m wide and 480m long. The site is located at the highest elevation within the property (Figure 3.1). To the west of the landfill lies a pond, as well as a small stream that flows southward along the west side of the property before draining into a swamp south of the property. The 200 by 80 m engineered pond is situated approximately 40 m west of the closed landfill. The pond was artificially created by landscapers and has a drainage gate leading to the discharge outlet via a culvert (Figure 3.2). The engineered pond is inferred to receive some overland runoff as well as shallow groundwater flow from the closed landfill. The perimeter of the pond is lined with *Typha* and *Phragmites*. East of the pond is a road cutting across the landfill in the north and south direction. At the west side of the pond there is a small inflowing stream. The inflowing stream is almost negligible during the summer months and sees higher flow during winter and spring months. The pond supports a variety of aquatic invertebrates, as well as newts, turtles, and small fish. There is also *Chara* (a common freshwater plant) covering the bottom of the pond, except for the edges and certain patches in the north end of the pond.

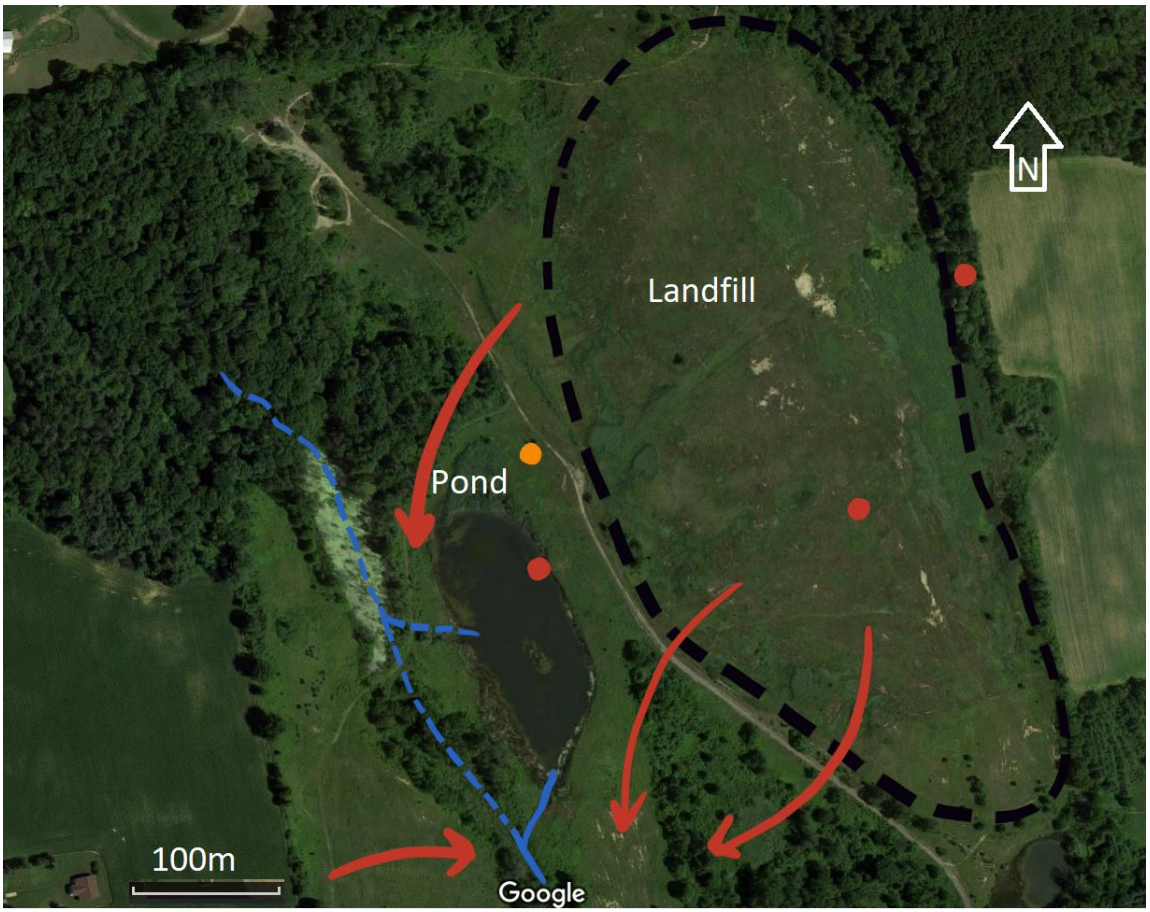

Figure 3.1. Satellite image of HB site from Google Maps. Landfill (right and outlined by dotted line) and pond (left) are labelled. Red arrows indicate approximate groundwater flow directions (May 2018 from WSP report). Red dots indicating sample locations from Propp et al. (2021). Orange dot indicates Monitoring Well 18R. Blue lines indicate streams.

Figure 3.2. Bird's eye view of the artificial pond to the west of the landfill. *Chara* (aquatic plant) is shown as the darker areas within the pond. There is a greater amount of phragmites at the north-east end of the pond.

According to the landfill report (WSP, 2018), the site is within an area that consists of clay to silty clay till moraines with alluvial silt, sand, and gravel covering the lower areas. The site is also situated within an undrumlinized till plain. Towards the north of the site, there are glaciofluvial outwash deposits consisting of sand, gravelly sand, and sandy gravel. Towards the south, there is Port Stanley till consisting of silty-to-silty clay till, as well as a bog deposit at the southern boundary. These overburden deposits range from 29 to 46 m in thickness, increasing in thickness from east to west. Bedrock was not encountered during the intrusive investigations but consists of Middle Devonian limestone and dolostone of the Detroit River Group (WSP, 2018).

Based on the culmination of hydrologic investigations performed (summarized in WSP, 2018), the groundwater flow system of the site comprises four hydrostratigraphic units. On top, there is a sand and gravel unit with a mean hydraulic conductivity (K) of $2.9x10^{-1}$ cm/s for the coarse sediments, and $2.6x10^{-3}$ cm/s for the fine sediments. Below that there is an upper clayey silt unit with a mean K of $8.8x10^{-5}$ cm/s. Thirdly, there is a confining/semi-confining lower clayey silt unit with a mean K of $6.5x10^{-6}$ cm/s and was inferred to have weak downward hydraulic gradients. Finally, there is a lower sand and gravel unit with a mean K of $3.6x10^{-1}$ cm/s for the coarse sediments, and $6.1x10^{-5}$ cm/s for the fine sediments. The thickness and lateral extent of the lower clayey silt unit is unknown. The hydraulic conductivity tests were performed in-situ (James F. MacLaren Ltd., 1979 and MacLaren Engineers, 1982). The two upper units represent the shallow groundwater system while the lower unit represents the deeper groundwater system.

Within the pond, there is organic rich sediment, black in colour and about 30 cm thick, hosting aquatic vegetation.

The groundwater in the shallow flow system flows to the southwest across most of the site. Based on the groundwater elevation there appears to be a mound at the landfill site causing radial groundwater flow away from the landfill in the east and southeast direction. However west the creek, the shallow groundwater flows towards the east (towards the creek). Therefore, throughout the site, the groundwater appears to converge towards the creek. Furthermore, the synthetic pond likely acts as a discharge zone.

As part of the annual monitoring, groundwater samples have been routinely collected from a series of monitoring wells at the site (WSP, 2018). The samples were analyzed for major and minor ions, nutrients and organics, and dissolved metals. Select wells were analyzed for volatile organic compounds (benzene, 1,4-dichlorobenzene, and vinyl chloride). Concentrations of chloride, alkalinity, potassium, boron, iron, and ammonia, total Kjeldahl nitrogen, vinyl chloride, benzene, and 1,4-dichlorobenzene were higher compared to the background concentrations in several monitoring wells in the upper aquifer groundwater at the site. However, the leachate strength at the site is deemed weak because chloride and sodium concentrations tested at the leachate well (Well 41) are below their Ontario Drinking Water Quality Standards. The 2018 concentrations were within the historic range, meaning previous site assessments found similar concentrations of the parameters. The report states that a decreasing trend suggests attenuation of the plume through hydraulic migration and microbial degradation. Additionally, the deep groundwater flow system has no clear evidence of leachate influence. Finally, the pond

surface water, sampled annually, appears to be weakly affected by the landfill according to the report in 2018, because of elevated concentrations of alkalinity, chloride, potassium, and sodium.

A landfill leachate survey of historic landfills conducted as part of the broader investigation in 2018 by Environment and Climate Change Canada tested for various contaminants of emerging concern in samples from two leachate-impacted monitoring wells on the HB landfill site, along with discharging groundwater from the east edge of the pond (Propp et al., 2021). The investigators concluded that there were landfill leachate impacts based on the presence of emerging contaminants in their water samples.

4.0 Methodology

4.1 Shallow Groundwater Sampling at the Study Pond

To delineate the general extent of the leachate-affected plume discharging to the pond and identify areas for focused study, a screening assessment of the groundwater entering the east side of the pond was performed in May 2019 (extended further south in June) and one in a line across the pond in July 2019. This assessment included shallow discharging groundwater below the pond sediment interface and a few seep samples from the edge of the pond. These samples were measured for common groundwater geochemistry and contaminants (described further below). Subsequently, more permanent groundwater sampling devices were placed at most of the same sample locations but only at locations with high concentrations of leachate indicators or at locations that help delineate the plume extent. Most of the solution samplers were installed along an east-west line across the pond called “Transect E-W”, as well as a north-south transect along the east edge of the pond called “Transect N-S” (Figure 4.1). Just north of and parallel to Transect E-W, there is a shorter transect (5 sample locations) a part of the preliminary screening.

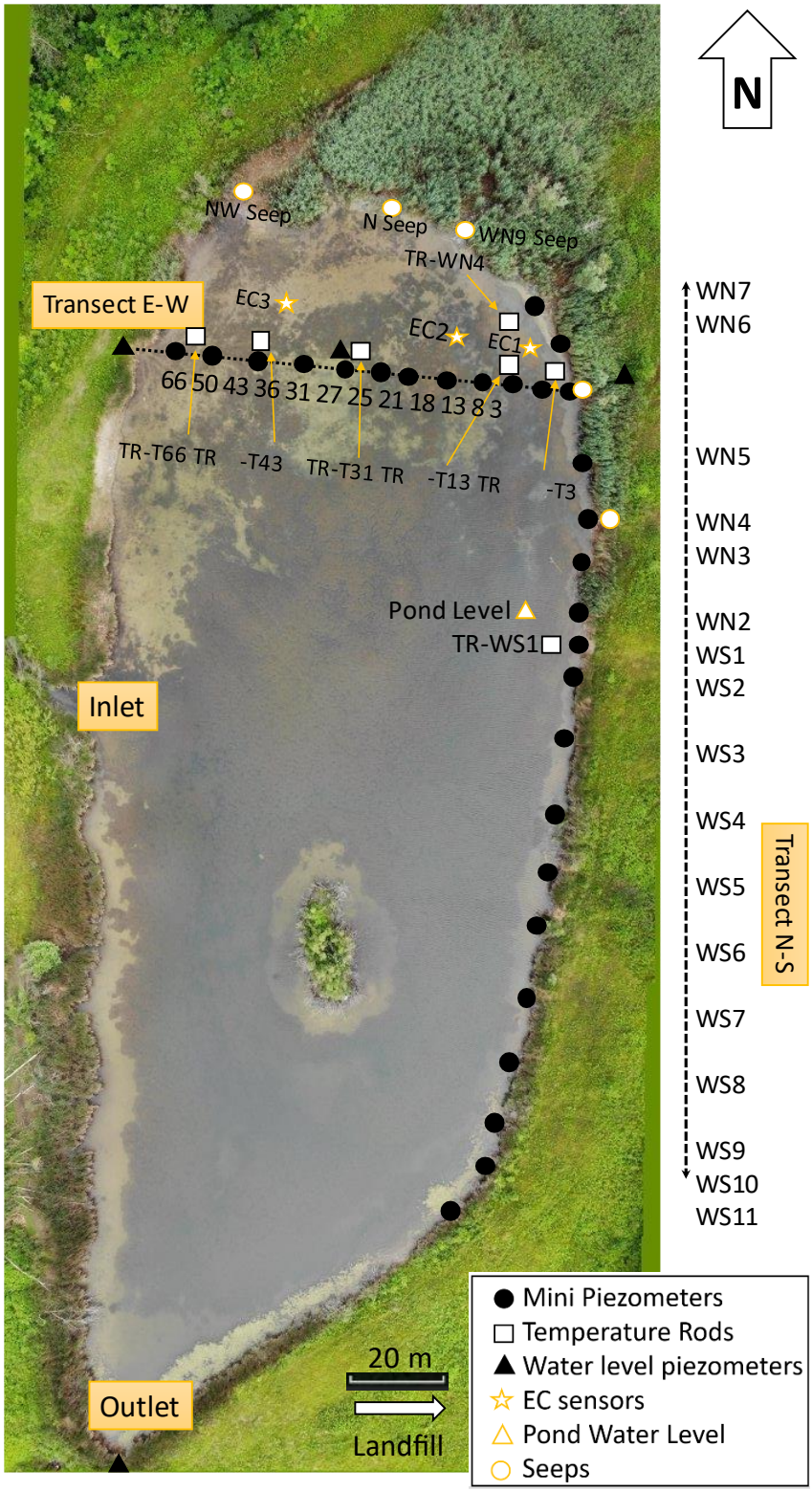

Figure 4.1. Bird's eye view of the pond and the sampling transects. Instrumentation comprised of mini-piezometers (E-W - locations numbered according to distance (m) from east shore; N-S - locations indicated by relative position north (N#) or south (S#) of the central location, first measured by Propp et a. 2021), along with additional monitoring equipment; electrical conductivity data loggers (EC sensors), water level piezometers, temperature rods, and seep locations. The inlet is on the west side of the pond and the outlet is to the south. The landfill is to the east of the pond (see Figure 3.1).

The dates of sampling groundwater and the locations, as well as the analyses conducted are summarized in Table 3.1. The initial screening assessment along the Transect N-S consisted of 17 sampling locations total, spanning 5 to 20 metres in between. There were also 12 sampling locations spanning every 4 to 16 metres along Transect E-W. The spacing of the sampling locations varied because some areas did not produce sufficient groundwater flow for sample collection. The mini-profiler system (see Roy and Bickerton, 2010) used to collect the groundwater samples consisted of an 18 cm stainless steel drive point with sampling ports, which was attached to an ¼-in polyethylene tubing inserted into a ⅝-in hollow rod. The mini-profiler system was driven to various depths ranging between 14 and 83 cm within the sediment with a hammer drill (Figure 4.2). The tubing was connected to a peristaltic pump with Master flex tubing (Figure 4.3). While the rod was drilling into the sediment, pond water from a second stainless steel drive point attached onto the opposite end of the peristaltic pump, and immersed in the pond surface water, was pumped into the sediment to prevent clogging of the ports. The groundwater was then pumped into a graduated cylinder by reversing the flow, from which electrical conductivity, temperature, dissolved oxygen, and pH were measured using hand-held meters (YSI Professional Plus, and YSI ProDO probe, Hoskins Scientific). Groundwater samples were collected to be analyzed for ammonium, artificial sweeteners, SRP, and various anions. The mini-profiler was subsequently removed and used for the next sample location. Before each new location, the tubing was replaced to avoid cross contamination.

A total of fifteen solution samplers (essentially mini-profiler rods left in place; Figure 4.4) were installed along both transects, 11 in Transect E-W and 4 additional ones in Transect N-S (Figure 4.1) at many but not all the sampling locations from the screening assessment. The solution samplers were installed at depths from 10 to 20 cm with the intent to target the endobenthic zone. The solution samplers were used to collect a full suite of shallow groundwater samples (i.e., analyses including VOCs, anions, cations, SRP, ammonium, dissolved metals, artificial sweeteners, and PFAS) on August 22, 2019 (Sampling Campaign 1) and December 9 and 10, 2019 (Sampling Campaign 2). Sampling groundwater from the solution samplers was similar to using the mini-profiler system in which Master Flex tubing was connected to a peristaltic pump and fed into a graduated cylinder where field parameters were measured, and samples were collected (Figure 4.3).

Figure 4.2. Photograph of Tammy Hua demonstrating the use of a hammer drill to install a mini-profiler into the subsurface (not HB site). Tubing is pumping water into the ground to prevent clogging of ports.

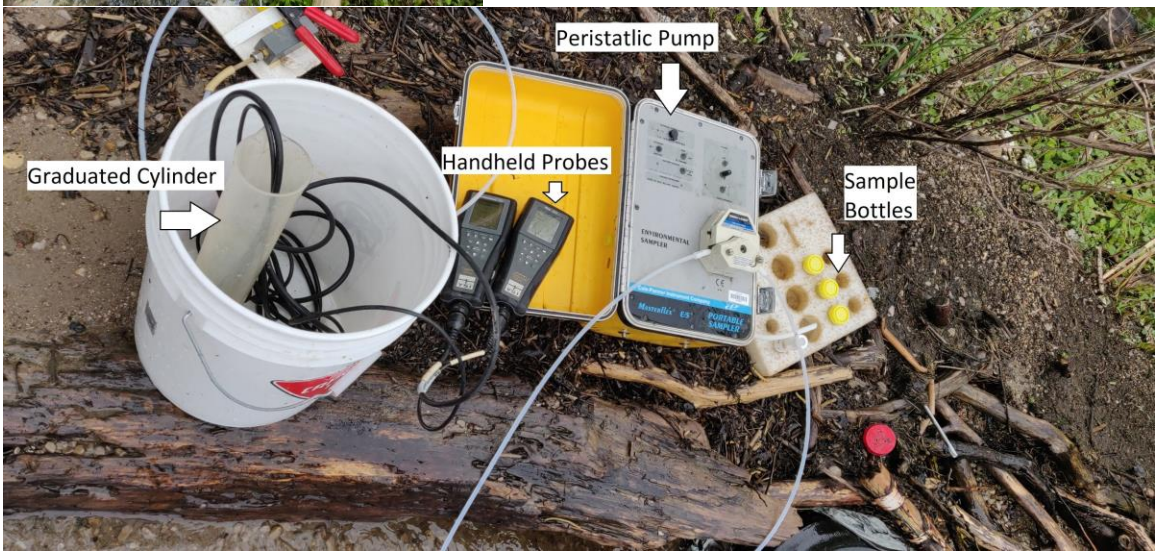

Figure 4.3: Photo of part of the mini-profiler system. Photographed here is the peristaltic pump with tubing leading from the mini-piezometer or solution sampler to the graduated cylinder. The graduated cylinder is where handheld probes can measure groundwater and surface water parameters. Sample bottles wedged in a Styrofoam tray are also pictured here.

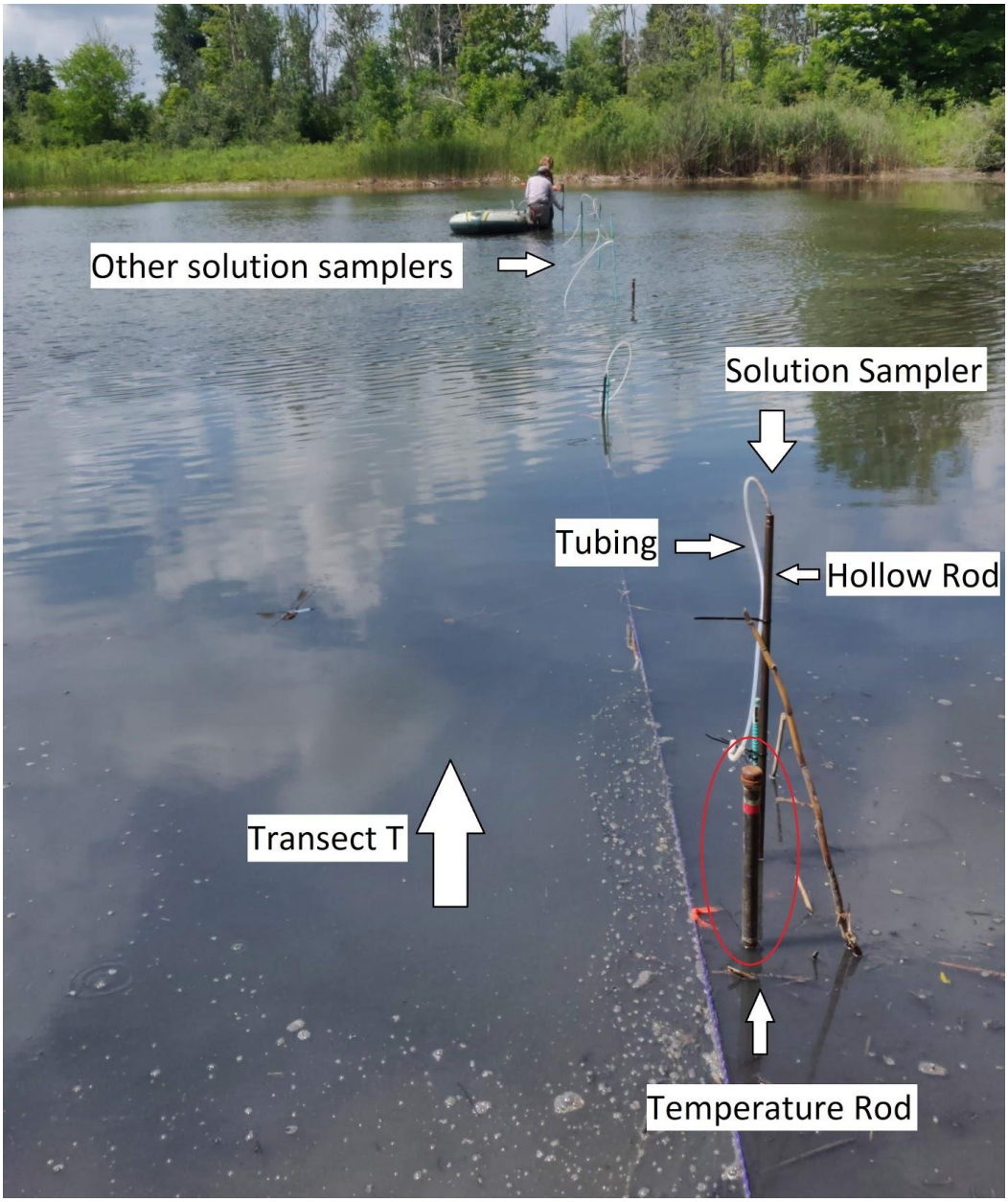

Figure 4.4. Photo of Transect E-W and the semi-permanent solution samplers. Solution sampler's metal hollow rod is sticking out of the pond surface, along with tubing that gets hooked onto a peristaltic pump (see Figure 4.3). Temperature rod sticking out of the pond surface (circled in red, schematic diagram below).

Table 4.1. Dates of sampling groundwater in 2019. Screening used a temporary mini-profiler system (drive point system) with more limited parameters, and campaigns used a permanent drive point system.

Dates of Sampling	Type of Sampling	Parameters/Analyses Conducted	No. of Locations
31-May	Screening for Transect N-S	NH_4^+, EC, Anions, SRP, Artificial Sweeteners (AS)	12
26-Jun	Screening for Transect N-S (WS7 to WS10)	NH_4^+, EC, AS	4
11-Jul	Screening for Transect T	NH_4^+, EC, AS	17
22-Aug	Campaign 1 for Transect N-S and Transect T	NH_4^+, EC, Anions, SRP, AS, VOCs, Dissolved Metals, PFAS, Alkalinity	15
29-Aug	Additional location sampled along Transect N-S (WS11)	NH_4^+, EC, AS	1
9/10-Dec	Campaign 2 for Transect N-S and Transect T	NH_4^+, EC, Anions, AS, VOCs, Dissolved Metals, Alkalinity	13

4.2 Surface Water Sampling

Approximately every month (during each of the two sampling campaigns, and periodically in between), surface water samples were collected at the outlet and pond edge (Figure 4.1). Surface water samples were collected by drawing stream water up through a syringe and then inputted into sample bottles. For some analyses, the stream water was filtered. Oftentimes, only ammonium and artificial sweeteners were sampled in between the sampling campaigns. Surface water samples were handled and stored similarly to the groundwater samples, as described below.

4.3 Water Sample Handling and Chemical Analyses

Collected samples were placed into a cooler with ice packs during transport, and then refrigerated or frozen until analysis. The sample handling details for the groundwater and surface water samples are listed in Table 4.1. Analyses were performed in Environment and Climate Change Canada labs at the Canada Centre for Inland Waters (Burlington, ON). SRP was measured with a Thermo Scientific Evolution 160 spectrophotometer using a mixed reagent of ammonium molybdenate and antimony potassium tartate (absorbance measured at 885nm). Ammonium was analyzed using a Beckman Coulter DU 720 general purpose spectrophotometer and a phenolhypochlorite reagent (absorbance measured at 640 nm). A set of 71 VOCs, largely chlorinated solvents and petroleum compounds were analyzed with a Teledyne Tekmar Aquatek 70 autosampler, a Teledyne Tekmar 3100 sample concentrator purge and trap, an Agilent G1530A gas chromatograph, and a HP/Agilent 5973 mass selective detector. Anions were analyzed with a Dionex 2500 ICS ion liquid chromatography system. Trace metals and cations were analyzed using Inductively Coupled Plasma-Sector Field Mass Spectrometry (ICP-MS, NLET methods #2003) at the National Laboratory for Environmental Testing. Alkalinity was analyzed using HACH digital titration method 8203 with 1.6 N H_2SO_4. AS were analyzed with a Dionex 2500 ICS ion liquid chromatograph system combined with an Applied Biosystems AB Sciex QTrap 550 triple quad mass spectrometers (IC/MS/MS). PFAS were extracted using weak-anion exchange (WAX) solid phase extraction (SPE) and then analyzed using ultra high-performance liquid chromatography tandem mass spectrometry (UHPLC-MS/MS).

Table 4.2. Details on water sample handling and storage. Detailed list of compounds analyzed can be seen in Table A2 and Table A1 for PFAS.

Analyte	**Volume Collected / Bottle Type**	**Filtration (polyethersulfone membrane filter)**	**Preservation and Storage**
PFAS (27 compounds, Table A1)	0.5L polyethylene - MEOH rinsed	None	Stored in fridge 4℃
Dissolved metals (50 compounds, Table A2)	125ml polyethylene	0.45µm	pH < 2 with nitric acid 70% (M=15.8), stored in fridge 4℃
Anions (7 compounds, Table A2)	30ml polyethylene	0.45µm	Stored in fridge 4℃
Ammonium	30ml polyethylene	0.45µm	pH 5-6 with 10% hydrochloric acid; frozen until analyzed
Artificial Sweeteners (11 compounds, Table A2)	30ml polyethylene	0.45µm	frozen until analyzed
Volatile Organic Compounds (71 compounds, Table A2)	40ml glass with septa	None	pH <2 with NaHSO4, no headspace, stored in fridge 4℃
Soluble Reactive Phosphorus	40 ml glass	0.45µm	Stored in fridge 4℃
Alkalinity	125ml polyethylene	None	Stored in fridge 4℃

4.4 Water Level and Flow Measurements

4.4.1 Stream Discharge

The stream discharge at the outlet of the pond, which exits via a drain and attached culvert, was determined by stream gauging using the midpoint method (Turnipseed and Sauer, 2010). The vertically averaged velocity was measured every 5 cm across the culvert by moving the flow meter (Global Water Model FP101; range of 0.1-4.5 m/s, accuracy of 0.03 m/s) up and down the full water depth. However, measurements after August were incorrectly done at the edges of the culvert, with depth measured to the sediment bottom while velocity was averaged to the culvert bottom. These depth readings were adjusted based on previous measurements of the distance between the sediment bottom and culvert, assuming any erosion of the sediment was negligible, for which there was no visual evidence over the study period. Still, these discharge values likely had slightly greater uncertainty.

At times of lower flow, discharge measurements suffered from having too many velocity values below the quantifiable limit, approximately 0.4 m/s. These values register as 0 m/s and were typically assigned that value in the discharge calculations. Therefore, the discharge calculated could be underestimated. To test this, discharge was calculated in two ways, with the 0 m/s readings assigned 0 m/s and 0.4 m/s. The percent difference between the original discharge to the adjusted discharge was then calculated, with values 10% or less signaling an acceptable set of measurements. A 10% or greater difference raised concerns because it meant that the measurements did not capture all the flow, and

so these measurements were omitted. The uncertainty was likely higher for these smaller but acceptable discharge values, though.

The rating curve was calculated by plotting stage level (described below) and discharge from the outlet from the same time. The rating curve would provide interpolation of outlet discharge between manual discharge measurements for all continual stage measurement times. Unfortunately, there was too much variation and uncertainty in the data to provide a reliable rating curve. The discharge was plotted with pond level data as well to see if the curve would improve with this water level data set, but it was still not reliable.

4.4.2 Piezometers and Water Levels

Three piezometers were installed along Transect E-W using direct push methods and hand augers (Figure 4.5). The east piezometer, made of PVC plastic and fully screened, was installed July 30, 2019. The middle and west piezometers were made of stainless steel with a 25 cm screen length at the bottom and were installed on August 1, 2019. Each piezometer had a pressure transducer (Micro-Diver©, Van Essen) installed near the bottom of the screened section. The Micro-Divers were tied with a fishing wire that was then attached to the cap or top of the piezometer. These Micro-Divers were set to log pressure (to be converted to water levels) and temperature every 15 minutes.

A pressure transducer (Solinst) was installed into the stream at the outlet (end of culvert) on July 4, 2019 to monitor the outlet stream stage. The transducer was placed into a slotted PVC pipe that was pushed into the streambed. The outlet pressure transducer measured and logged total pressure, temperature, and electrical conductivity every 15

minutes. Another pressure transducer was installed on July 4, 2019 in the middle of the pond (Figure 4.1) to measure changes in pond level. In addition, a Micro-Diver was installed in one of the on-site monitoring wells (Well 18R) on October 23, 2019 to monitor pressure and temperature every 15 minutes at greater depths but still within the shallow groundwater flow system. Well 18R is around 65 m northeast from the pond, and has a depth of 5.7 m from the ground surface (WSP, 2018).

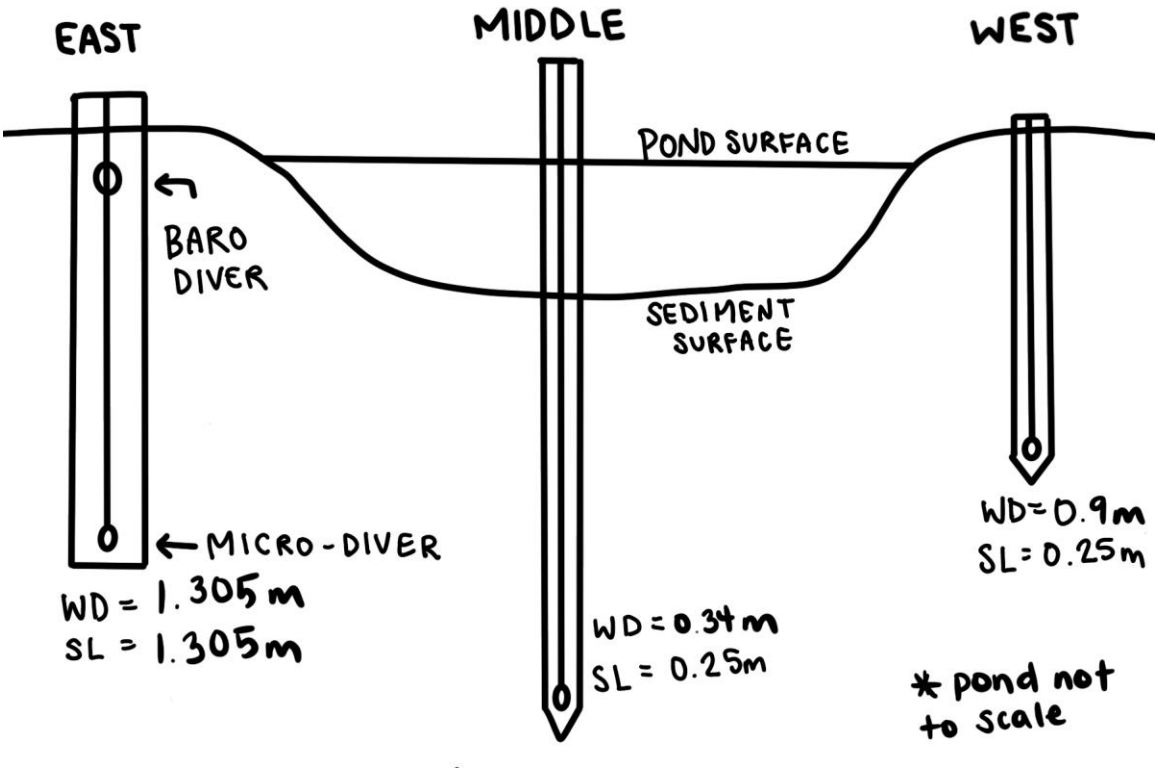

Figure 4.5. Schematic diagram of piezometers across Transect E-W. Installed with barometric diver and micro divers (depicted as ovals at the bottom of each piezometer). WD = well depth below ground surface, SL = screen length. Well depths and pond are not to scale.

All the pressure transducers required barometric pressure compensation to convert the measured pressure to water head level. A barometric pressure logger (Micro-Diver) was deployed July 4, 2019 on the north side of the pond but was lost due to vandalism. Consequently, for the period from July 12 to September 12, 2019, barometric pressure from a barologger near the city of Woodstock (~17 km away) was used instead. A second Micro-Diver was installed on-site on September 12, 2019 at the top of the east piezometer to measure barometric pressure (Figure 4.1). The barometric data from the east piezometer ended on May 19, 2020 (memory full but could not retrieve the data due to COVID-19 travel restrictions), so barometric data from a weather station nearby was used (Delhi; ~22 km) from May 20, 2020 to June 27, 2020. There were slight differences between the different barometric data sets as their locations were different. The average pressure difference between the off-site and on-site location for overlapping time periods was used to adjust the off-site barometric pressure such that it better represented the conditions at the HB site. To assess potential pressure sensor drift, water levels for the piezometers around the pond were periodically measured using a water level tape (Heron Instruments dipper-T), around the same time the Micro-Divers were being downloaded.

During the screening assessments, a hydraulic potentiomanometer (see Winter et al., 1988) was used at most sampling locations to determine local vertical hydraulic gradients. The potentiomanometer was connected to the polyethylene tubing (Masterflex) hooked up to a peristaltic pump. One end of the tubing was attached to the mini-profiler system installed in the sediment bed and the other end was connected to a steel drive point submerged in the pond surface water. With one end in the groundwater and one end

in the surface water, the potentiomanometer was therefore hydraulically connected to the groundwater and surface water. A vacuum was created in the potentiomanometer, drawing water up into the two clear tubes representing either the groundwater or surface water, while still maintaining the head difference between the two. The dominant system would fill the corresponding tube more.

4.5 Temperature-based Groundwater Measurements

4.5.1 Temperature Depth Profile for Groundwater Flux

Vertical temperature profiles required for calculating groundwater flux at a given location were measured using temperature rods equipped with five Thermochron iButtons (Figure 4.6). Seven temperature rods consisting of 3/4" iron rods 152 cm long with a tapered point (as in Fitzgerald et al., 2015) were installed, each near a solution sampler. More specifically, five were installed along Transect E-W, and two additional ones along Transect N-S (Figure 4.1). The rods were installed manually using a sledgehammer and driven down to a depth of 76.5 cm below the sediment surface (excluding low-density sediments on top) for temperature rods TR-T31, TR-WS1, and TR-T13 and 86.5cm below the sediment surface for temperature rods TR-T3, TR-WN4, TR-T43, and TR-T66. Wooden dowels attached by fishing line were used to space the iButtons at known depths. The first four iButtons for all rods were installed at depths of 0.3 cm, 9.9 cm, 19.5 cm, and 39.1 cm below the sediment surface. For some rods, the fifth and deepest iButton was installed at 78.7 cm while others were installed at 88.7 cm below the sediment surface. These iButtons were set to log temperature readings every 15 minutes and had an accuracy of 0.125ºC. There were two possible settings for the iButtons resolution: 0.5°C

for 8 bit, and 0.0625°C for 11 bit. Unfortunately, the lower resolution setting was accidentally chosen. The iButtons were removed every few months to download the data, and then were replaced in the same position in the same rod.

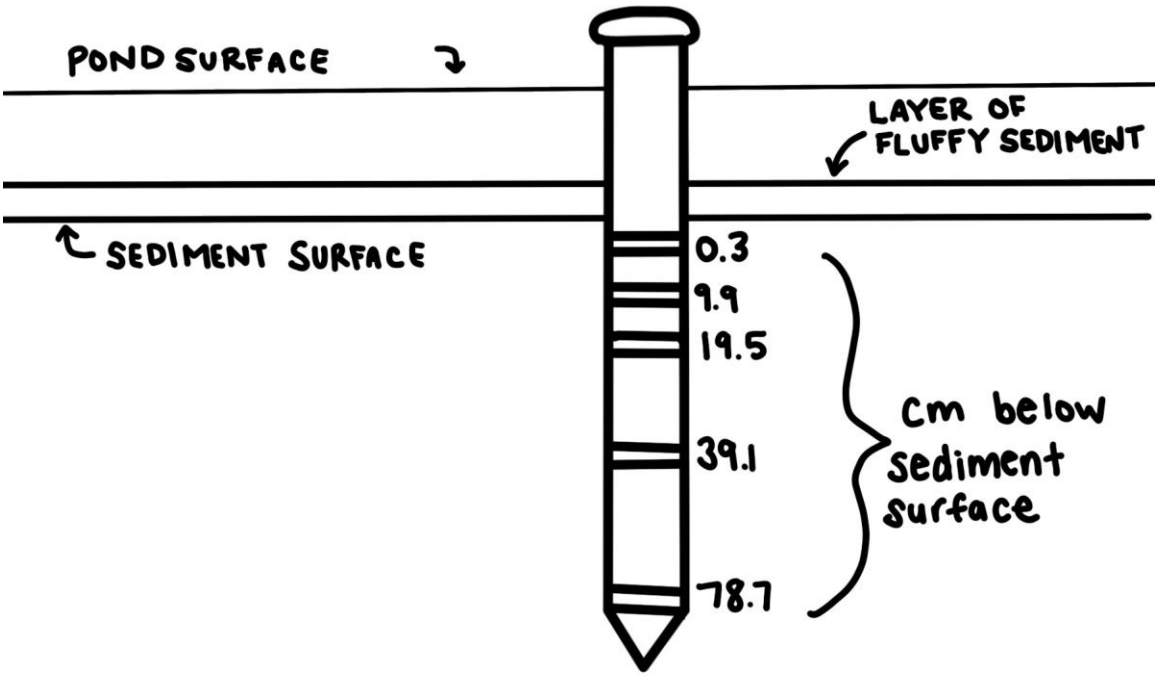

Figure 4.6. Schematic diagram of a temperature rod equipped with 5 iButtons. In reference to the sediment surface.

The iButtons were calibrated all together relative to a single "master iButton" before initial deployment and following the final download. The comparison of the two calibration values showed that there was little or no drift in temperature for all the iButtons. Therefore, only the first calibration value was used for the entire period. There is a gap in the continual data between November 2019 and April 2020 because the pandemic prevented the downloading of data before it was overwritten.

Groundwater flux was calculated from the temperature profile for each temperature rod using an analytical model called FLUX-LM. FLUX-LM is an Excel solver by Kurylyk et al. (2017) which estimates vertical 1D fluxes using a point in time or constant in time temperature depth profile (and saturated sediment thermal conductivity). The "LM" stands for layered media which means it can calculate the flux for horizontally layered porous media too. Here, it was assumed that there was only one layer within the pond sediment covered by the temperature rods. This solution is based on a steady state equation by Bredehoeft and Papadopulos (1965) in which the solutions are either positive (indicating discharge) or negative (indicating recharge) groundwater flux. Bredehoeft and Papadopulos' (1965) solution is best used when there is a lack of diurnal oscillations in temperature signals. Here, data with a diurnal signal was processed with a 24 hour moving average to emulate the quasi-steady state, as suggested by Kurylyk et al. (2017). Bredehoeft's solution requires a measurable contrast between surface water and groundwater temperatures, so it may not be applicable for extended periods in the spring and fall season in temperate climates, including this site. It is best to encompass as many sequential days with a steady temperature trend as possible. Some parameters are set within the model, such as the volumetric heat capacity of water, and the thermal conductivity of the sediment. Thermal conductivity (W/m ℃) was set at 1.77 W/m ℃ which is within the range for sand to sandy gravel to sandy loam based on values reported in Lapham (1989). However exact conditions from each location will vary. Note that fluxes with an absolute value less than 10 m/yr (i.e., whether discharge or recharge conditions), had an essentially linear profile (considering the uncertainty in the

temperature data measurements) and cannot be quantitatively distinguished, nor the actual direction of flow determined.

A benefit of using FLUX-LM is that it does not calculate the flux within the context of the sediment but within the boundaries of the depth measurements provided. Therefore, it negates the issue of having to know the exact positions of the iButtons below the pond sediment surface, meaning minor erosion and sedimentation will not negatively impact the results, unless an iButton is no longer within the sediment or within its assigned layer. In this study, the top iButton (0.3 cm depth) was positioned right at the top of the denser sediment, and so was potentially not representing the layers sediment conditions. Therefore, the groundwater flux and the associated root mean square error (RMSE) was calculated for the full profile with the top iButton and for the profile without the top iButton. The flux (with or without the top iButton) with the better RMSE was applied for the calculations and assessments.

Figure 4.7. Photograph of a space in between each dowel segment used to hold iButtons and separate them at discrete depths in the temperature rods.

4.5.2 Temperature Mapping

Measuring temperature just below the sediment surface can map zones of higher groundwater discharge. Temperature mapping is because groundwater is colder in summer and warmer in winter than the pond water above. Here the sediment temperature was measured using a handheld thermometer with a 10 cm probe pushed into the sediment (temperature made at its tip). The sediment temperature was mapped on July 11, 2019 and December 10, 2019 along Transect E-W at each solution sampler location (Figure 4.1). On July 4, 2019, sediment temperature was also mapped along the north

portion of Transect N-S (19 m total) at every one meter starting at location WS1 (Figure 4.1). At each meter along Transect N-S the sediment temperature was measured 0 cm, 30 cm, and 60 cm perpendicular to the east shore. While temperature mapping, the surface water temperature was also measured for comparison.

4.6 Sediment Property Measurements and Calculations

Sediment samples were collected from cores removed prior to installation of the east and west piezometers for grain size distribution analysis (Figure 4.1). Due to the pandemic restrictions on laboratory access, the sediment collected was not able to be analyzed. However, personal observations of sediment properties were recorded. Additionally, due to the coarse material, a sledgehammer was used to install the metal piezometer for around 130 cm of the piezometer depth.

4.7 Electrical Conductivity Monitoring

Three HOBO Saltwater Conductivity/Salinity Data Loggers were installed north of Transect E-W at approximate distances of 10 m, 20 m, and 40 m from the east shore (Figure 4.1). All three loggers were programmed to measure electrical conductivity and temperature every 15 minutes. The loggers were collected to download data onshore every few months and then returned to their original positions. There was no data after February 10, 2020 because the loggers' memory storages were filled, and it was not possible to download and clear space due to COVID-19 travel restrictions. An equation from Hayashi (2004) was used to correct the electrical conductivity to a standard temperature of 25°C (resulting in specific conductance).

5.0 Results and Discussion

5.1. Sediment Observations

The shallow soil was observed during coring prior to piezometer installment at the east and west shores. A rough classification at each location was determined based on personal observations. The east piezometer location (Figure 4.1) had topsoil for the first ~30 cm, which progressed into silty sand for the next ~100 cm, and then transitioned into a sandy gravel layer making it difficult to manually dig deeper. The west piezometer (Figure 4.1) subsurface consisted of mostly large pebbles with a sandy matrix for the full depth of the piezometer (91 cm). These observations fit with those reported in the WSP 2018 landfill report.

5.2 Groundwater - Pond Flow System

5.2.1 Water Level Measurements

Continuous measurements of the water levels of the pond, piezometers and monitoring well (locations shown in Figure 4.1, 3.1, respectively; associated depths given in Table 5.1) are shown along with daily precipitation data obtained from a nearby weather station (Delhi; ~22 km from the site) in Figure 5.1 and 5.2. There was a plan to survey the elevations of each monitoring level in Spring 2020, but due to COVID-19 travel restrictions it could not happen. The elevation survey would have allowed for quantitative comparisons of hydraulic head levels between each location. Therefore, it was only possible to compare relative temporal patterns between each location, noting that historic data (WSP, 2018) and measurements of this study (Sections 4.3.2) do indicate groundwater flow to and discharge into the pond.

There were several issues that affected some of these water level data sets that must first be mentioned. The pond level and the west piezometer had a maximum stage level limit imposed by either the pond outlet drain or the water level reaching the top of the piezometer (approximated by horizontal red line in Figure 5.2), respectively. Another issue came up with the diver in the middle well. From September 26, 2019 to November 15, 2019 the diver read erroneously, and the cause is unknown. The Micro-Diver was installed in Well 18R on a later date (October 23, 2019) compared to the other divers. Additionally, there was a problem with the barometric pressure compensation during the winter season as the barometric diver appeared to have had a measurement lag during precipitation events. The measurement lag could have been because of a slow response to changes passing through snow covering the well cap, although this is uncertain. The barometric error was depicted by sharp dips in the data during the winter in 2020. However, this discrepancy was not seen in the east piezometer data because the barometric diver was located within the same piezometer, and therefore both probably experienced the same lag from snow covering the well cap. Finally, there were occasional sharp increases in the east piezometer water level of 10-20 cm (i.e., August 18, September 11, October 2, October 16; Figure 5.1), which occurred during precipitation events. These responses are attributed to overland runoff flowing down into the fully screened piezometer.

Continuous measurement of outlet stream stage was also measured, and outlet stream discharge was measured (2-20% uncertainty) periodically throughout the year (Figure A1). Unfortunately, the measured outlet discharge did not produce a useful rating

curve for interpolating the outlet discharge over the year. However, the measured outlet discharge appeared to increase towards the winter season, similar to the pond level. The stream stage did not follow trends found in the pond level from winter 2019 to summer 2020. Perhaps there were changes that happened at the stage area (culvert outlet), which altered the stage positions or sediment bottom topography and caused this discrepancy.

The water levels at each location displayed similar seasonal trends with a lower level in the summer and the highest level in the wintertime (Figure 5.2). This seasonal trend reflected greater evaporation and evapotranspiration occurring in the summer, while precipitation had no strong seasonal pattern. The seasonal ranges of each water level are summarized in Table 5.1. The pond water level had a seasonal range of ~30 cm while the seasonal range on the east shore had a range of ~40 cm, which indicates that the hydraulic gradient from the onshore piezometers to the pond is greatest in the wintertime. Well 18R has a seasonal range of over one meter which is corroborated with past annual measurements by the 2018 landfill report (Figure C-6; WSP, 2018).

Contrary to the east piezometer, the west piezometer decreased in water level throughout the summertime rather than remaining steady and increased earlier through the fall (Figure 5.2). Likely, the differences between the east and west piezometers indicate different groundwater flow systems, with different behaviours, affecting the east and west sides of the pond.

On a shorter timescale there were daily fluctuations in the water level signals for all locations except for the deeper monitoring well, Well 18R (Figures 5.1 and 5.2). The timing of the peaks and dips for each location are summarized in Table 5.2. Figure 5.3

depicts the diurnal pattern in water levels for the pond, east piezometer, and middle piezometer from August 4 to 8, 2019, when the diurnal signal was strongest. Generally, the water levels increased throughout the night and were at their lowest during the mid-afternoon. The magnitude of the diurnal fluctuations decreased and eventually disappeared in late fall, and slowly increased again in the spring (Figures 5.1 and 5.2). These patterns suggest that these daily fluctuations found in the data were associated with evaporation directly from the pond surface and possibly also with evapotranspiration from the nearby surrounding terrestrial plants (Rosenberry et al., 1999). Plant activity was highest during the afternoon and induced terrestrial plants to take up soil water and potentially groundwater, reducing groundwater head levels for shallow water tables. The uptake of water from the plants could reduce the hydraulic gradient to the pond and, therefore, the total groundwater discharge into the pond, potentially adding to the daily fluctuation in pond level. However, the fluctuating pond level would influence the hydraulic gradient and could be the cause of the fluctuations observed in the three piezometers. To facilitate a closer comparison, the pond and piezometers water levels were normalized to the mean in Figure 5.3. The west and middle piezometers closely followed the pond level (Figure 5.3) suggesting that they are influenced by the same factor (pond evaporation). Compared to the other piezometers and pond level, the east piezometer showed the greatest range in daily fluctuations, which indicates another factor, likely evapotranspiration from nearby terrestrial plants, is affecting it. Greater evapotranspiration losses may be expected at the east shore piezometer location, given there is dense vegetation and a shallow water table. Diurnal signals were not detected for

Well 18R, likely because the water table was much deeper than the roots zone of influence.

The pond and piezometer water levels also showed response to precipitation and snowmelt events (Figures 5.1 and 5.2; Table 5.1), again with the east piezometer being the most responsive and likely indicating recharge to the shallow water table. Well 18R had a less flashy response to precipitation events, likely because the recharge water would have to percolate through a greater depth of sediment, and the flow patterns may change as the aquifer is adjusting to recharge input.

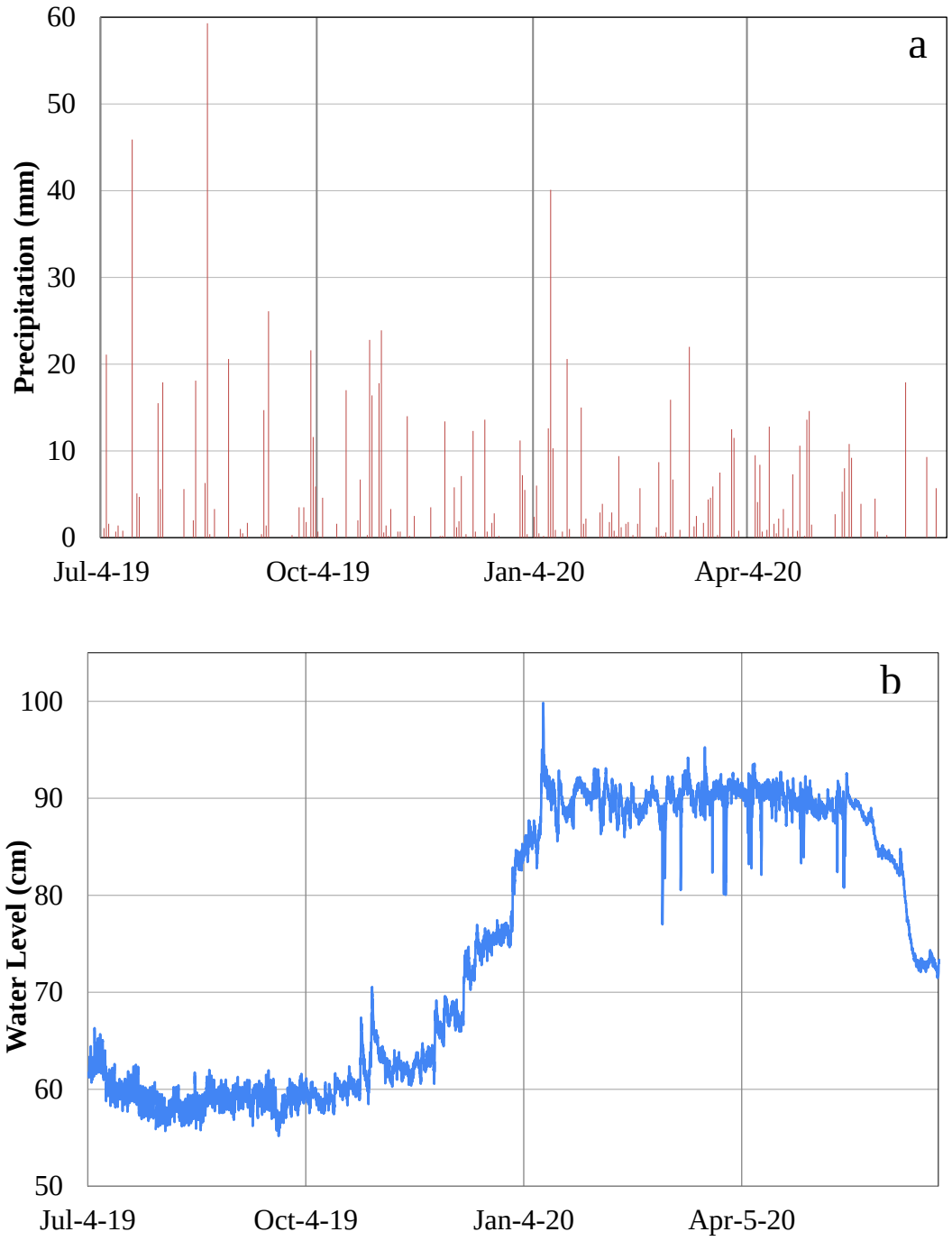

Figure 5.1. a) Precipitation (cm) b) pond water level (cm) over time. Steep declines in water level data are due to problems with barometric pressure compensation for the winter (mentioned above).

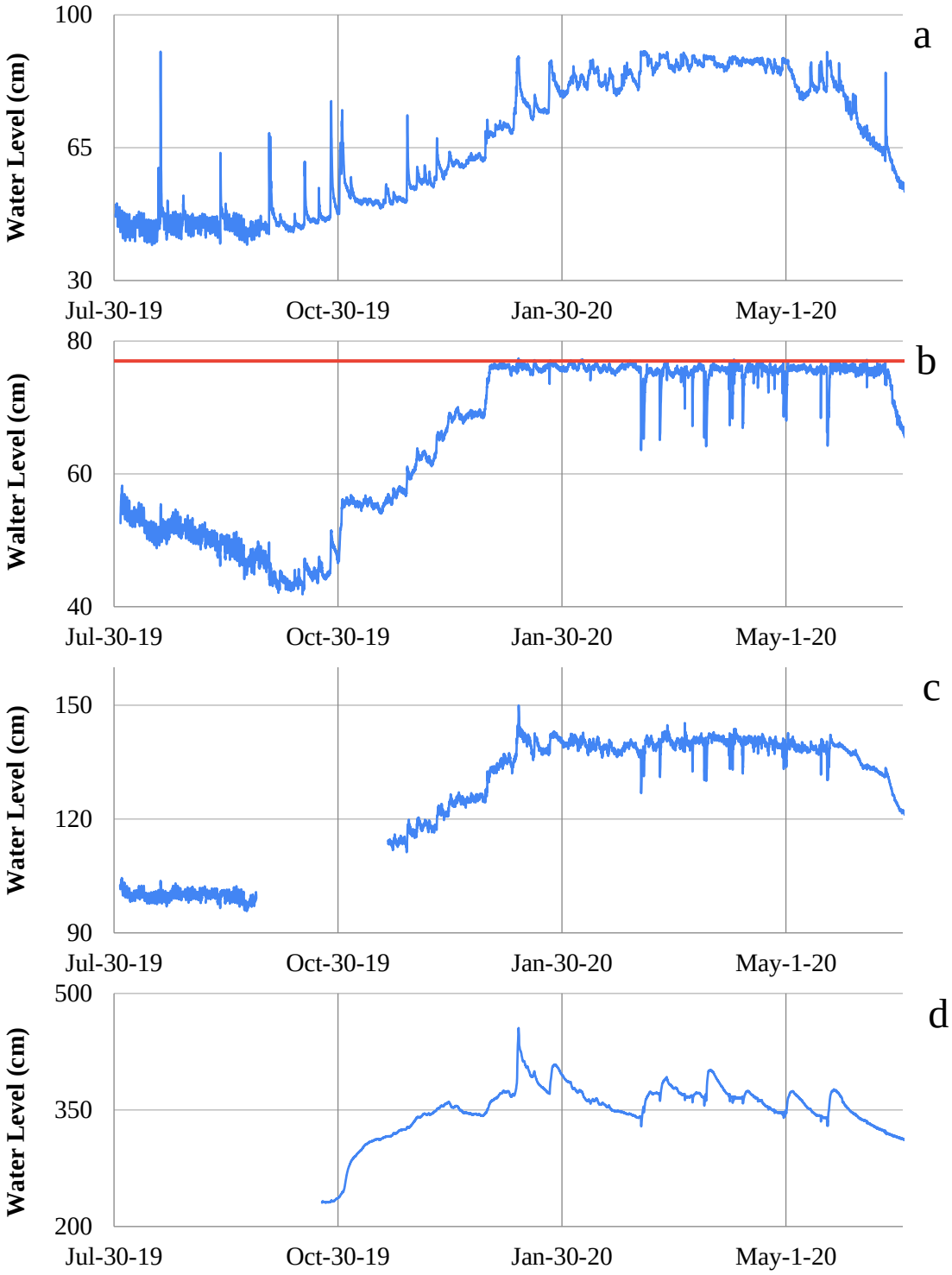

Figure 5.2 Water levels (cm) measured over time. a) east piezometer b) west piezometer c) middle piezometer d) Well 18R (see Figure 4.1 for locations). The maximum height in the west piezometer is indicated by a red line (~75 cm) in which the water level reaches in January 2020.

Table 5.1. Summary of water level responses or fluctuations at the diurnal (in August), seasonal, and event-based timescales. (*) indicates minimum value

Location	Depth Below Ground Surface	Aug 18 Rain Event	Jan 11 Rain Event	Feb 20-24 Snow Melt	Diurnal Signal	Time of Diurnal Signal	Seasonal Range
Outlet		15cm	7cm	1.5cm	2cm	7am - 7pm*	15cm
Pond		5cm	8cm	2cm	4cm	7am - 3pm*	30cm
East	1.305m		9cm	6cm	6-8cm	8am - 4pm*	60cm
West	0.9m	6cm		1cm	3cm	7am - 2pm*	
Middle	0.34m	3cm	8cm	2cm	3-4cm	7am - 3pm*	53cm
18R	5.72m		72cm	-3.5cm			225cm

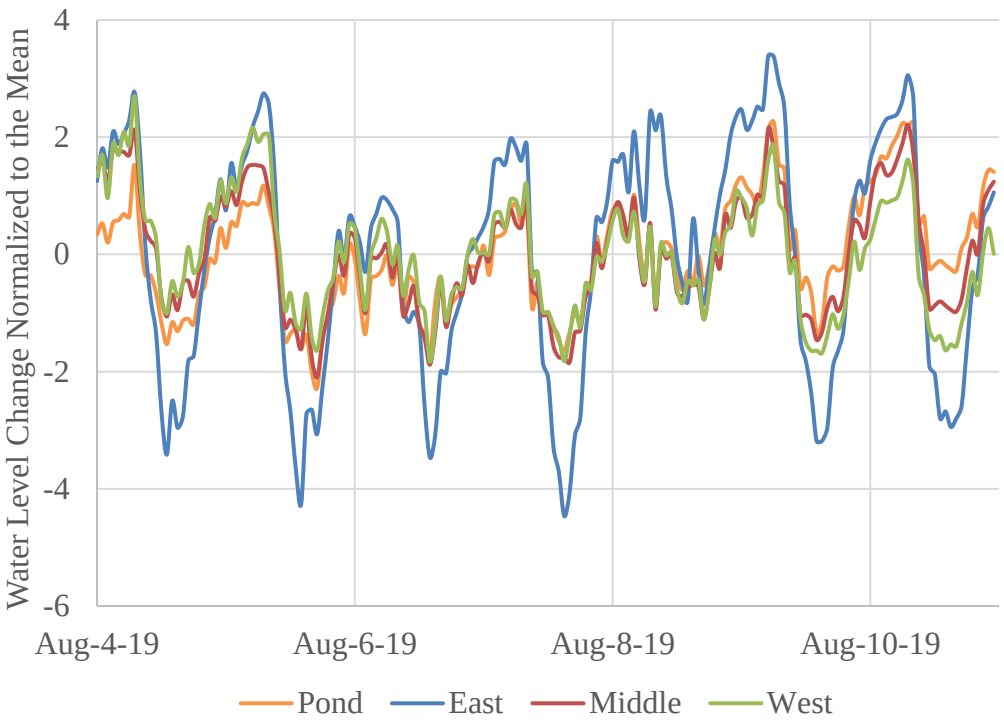

Figure 5.3. Illustrating water level fluctuations of east, middle, and west piezometers and the pond. See Figure 4.1 for locations. The red indicates a rain event of 5.6 cm on August 8, 2019. Data was normalized (each data set subtracted from its mean) for comparison purposes.

5.2.2 Groundwater Flow Direction and Flux

Potentiomanometer measurements between pond and groundwater hydraulic head levels can provide an indication of water flow direction across the pond sediment interface. The vertical hydraulic gradient was calculated by dividing this measured difference in hydraulic head (cm) by the distance between the measurements, which in this case is the depth below the sediment interface of the mini-profiler (cm). Figure 5.4 depicts the vertical hydraulic gradient at various positions across Transect E-W on July 11, 2019. All locations had a positive hydraulic gradient, which indicated a driving force for upward groundwater flow into the pond (i.e., negative flux, defining recharge conditions as

positive) at that point in time. The variation in hydraulic gradient may reflect variation in groundwater flux and/or hydraulic conductivity. Note that there was visual evidence of groundwater seeps along the east, west and north edges of the pond in the northern portion, most notably at location WN4 in Figure 4. The large groundwater seep at WN4 provided another indication of groundwater discharge to the pond in this general area. Seeps were not evident along the south shore.

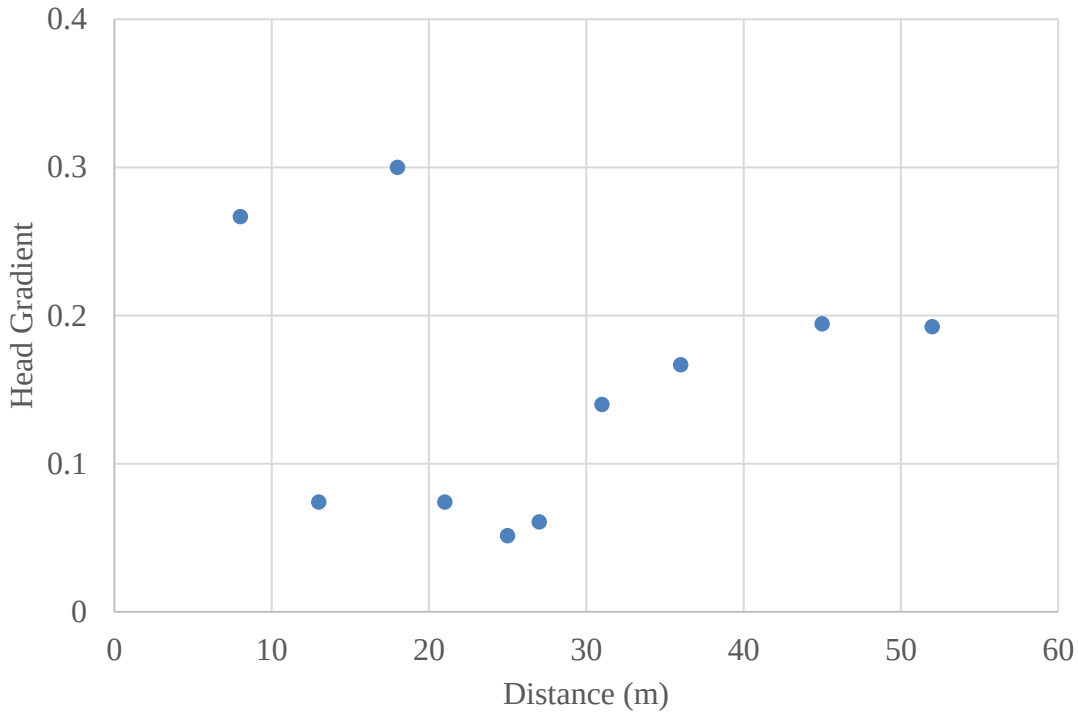

Figure 5.4. Hydraulic head gradient across Transect E-W (0 is the east shore) on July 11, 2019. Hydraulic head gradient (groundwater head - pond head) across the pond sediment interface calculated with potentiomanometer groundwater-pond head-difference measurements divided by depth of the mini-piezometer. Positive values indicate a driving force for upward flow conditions.

Sediment temperature was measured with a handheld thermometer probe, pushed about 10 cm into the subsurface. Sediment temperature measurements can provide indications of groundwater flow direction based on the premise that groundwater is cooler than the surface water in the summer and vice versa during the winter. The sediment temperature along the Transect E-W decreased towards the middle of the pond (~25-30 m positions) and increased towards the edges of the pond in summer, July 11, 2019 (Figure 5.5). Meanwhile on December 10, 2019, the sediment temperature was highest in a similar area, at around 18-27 m, though there was less of a range in sediment temperature due to the surface water temperature being like the ground water. The lower sediment temperature was in the summer and higher sediment temperature in the winter suggested a higher groundwater flux zone in the area around ~25 to 30 m position. Personal observations in summer indicated no other major cold spots existed for other parts of the transect in between the measurement points.

Sediment temperatures were also measured along a smaller section of Transect N-S on July 4, 2019 (Figure 5.6). Sediment temperature was measured every meter for 19 m starting at the WS1 position moving towards the north. Additionally, at every meter the sediment temperature was measured 0 cm, 30 cm, and 60 cm from the east bank. The sediment temperatures were overall less than the surface water temperature of 32.5℃ and decreased towards the north direction (Figure 5.5). Based on the geology of the landfill report, the shallow sediment extending from the landfill to the pond (around 5-8 m in depth) consisted of a sand and gravel layer suggesting high hydraulic conductivity,

resulting in potentially greater groundwater discharge (WSP, 2018). Therefore, it makes sense that the temperature decreased towards the north.

The temperature rods were designed to measure the vertical pond sediment temperature profile (iButtons at 0, 10, 20, 39, 79, and 89 cm depths) at 7 locations in the pond (Figure 4.1), with readings covering July 30, 2019 to November 19, 2019 and April 3, 2020 to June 26, 2020. An example of collected data for temperature rod TR-T3 is given in Figure 5.7. The calibrated dataset of each temperature rods was plotted over time in Figures A3a, A3b, A4a and A4b. Surface waters have greater seasonal variation because they equilibrate with the atmosphere (warmer in summer, cooler in winter). Whereas groundwater tends to stay at a constant temperature despite the changing seasons. During the summer months, the surface water was warmer than the discharging groundwater, and therefore the temperature decreased with depth. During the winter months, the surface water became much cooler compared to the groundwater, and therefore the deepest iButton was reading warmer temperatures compared to the iButtons closer to the surface. The curvature of the profile indicates the magnitude of the flux. A straight line (but not vertical) signifies heat transport by conduction is dominant, indicating that there is no or little groundwater flux. A substantial curvature indicates a greater flux in groundwater. The direction of the curve indicates whether the groundwater is recharging (concave up) or discharging (convex up). The fall and spring seasons were transition periods where the surface water and the groundwater were similar temperatures, resulting in a vertically linear profile (Figure 5.7). During these transitions, the flux cannot be determined from the temperature profile data. Additionally, shallow

groundwater may be influenced by daily fluctuations in surface water temperature. The deepest depth will experience the least influence from the overlying surface water which heats up throughout the day and cools at night. Higher groundwater discharge will limit the depth influenced by daily fluctuations.

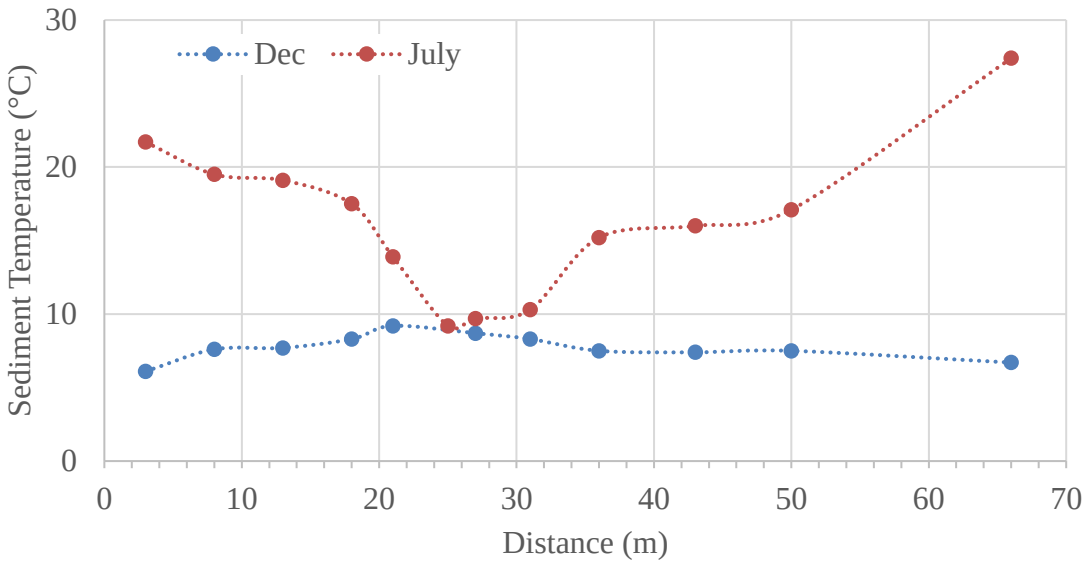

Figure 5.5. Sediment temperature at 10 cm depth plotted over distance along Transect E-W (0 m is east shore) for July 11, 2019 and December 10, 2019. Pond water temperature was around 27℃ and 4℃ on July 11, 2019 and December 10, 2019, respectively.

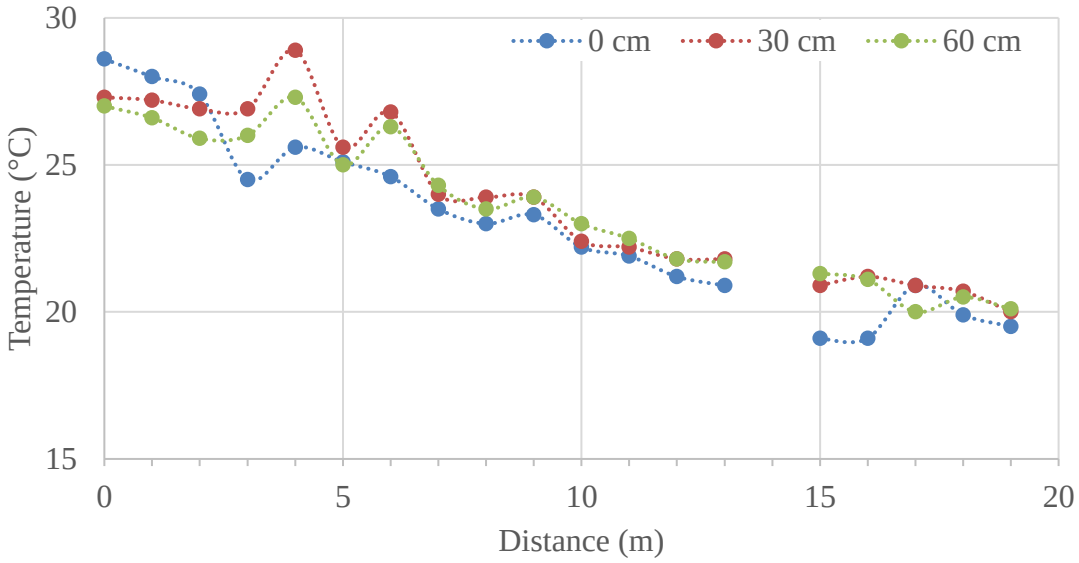

Figure 5.6. Sediment temperature at 10 cm depth plotted over short distance (north portion) along Transect N-S for July 4, 2019. Pond water temperature was around 32.5℃

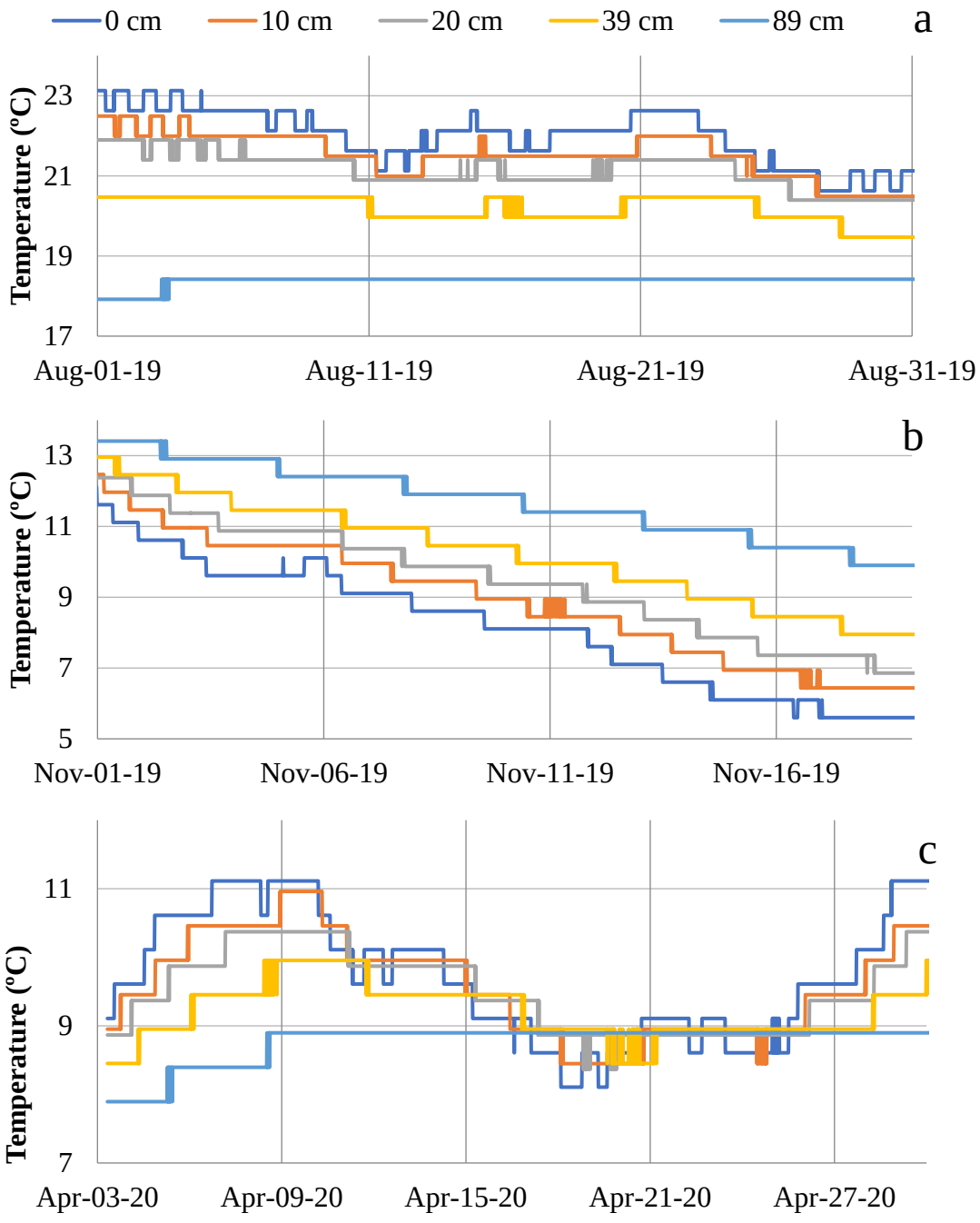

Figure 5.7. Temperature for 5 depths (0, 10, 20, 39, 89 cm) in the pond sediment measured using iButtons in the temperature rod TR-T3. a) August 1-31, 2019 b) November 1-19, 2019 c) April 3-30, 2020.

The set of plots in Figure 5.8 depict the average temperature depth profiles of each temperature rod for August (summer) and November (winter) 2019, respectively. Most notably, the profile for TR-T31 was almost vertical in both seasons and was colder in summer and generally warmer in winter compared to the other temperature rods, suggesting that TR-T31 was in an area with a very high discharge. TR-T31 was in the middle of the pond, and the area of high discharge matched with the sediment temperature mapping (cold spot in summer, warmer spot in winter). For the remaining rods, during the summertime, the profiles were cooler with depth, and vice versa for the wintertime. The temperature profiles were linear, however the general curvature for both seasons was convex upwards, which indicated upward groundwater flow. Some rods showed slightly more curvature than others, which indicated a greater groundwater flux.

Groundwater fluxes were quantified from the sediment temperature profiles using the FLUX-LM model (Kurylyk et al., 2018). FLUX-LM assumes a homogeneous, isotropic, fully saturated medium (or layers, but this was not done here) under steady-state heat transfer across a thermal gradient in the subsurface. Average groundwater flux was determined for time periods consisting of several days (typically 2-7 days). Only periods with stable average temperatures were used, typically indicated by the bottom iButton temperature not changing. It was not possible to do continuous time periods because of sudden changes to the profile caused by weather changes, or to assess the transition periods when the pond and groundwater were of similar temperature. Additionally, an average temperature for each iButton over one period was used to account for daily temperature fluctuations.

For much of the data there was an issue with the top (1st) iButton (i.e., at the sediment interface). The FLUX-LM model requires that the temperature decreases or increases monotonically with depth, but this was not always the case because of the top iButton. It was generally cooler than the 2nd iButton in summer. The reason for this is uncertain. Potentially the top iButton could have been positioned above the sediment or in the fluffy sediment layer, and the iButton was measuring the surface water temperature instead of the sediment temperature, with the latter experiencing more heating during the day from the sun. To accommodate this issue, two flux values per period were calculated, one including the top iButton and one excluding the top iButton (ignoring the top 10 cm of the profile). An example demonstrating a poor fit to the temperature profile in FLUX-LM (top iButton included), and a better fit (top iButton excluded) is shown in Figure 5.9. The root mean square error (RMSE) was used when deciding which output was more reliable. Generally, model outputs calculated without the top iButton had a lower RMSE.

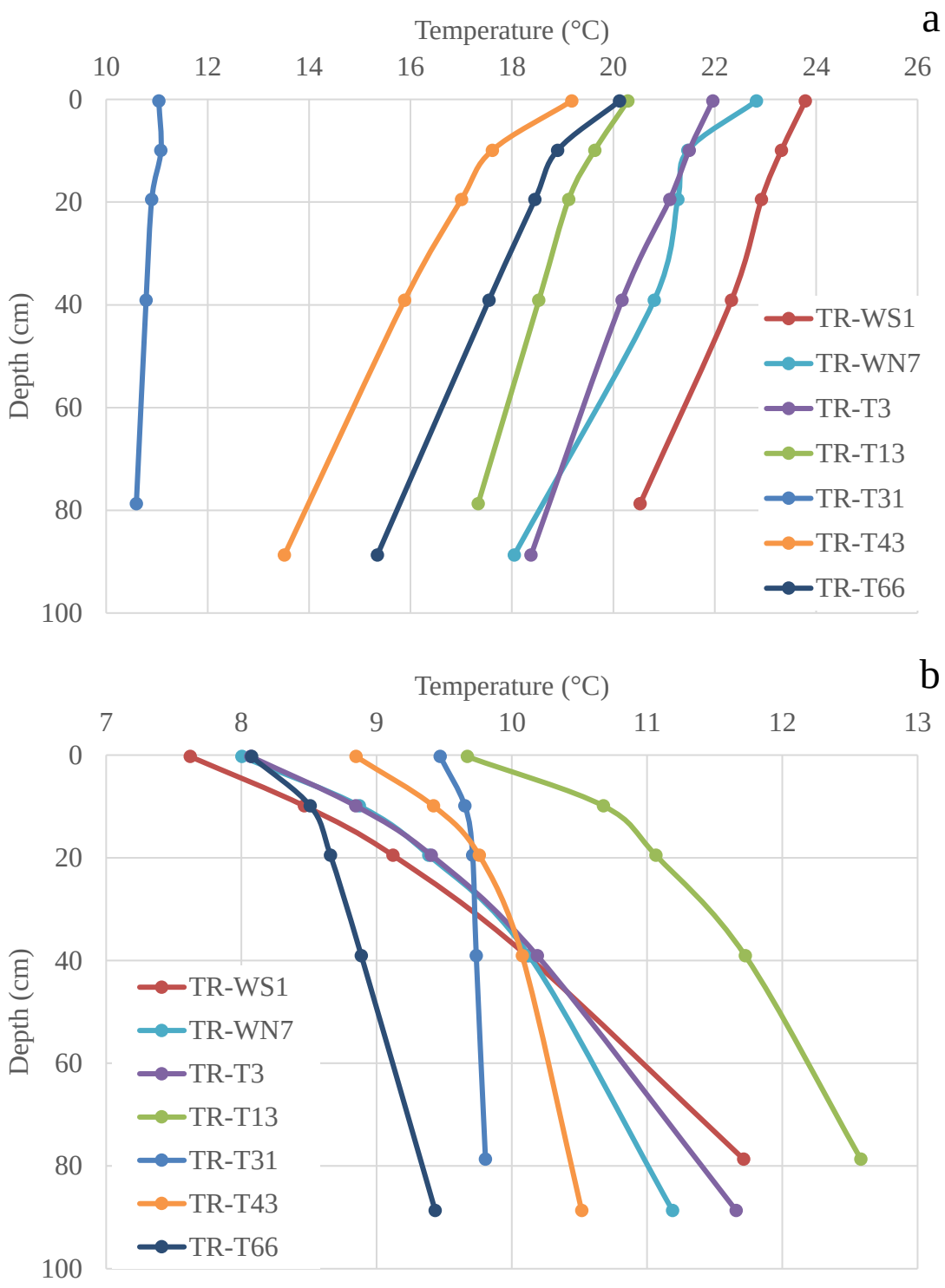

Figure 5.8. Monthly average temperature depth profiles for a) August and b) November for all temperature rods.

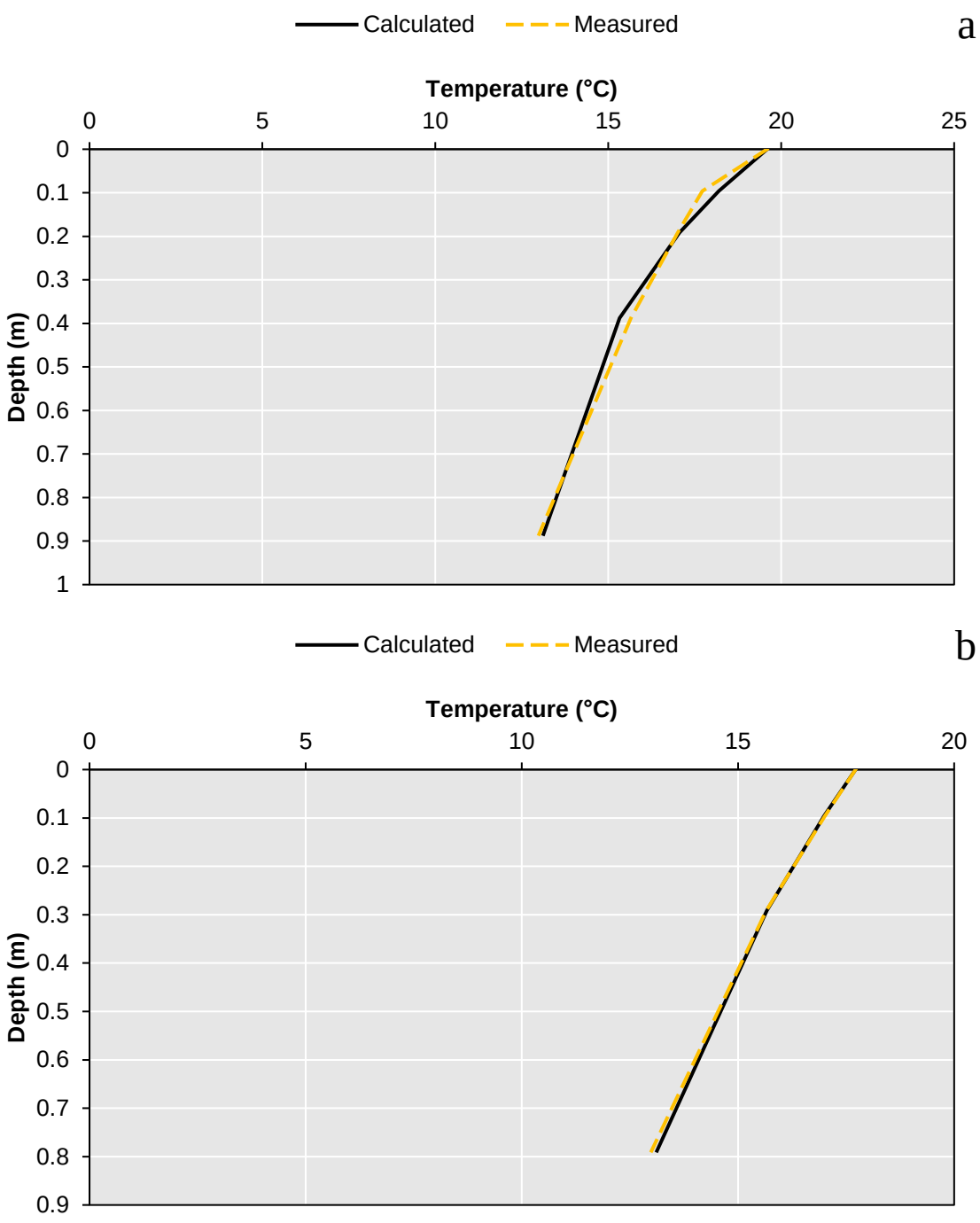

Figure 5.9. Measured temperature profile and FLUX-LM model output for TR-T43 for the period July 30-August 7, 2019. a) including the top iButton (RMSE = 0.26), and b) excluding the top iButton (RMSE = 0.06).

The flux is plotted over time for each temperature rod, except for rod TR-T31 (explained further below), to show temporal trends in the data in Figure 5.10. An RMSE > 0.1 was deemed less reliable and depicted as an open symbol. Around 90% of the flux was calculated without the top iButton and in only three calculations the RMSE was greater than 10%. The low fluxes within +/-10 m/yr, which have a linear profile and are essentially indistinguishable by the model, were depicted by the grey zone in Figure 5.10. Much of the data indicated low fluxes and were within the grey zone. Few locations depicted some recharge conditions, but most others suggested discharge dominant conditions. Generally, there were greater discharging conditions in the middle of the pond (around 31 m) than the edge.

It was difficult to clearly assess seasonal patterns due to limited data through spring and fall periods, but generally the highest discharge occurred in the winter months. TR-WN7 and TR-WS1 showed a temporal pattern in the flux, compared to the other temperature rods. When it was summertime, the flux at TR-WN7 and TR-WS1 were either low or recharging which makes sense when it is the dry season. During the cooler months there was higher discharge (Figure 5.10). The seasonal trends found in the temperature data corroborated with the seasonal pattern found in the water level data (low in summer, high in winter). For example, with TR-WN7, there was a decreasing trend as it got closer to wintertime. Then during the spring season, the transition to warmer temperatures, the fluxes were fluctuating around the x-axis (0 m/yr). TR-WS1 and TR-WN7 are near the edge and may be more affected by drawdown of the water table by

vegetation evapotranspiration (daytime) near the pond. Some rods such as TR-T13 had mostly negative (discharging) values which indicated a discharge zone.

The steep vertical temperature profile measured for TR-T31, indicated high groundwater discharge. FLUX-LM cannot easily determine the groundwater flux as one of the requirements of the model is a temperature gradient that changes monotonically with depth. Only two time periods worked with FLUX-LM, July 30 to August 8, and August 19 to October 8, and each gave a similar RMSE over a range of fluxes from -50 m/yr to -100 m/yr. For plotting purposes (Figure 5.11), the flux at TR-T31 will be assumed as -75 m/yr for the summer of 2019.

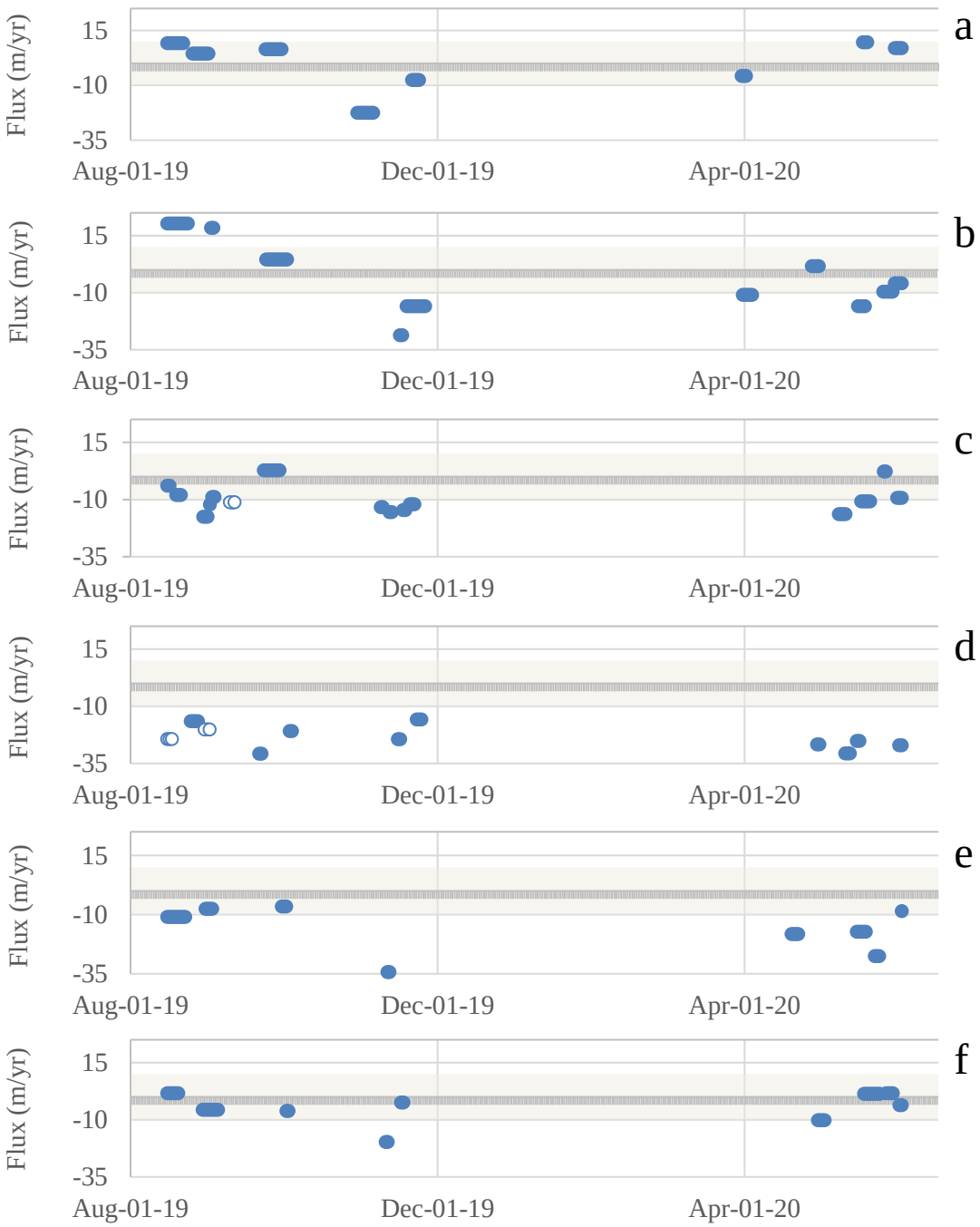

Figure 5.10. Groundwater flux values (negative value indicates discharge into pond) calculated with FLUX-LM (Kurylyk et al., 2018) plotted over time for each temperature rod, except for TR-T31. a) TR-WS1 b) TR-WN7 c) TR-T3 d) TR-T13 e) TR-T43 f) TR-T66 +/- 10 m/yr is the minimum threshold for quantification with this model (grey shaded area). Open symbols are for values with a RMSE value >0.1, while closed symbols are for values with RMSE <0.1. There is a missing data period from December 2019 to April 2020, due to loss of data (mentioned above).

Figure 5.11 includes the groundwater flux measurements along Transect E-W for three time periods (August to Mid-September, November, May to June), which had reasonably reliable data from FLUX-LM. Similar to the hydraulic gradient (Figure 5.4) there was indication of discharging conditions across Transect E-W. Additionally, the sediment interface temperature (Figure 5.5) and the groundwater flux depicted an increasing trend towards 25-31 m along Transect E-W. The groundwater flux then decreased towards the edges of the pond. The calculated flux showed a peak at 31 m during the summertime in 2019, but this high flux was not quantifiable, though likely higher, during other periods. Temporally, the groundwater flux was higher in the wintertime compared to the summertime.

The spatial coverage of groundwater flux calculated using the vertical temperature profiles was limited by only having seven temperature rods total, 4 across Transect E-W and 3 across Transect N-S. Therefore, the sediment interface temperature measurements discussed above were used to help interpolate the groundwater flux between the temperature rods. The sediment temperatures from July were plotted against the associated groundwater flux measured in August at those same locations (Figure 5.12). Then, a logarithmic trend line that best fit the data (R^2 value of 0.84) was used to calculate an interpolated groundwater flux at the remaining sediment temperature measurement locations, representing the summer conditions. The fit was poorer for the winter data (R^2 value of 0.32), likely because the surface water temperature is closer to the groundwater temperature, and therefore the contrast is less. The interpolated data revealed a greater area with higher discharge (25-31 m). It was also important to note that

flux patterns may be different between the measurement points, though no major discharge zones were believed to be missed. However, there could be discrete locations with high flux due to preferential flow.

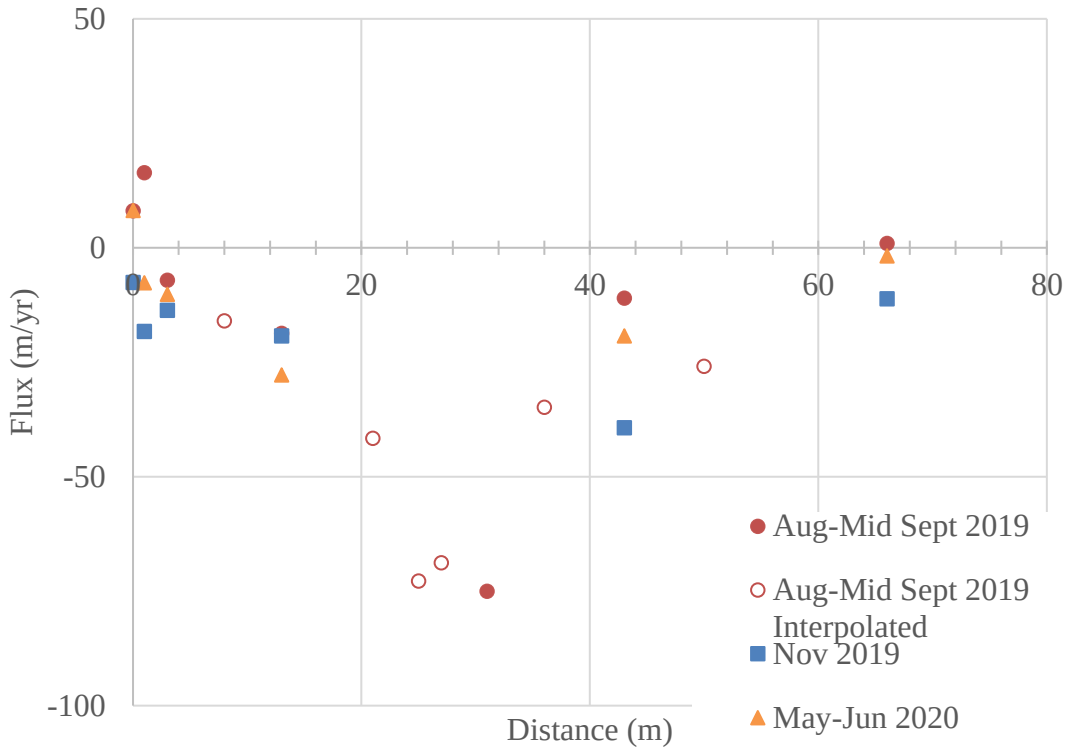

Figure 5.11. Seasonal average groundwater flux for August - Mid September 2019, November 2019, and May - June 2020 calculated using FLUX-LM, and including August - Mid September interpolated groundwater flux (from sediment temperature measurements), plotted with distance across Transect E-W. Note that the flux for 31 m is set at -75 m/yr for plotting purposes but ranges from -50 m/yr to -100 m/yr and is likely higher in the wintertime.

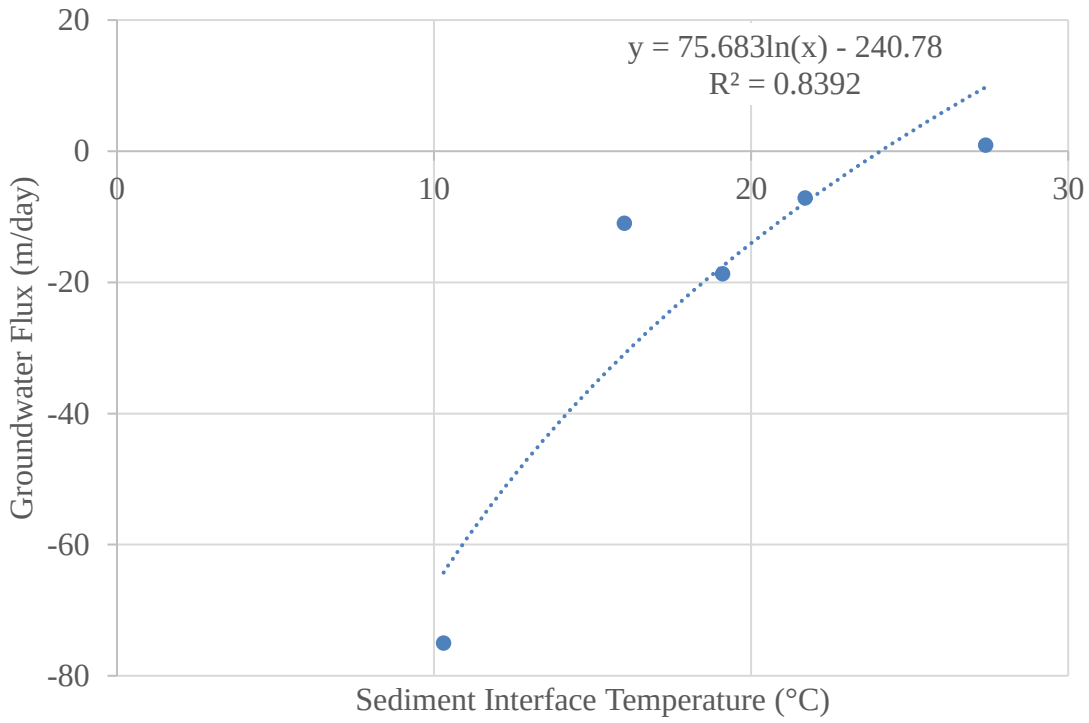

Figure 5.12. Sediment surface temperature (July 11, 2019) versus groundwater flux (August 22, 2019) calculated with FLUX-LM (Kurylyk et al., 2018) measured at the same locations along Transect E-W. Logarithmic relationship used to calculate interpolated groundwater fluxes. R^2 value= 0.84. Note that the flux for 31 m is set at -75 m/yr for plotting purposes but ranged from -50 m/yr to -100 m/yr in late summer 2019.

Finally, personal observations provided several other lines of evidence for the presence and nature of groundwater discharge to this pond. First, variable ice cover in the wintertime indicated areas of higher groundwater discharge as well as preferential flow paths for discharging groundwater. Holes in ice cover could be the result of the continuous influx of groundwater that can prevent ice from forming above that area (Kidmose et al., 2013; Sebok et al., 2013). Pictures of ice holes, an indication of preferential flow pathways, can be seen in Figure 5.13. Based on the periodic visits to the site, the northwest portion of the pond did not have any ice cover throughout the winter (Fig. 5.13). The lack of ice cover in the northwest portion of the pond was likely due to

higher groundwater input in this area (Kidmose et al., 2013). Secondly, through personal observations there were iron-stained groundwater seeps along the banks of the east shore, at the north end of the pond, and other non-stained seeps along the west shore, all in the northern portion of the pond. These groundwater seeps can also disrupt ice formation, as they can create overland flow to the nearshore area. Thirdly, there were personal observations of iron staining on the aquatic plants (*Chara*) in the north-east portion of the pond.

The distribution and magnitude of groundwater flux to the pond has implications for the contaminants input to the pond from the leachate plume. Specifically, the contaminant flux is the mathematical product of groundwater flux and contaminant concentrations. However, groundwater discharge may also affect the aquatic ecosystem through its control on the temperature of the sediment and overlying water. Temperature, particularly warmer temperatures will increase the growth, and metabolism of the organisms (Brett, 1974). A high discharge zone such as TR-T31 was very cold since groundwater is cooler than surface water in the summertime. Low temperatures can potentially slow down growth and metabolism of affected organisms. Although our study is focused on the contaminants, temperature patterns that could potentially affect organism's metabolism was a side observation from temperature and groundwater flux data.

a

b

Figure 5.13. Evidence of a) ice holes and b) unfrozen sections of the pond (looking north) during the winter season. (Photographed by Jim Roy)

5.2.3 Pond Outlet Discharge and Turnover

The outlet stream discharge was plotted along with the outlet stage data in Figure A2, noting that the percent error in the discharge measurements could range from 2-20% (Turnipseed and Sauer, 2010), but was expected to be relatively high for low discharge values at the site. Unfortunately, the data was not reliable enough to create a rating curve. The discharge values roughly followed the trends observed in the water level at the outlet, with the lowest values in the late summer and higher values in the winter. There was a noticeable spike on August 18, 2019, the day of a large precipitation event.

A very rough estimate of the pond's average turnover time or residence time was calculated using estimates of the pond volume divided by the average outlet discharge during the summer and winter season. The pond is about 11,700 m^2 (estimated using Google Earth). The depth of the pond was crudely estimated to be around 0.4-0.6 m based on pond water level measurements during the respective season given the uncertainty of the pond's bathymetry. The residence time for the pond was 12 to 19 days for the summer, and 9 to 14 days for the winter. The residence time of the pond could affect reactions in the pond (e.g., volatilization of VOCs and nitrification of ammonium to nitrate).

5.3 Landfill Leachate Plume Chemistry

5.3.1 Discharging Plume Footprint

Over the course of the field season, there were multiple locations sampled along Transect E-W and Transect N-S on different days. Each sampling time of groundwater using the mini-profiler system, or solution samplers is summarized in Table 4.1. Transect N-S and Transect E-W were designed to provide rough delineation of the spatial extent (or footprint) of landfill plume discharge to the pond and possible changes over time. Note that the east location (T3) was from Transect E-W and was also applied to Transect N-S when plotting the data. Electrical conductivity (EC), ammonium, saccharin (SAC), and chloride are landfill leachate indicators that will be discussed to show spatio-temporal variation. The more limited PFAS data are discussed in Section 5.3.3.

During the preliminary screening of Transect N-S in May, elevated concentrations of saccharin, chloride, ammonium, nitrate, and electrical conductivity were found from 0 m to 30 m north (WS1 - WN7; Figure 5.14). An exception at 30 m south also had elevated concentrations of saccharin and electrical conductivity (EC), with the concentration of saccharin approximately 6 times greater than at all other locations. However, this spike was not measured in subsequent sampling campaigns, perhaps because the permanent sampler was at a slightly different location and/or depth (required to be able to draw water). Furthermore, there was evidence of high saccharin at -85 m along with elevated electrical conductivity compared to background measurements. Subsequent sampling campaigns sampled fewer locations along Transect N-S and therefore temporal data is less evident (Figure 5.14). Nevertheless, starting at 0 m along

Transect N-S, the four constituents showed an increasing trend towards the northern portion of the pond.

Transect E-W was sampled in July, August, and December for various constituents (Table 4.1). Elevated concentrations of saccharin, ammonium, EC, and chloride were found at the east side at the pond (Figure 5.15), closest to the landfill. The elevated concentrations of the plume reached 25 m (July 11); subsequent groundwater samples at 25 m were not obtained due to poor flow conditions from the solution sampler. The concentrations found at 25 m likely represented the bottom of the plume. At 27 m and onwards (towards the west) the concentrations were representing background groundwater concentrations. This extent of the plume across the pond was consistent through the 3 sampling dates. Generally, there were peaks in concentrations for all four indicators at 8 m and 21 m indicating vertical spatial heterogeneity within the plume. Lower concentrations near the shore may represent the top of the plume where attenuation factors such as dispersion occurs. However, this was not fully supported by the redox data mentioned later. There could also be microbial degradation affecting this area; however, chloride followed the same trend as other parameters suggesting that microbial degradation was not the dominant process affecting the near-shore concentrations. Overall, source variability was likely the reason for internal spatial variability. Over time, the concentrations tended to stay around the same range. However, one noted change for saccharin at 3 m suggested a change in plume position over time. More specifically there was likely vertical movement of the plume from summer to winter, with its increased amount of recharging groundwater.

Several seeps (groundwater discharging to the land adjacent to the pond) along the east, north and west shores were sampled from May 31, 2019 to January 23, 2020 and periodically in between (Table 5.2). Areas of the highest saccharin concentrations and ammonium concentrations were located along the east shore at 20 m and 30 m north, where the plume is indicated by Transect N-S. The seeps along the northwest to west shores had low concentrations of SAC and ammonium but showed detectable concentrations of nitrate along with high chloride. These areas were not within the landfill plume footprint. The groundwater concentrations found in the middle of the pond and the west of Transect E-W, along with northwest seeps were similar. Similar chemical compositions may indicate that groundwater from the west was discharging into the middle of the pond. For example, both locations had chloride concentrations of around 35-45 mg/L, sulfate concentrations of 30-40 mg/L, 0-0.4 mg/L of ammonium, and non-detectable to low concentrations of saccharin.

Together the concentrations of landfill indicators for the transects and seeps, along with the dissolved metals, VOCs, and other major ions (Figures A6a, A6b, and A6c) indicate that the landfill plume footprint extended 120 m or more along the east shore on the north end and extended to around 25 m from the east shore. Concentration patterns within the plume footprint, particularly along Transect E-W, were more variable between contaminants. As noted, saccharin and ammonium and chloride patterns are elevated towards the east end of the pond with peaks at 8 m and 21 m and dissipated at 27 m (Figure 5.15). Along Transect N-S, the elevated concentrations were found at the northern side of the pond (Figure 5.14).

While it seems obvious that elevated concentrations of these leachate indicators means that the plume is from landfill, there are other sources of these indicators. Some alternate sources include road salt (Cl), wastewater (SAC, NH_4, Cl), agricultural fertilizers (Cl, NH_4, possibly SAC for manure). However, acesulfame and sucralose are expected to be found in modern wastewater but not for old landfills (Roy et al. 2014). In this study, acesulfame and sucralose were < 5 ng/L, eliminating wastewater as a contributing source. Chloride and bromide ratios are helpful in determining sources (Mullaney et al., 2009). Landfill affected samples have lower Cl/Br ratios (~150-200) while ratios for water influenced by road salt (>5000), fertilizer (~510) and wastewater (~300-1400). In this study, where bromide levels were above detention limits, the Cl/Br ratios ranged from ~200-300 which fits with the landfill source identification. Furthermore, detection of VOCs like methylene chloride, 1,1,2-trichloroethylene, 1,1-dichloroethane, ethylbenzene, benzene, and trans-1,1-dichloroethylene, as found in many of the plume footprint samples, is not expected in any of those sources, but common in landfills (Sabel & Clark, 1984).

Table 5.2. Concentrations of various constituents (saccharin, ammonium-N, nitrate, chloride, and sulfate) in groundwater seeps around the pond. Locations starting from the east and move around the perimeter of the pond in counterclockwise direction. Location detailed in Figure 4.1

Location	Date Sampled	Cl^-	NO_3	SAC	NH_4	SO_4
WS1	04-Jul-19	64.69	0.41	179	4.1	18.92
	22-Aug-19	59.33	0.1	151	2.21	18.49
	23-Oct-19	58.3	0.23	151	4.56	24.03
	19-Nov-19	50.47	0.59	275	5.31	19.21
WN4	31-May-19	118.75	0	3155	53.88	1.11
	02-Dec-19	296.65	0.33	3530	87.74	1.63
	23-Jan-20	256.27	0.41	2289	68.83	2.83
T3	02-Dec-19	67.25	7.45	132	7.07	24.51
WN7	31-May-19	9.37	0	756	43.31	10.85
WN9	31-May-19	119.94	0	345	74.24	14.83
	02-Dec-19	347.98	18.43	243	64.36	19.38
North	02-Dec-19	250.33	10.19	11	15.01	30.67
North West	02-Dec-19	36.77	5.44	5	0.05	30.78

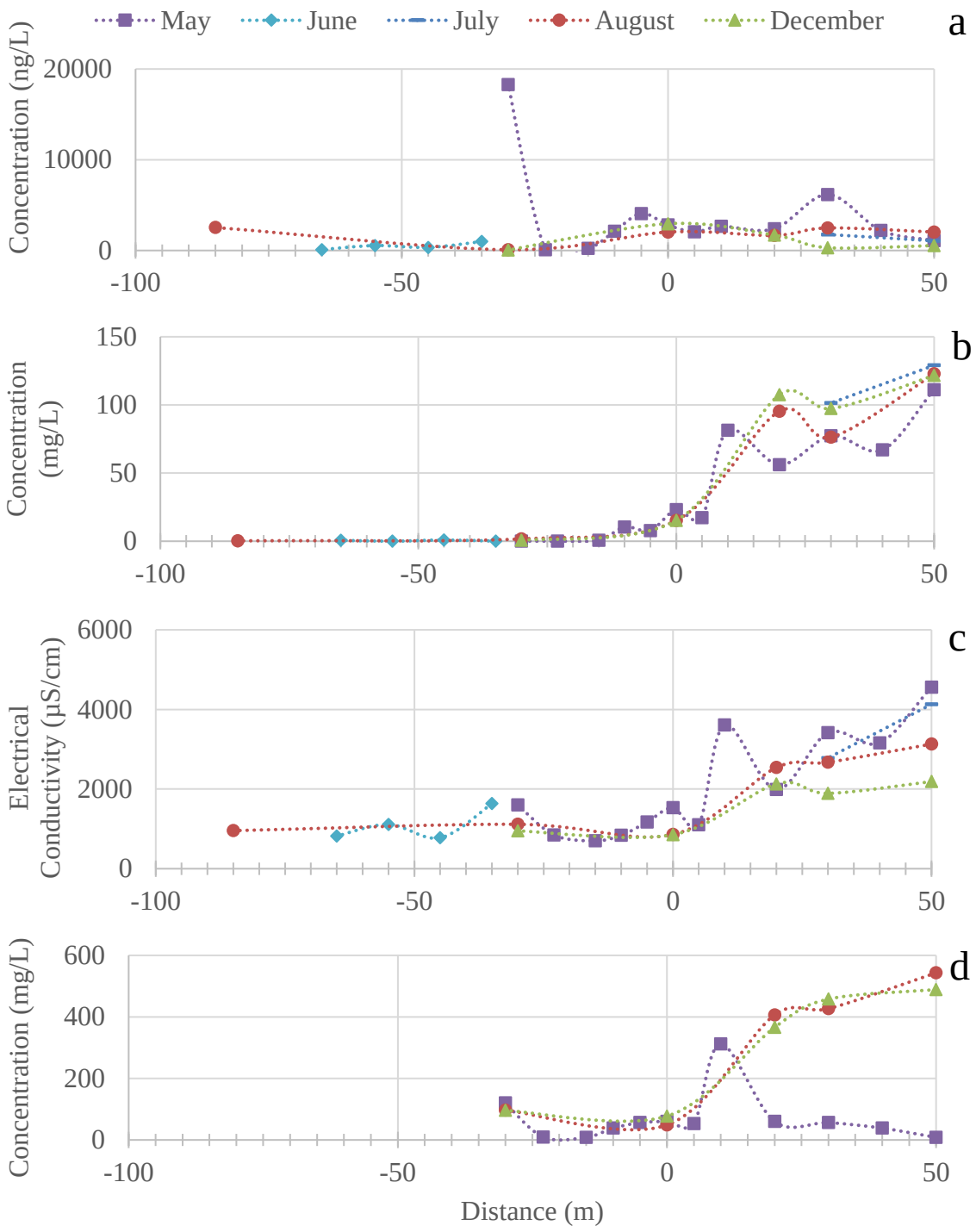

Figure 5.14. Concentrations of a) saccharin, b) ammonium-N, c) electrical conductivity, and d) chloride along Transect N-S (Figure 4.1) in May, July, August, and December. Where WS1 = 0m and the northern section is positive distance. Chloride was not measured in July or for WS11 in August.

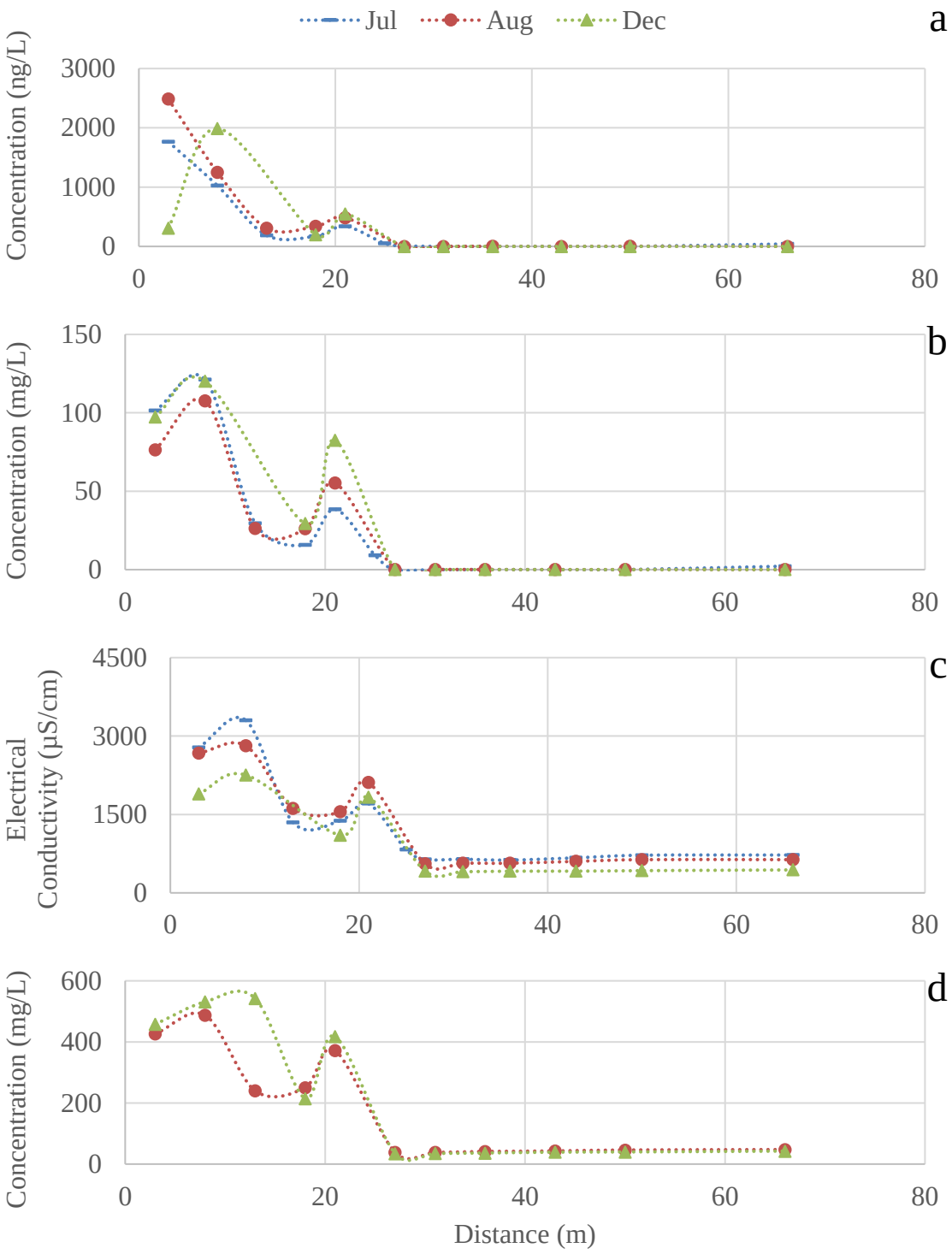

Figure 5.15. Concentrations of a) saccharin, b) ammonium-N, c) electrical conductivity, d) chloride concentrations along Transect E-W (Figure 4.1) for August, and December sampling campaigns. Landfill located to the left of the graph.

5.3.2. Geochemistry (Redox)

McMahon and Chapelle (2008) created a framework for assessing the geochemical redox conditions in regional aquifer systems. The framework was based on threshold concentrations for oxygen, nitrate, sulfate, and dissolved manganese and iron. The framework distinguishes between oxic, suboxic, nitrate-reducing, manganese-reducing, joint iron-sulfate reducing, and methanogenic redox conditions. The prescribed thresholds have been adjusted somewhat to accommodate site conditions, as recommended by McMahon and Chapelle, and probe/measurement concerns (Tables 5.3a and 5.3b). For example, dissolved oxygen was measured above ground and therefore could be altered when being transported into a graduated cylinder. Additionally, the probes needed time to equilibrate and due to time constraints, the oxygen levels were recorded prematurely before moving onto the next site (it was often assumed that oxygen would be low). Consequently, the threshold for oxygen was raised to 1.2 from 0.5 mg/L for this site, and because manganese and iron concentrations were also generally high for this site, their thresholds were changed to 0.15 and 0.25 mg/L, from 0.05 and 0.1 mg/L, respectively.

Redox conditions ranged from highly reducing methanogenesis to less reducing nitrate-reducing for August and December data (Tables 5.3a and 5.3b). A conceptual model was created to illustrate the redox conditions within the plume (Figure 5.16). The conditions within the plume footprint ranged from methanogenesis to iron-sulfate reducing while conditions outside the plume (Transect E-W only) ranged from nitrate reducing to manganese reducing conditions (Figure 5.16). The middle of the pond around

27-36 m, a high discharge zone according to the groundwater flux data, was a nitrate-reducing zone. At 27 m to 31 m the high nitrate levels were likely from other sources (e.g., agricultural fertilizer), however, the ammonium at the plume fringe could be contributing also. The edge of the plume was at 27 m and because there was not an abundance of organics, there may have been enough oxygen to mix with the ammonium (source unknown) causing nitrification and the creation of nitrate. Otherwise, background groundwater (west side of pond) appeared to be Mn-reducing, likely it had lower nitrate concentrations from its source. At 21 m, redox data showed that it was within the plume since it was still iron reducing. The top of the plume was likely suboxic as there was mixing of fresh water from infiltration. Along Transect N-S (more limited set of sample locations; all in plume footprint) the conditions were iron-reducing with a zone of methanogenesis at location WN7, in which there were also iron-staining groundwater seeps.

Table 5.3a. Concentrations of redox parameters (mg/L) and assigned redox condition according to modified criteria of McMahon and Chapelle (2008) for samples of Transect E-W and Transect N-S (Figure 4.1) from the August sampling campaign. Highlighted (green) boxes indicate concentration exceeding the prescribed threshold. Mixed means the criteria for more than one redox process are met.

	O_2	NO_3^-	Mn_2^+	Fe_2^+	SO_4^{2-}	Redox Process
Threshold	1.2	0.5	0.15	0.25	0.5	-
HB19-T3	0.2	0	0.103	13.6	0	Methanogenesis
HB19-T8	0.54	0.12	0.109	17.7	0.05	Methanogenesis
HB19-T13	0.86	0.11	0.252	5.59	6.84	Fe-SO_4 reduction
HB19-T18	0.35	0	0.319	4.14	9.2	Fe-SO_4 reduction
HB19-T21	1.08	0	0.333	8.17	0.67	Fe-SO_4 reduction
HB19-T27	0.86	6.2	0.137	0.0474	25.13	NO_3 reduction
HB19-T31	0.9	5.2	0.118	0.178	27.08	NO_3 reduction
HB19-T36	0.78	0.69	0.18	0.123	34.63	NO_3-Mn reduction
HB19-T43	0.94	0	0.211	0.162	36.17	Mn reduction
HB19-T50	1.5	0	0.212	0.357	35.76	Mixed
HB19-T66	0	0	0.248	0.0863	36.33	Mn reduction
HB19-TB	0.15	0.13	0.197	17.2	0.19	Methanogenesis
HB19-WN4	0.2	0.1	0.0715	21.5	0.04	Methanogenesis
HB19-WS1	0.3	0	0.157	7.8	8.7	Fe-SO_4 reduction
HB19-WS6	0.2	0	0.854	29.6	1.27	Fe-SO_4 reduction

Table 5.3b. Concentrations of redox parameters (mg/L) and assigned redox condition according to modified criteria of McMahon and Chapelle (2008) for samples of Transect E-W and Transect N-S (Figure 4.1) from the December sampling campaign. Highlighted (green) boxes indicate concentration exceeding the prescribed threshold. Mixed means the criteria for more than one redox process are met.

	O_2	NO_3^-	Mn_2^+	Fe_2^+	SO_4^{2-}	Redox Process
Threshold	1.2	0.5	0.15	0.25	0.5	-
HB19-T3	1.2	0	0.162	16.1	9.7	Fe-SO_4 reduction
HB19-T8	1.09	0	0.1	20.8	0.25	Methanogenesis
HB19-T18	2.2	0	0.312	5.22	10.88	Mixed
HB19-T21	0.45	0	0.365	9	1.96	Fe-SO_4 reduction
HB19-T27	0.6	5.06	0.139	0.0074	24.25	NO_3 reduction
HB19-T31	0.85	4.52	0.107	0.0376	26.82	NO_3 reduction
HB19-T36	0.6	1.41	0.176	0.202	31.44	NO_3-Mn reduction
HB19-T43		0	0.207	0.236	34.77	Mn reduction
HB19-T50	0.6	0	0.193	0.171	34.9	Mn reduction
HB19-T66	1.2	0	0.241	0.102	34.63	Mn reduction
HB19-TB	1.09	0	0.14	18.1	31.11	Fe-SO_4 reduction
HB19-WN4	0.5	0	0.0919	27.3	0.15	Methanogenesis
HB19-WS1	0.4	0	0.221	12.1	24.45	Fe-SO_4 reduction
HB19-WS6	0.5	0	0.973	41.1	2.8	Fe-SO_4 reduction

From August to December, the solution samplers near the shore had changed from methanogenesis to iron-sulfate reduction. Possible causes for this change could be due to changing flow conditions. Faster groundwater flow will reduce residence times and may not provide enough time for the conditions to reach methanogenic. Another cause could be changes in the vertical plume position and therefore showing natural spatial variability. More recharge on the hill during the wintertime (reduced evapotranspiration) could potentially push the plume deeper, meaning the top edge of the plume was more likely sampled at 3 m from shore. Other data contaminant data such as sweeteners, ammonium, or chloride could suggest dilution is occurring if there was a decrease in concentrations, although this was not evident in this study.

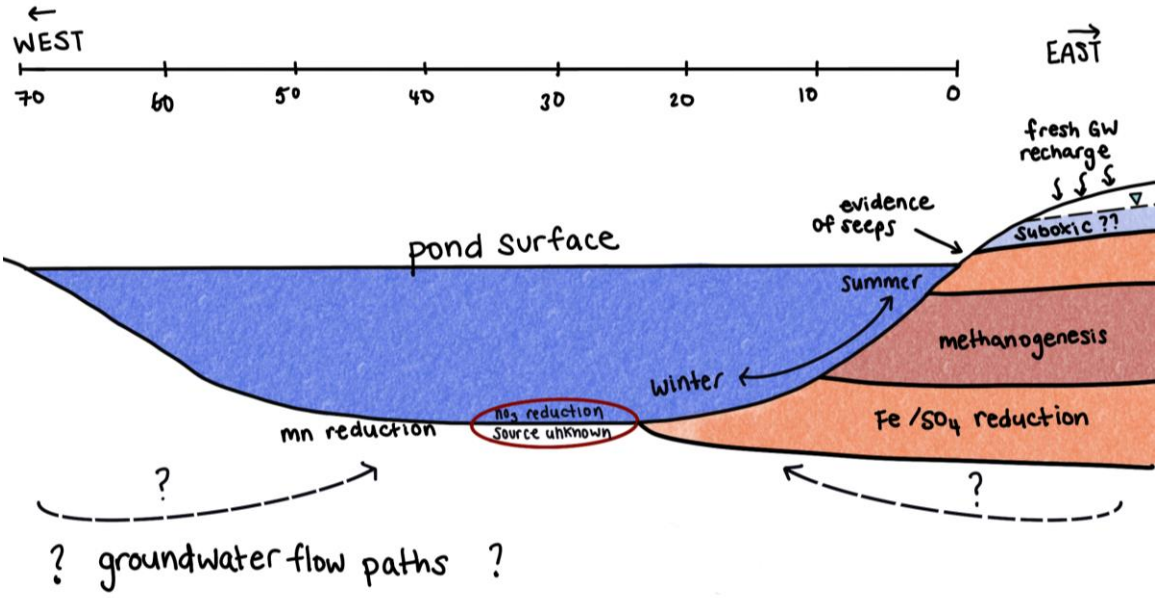

Figure 5.16. Conceptual model of leachate plume and redox conditions.

5.3.3 Plume Contaminants and Endobenthic Exposure

There were a variety of potential landfill contaminants analyzed, including 27 PFAS (Table A1). PFAS is of greatest concern here and so details of those PFAS detected, the relative composition and concentrations, and its spatial variability with respect to other landfill constituents will be discussed below. Note that there could be many precursors and other PFAS compounds not detected simply because they were not a part of the suite for analysis.

Figure 5.17 depicts concentrations of individual PFAS compounds at each sampling site along Transect E-W and Transect N-S. Of the 27 PFAS analyzed, 15 were not detected at a concentration >2 ng/L and are not shown in Figure 5.17. These compounds include; Perfluorodecanoic acid (PFDA), perfluoroundecanoic acid (PFUnDA), perfluorododecanoic acid (PFDoDA), perfluorotridecanoic acid (PFTrDA), perfluorotetradecanoic acid (PFTeDA), perfluorohexadecanoic acid (PFHxDA), perfluorooctanesulfonamide (FOSA), 4,8-dioxa-3H-perfluorononanoate (ADONA), sodium 8-chloroperfluoro-1-octanesulfonate (8ClPFOS (C8F16ClSO3)), 9-chlorohexadecafluoro-3-oxanone-1- sulfonic acid (9Cl-PF3ONS, F53B (C8F16ClSO4)), 11-chloroeicosafluoro-3-oxaundecane-1-sulfonic acid (11Cl-PF3OUdS, F53B (C10F20ClSO4)), perfluorododecane sulfonic acid (PFDoDS), hexafluoropropylene oxide dimer acid (HFPO-DA). Within the established plume footprint, the total PFAS concentrations surpassed 800 ng/L at all sample locations and generally had similar composition. In terms of the composition, the perfluorocarboxylic acids (PFCAs) were most abundant, particularly perfluorohexanoic acid (PFHxA), perfluorobutanoic acid

(PFBA), and perfluoropentanoic acid (PFPeA) (Figure 5.18). However, some perfluorosulfonic acids (PFSAs), namely perfluorobutanesulfonate (PFBS), and perfluorohexanesulfonate (PFHxS) were also found at substantial concentrations.

The concentrations of PFAS were elevated within the plume footprint along Transect E-W (Figure 5.17), and the total PFAS concentrations were highest at 8 m, and lowest at 13 m. The non-linear decline in concentration in Transect E-W showed spatial variability within the landfill plume, with a similar pattern to those of SAC, Cl, EC, and NH_4 (Figure 5.15). At 27 m and onwards the concentration of total PFAS became negligible (< 7 ng/L), and the PFAS composition changed as well. Most notably, the concentrations of PFHxA were negligible outside of the plume footprint, but most predominant within the plume footprint. The source for the low concentration PFAS found outside the plume footprint was likely not from the landfill. The high nitrate reduction zone found at 27 m and 31 suggested another potential contaminant source (potentially agricultural fertilizer) so this PFAS might be from atmospheric deposition. Along Transect N-S the total concentration of PFAS exceeded 2000 ng/L at WN4 to WN7 and was lower (~500 ng/L) for WS1 and WS6 (Figure 5.17). These spatial trends were seen in other leachate indicators as well, albeit the concentration peaks for PFAS on Transect N-S were located at the northern portion of the pond with detectable concentrations at WS1 and WS6. Furthermore, the composition of PFAS along Transect N-S was predominantly PFHxA for all locations and matched the composition for the locations on Transect E-W that were within the plume footprint (Figure 5.18). One slight exception was WS1, which had notably higher perfluorooctanesulfonate (PFOS) and

PFHxS than the others, indicating some variability in leachate composition within the plume and landfill.

Correlation plots showed high correlation between, PFAS, ammonium, saccharin, electrical conductivity, and chloride. Although they were not equally correlated, for example ammonium and EC might be more correlated than saccharin and EC. For the scope of this study, this high correlation just indicated that these contaminants came from the same plume. Notably, the other constituents were routinely sampled compared to PFAS, and less costly. The locations on the Transect N-S were the outliers on the correlation plot and might indicate differences within the landfill. This variability may be affected by various factors and processes. As mentioned before, different locations of the landfill would be filled at different times, therefore the leachate can have variable ages within the plume. Additionally, the spatial heterogeneity in the site geology will create different flow paths, which also affect residence times and in turn redox conditions. Locations near the shore were also likely more affected by precipitation inputs or lack of evapotranspiration as fresh groundwater inputs can move the plume downwards.

There was an earlier study by Propp et al. (2021) conducted in 2018 at this same site. Their first and second groundwater samples were from the leachate well and a second well respectively, while the third sample was also from the pond shoreline (aka WS1 in this study). Results comparing PFAS concentrations from this study to Propp et al. (2021) can be seen in Table 5.4. The sample analogous to WS1, had higher concentrations of PFAS compared to this study, however they both had predominantly PFHxA (Propp et al., 2021). Although the concentration at the leachate well (520 ng/L)

was similar to concentrations found at WS1 and WS6, concentrations 5 times higher were found near Transect E-W (2600 ng/L). This suggested that the leachate well meant to represent the concentrations found in the landfill leachate plume was not capturing the highest PFAS concentrations. This highlighted the spatial variability within the leachate plume itself and pointed to possible underrepresentation of the leachate plume concentrations by single leachate well.

Compared to modern landfills the concentrations are quite similar, although it was hard to compare between studies as there are thousands of different types of PFAS and not all studies analyze for the same ones. However, the composition was comparable to other landfill plumes. Hamid et al. (2018) found that PFCAs are more dominant in landfills, as well as short chain PFAS (C4-C7). As mentioned previously, short chain PFAS have higher mobility and solubility. Hamid et al. (2018) looked at a range of studies of researching modern landfills and found a range of 310-25,000 ng/L for PFHxA. This study had a maximum of 875 ng/L. Overall looking at the distribution between the studies in Hamid et al. (2018), it was evident that PFHxA and PFBS and PFOA, are the most predominant, much like at HB.

Some common contaminants (ammonium and chloride) were well above the water quality guidelines (WQGs) which indicates that historic landfills still present risk to the surrounding environment. Some maximum groundwater concentrations exceeded aquatic WQGs at locations within the plume footprint. For instance, ammonium and chloride exceeded their aquatic WQGs (10 mg/L and 120 mg/L, respectively) with max concentrations of 129 mg/L and 543 mg/L found at WN7, respectively (CCME, 2001;

CCME, 2011). Most PFAS compounds do not have guidelines. For example, only PFOS has aquatic water quality guidelines of 6800 ng/L and the max concentrations (62 ng/L at WN4) found at the site are negligible compared to its guideline (ECCC, 2018a). However, the PFOS WQG in Europe is 650 ng/L suggesting that guidelines may change, and therefore the concentrations found at this site may not be negligible in the future (Directive 2013/39/EU). Overall, there needs to be more toxicity information for PFAS.

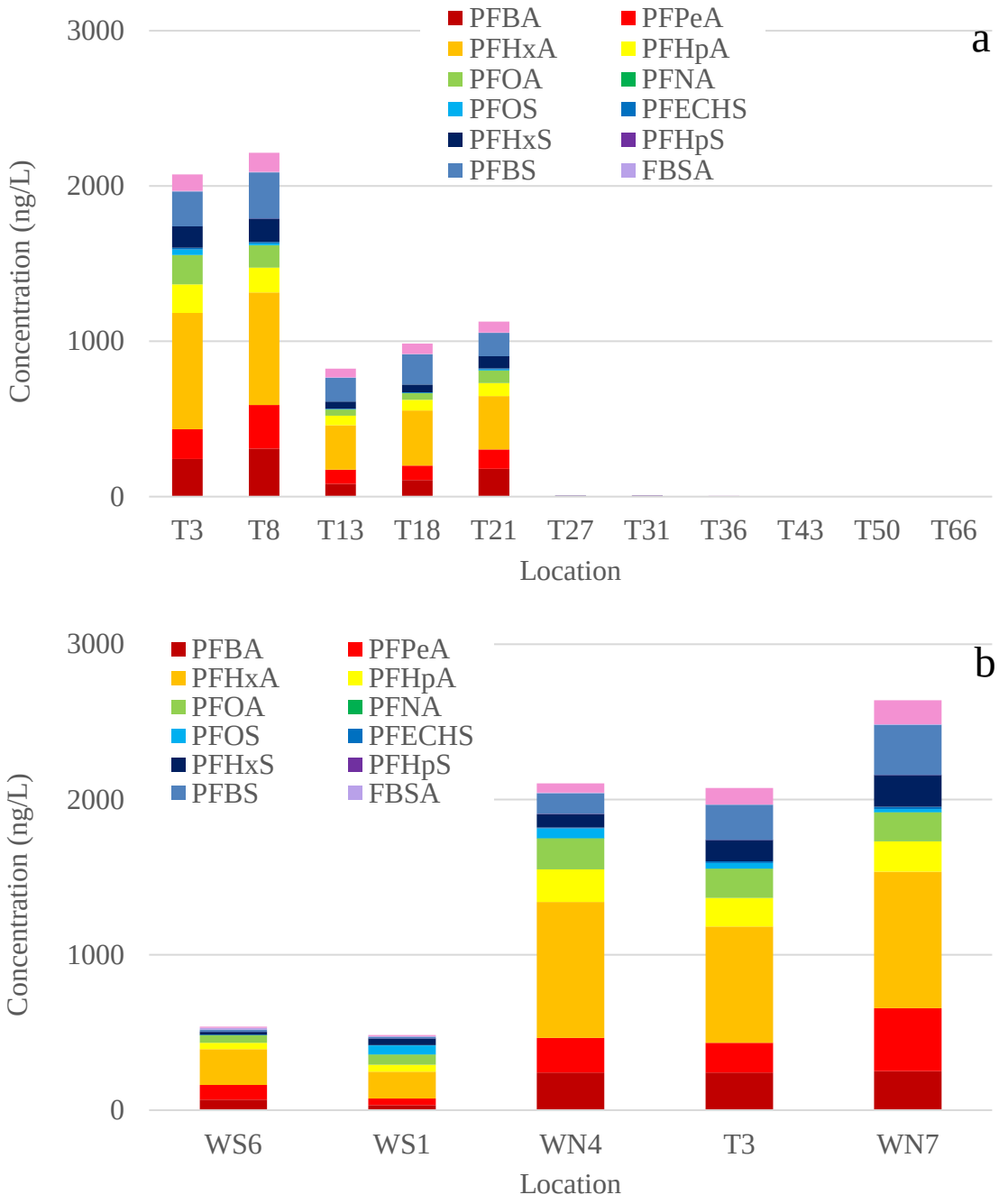

Figure 5.17. PFAS concentrations for August 22, 2019 sampling campaign. a) concentrations for Transect E-W b) concentrations for north south transect. Criteria for the PFAS concentration data is only PFAS compounds that have more than one sample greater than 2 ng/L are plotted.

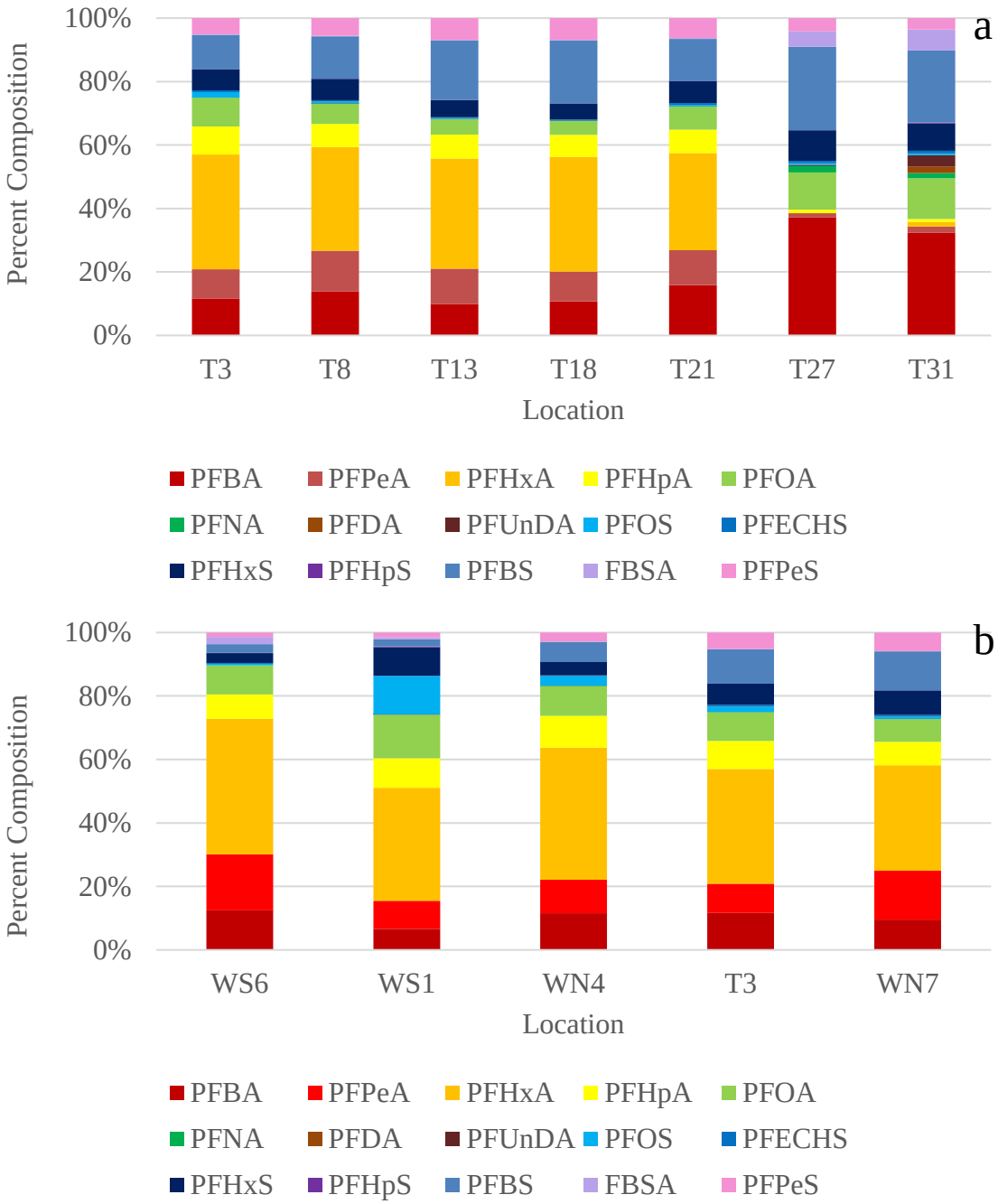

Figure 5.18. PFAS compositions for August 22, 2019 sampling campaign. a) composition for Transect E-W b) composition for Transect N-S. Criteria for the PFAS composition is that only locations that have total PFAS > 3 ng/L are included. This is because the field trip blanks have totals of PFAS of 0.6-0.7 ng/L and method blanks have up to 2.3 ng/L.

Table 5.4. Concentrations of total PFAS from this study (27 compounds) in August 2019 compared to Propp et al. (2021) sampled in 2018 (17 compounds). Note that only the same compounds tested in both studies were used to calculate total PFAS so that they are comparable.

	Total PFAS (ng/L)	
Location	**Propp et al. (2021)**	**This study**
Well 41 (leachate source)	520	-
Groundwater ~15cm (endobenthic zone)	Max ~1500	Max ~2600
Pond Surface Water (lentic zone)	-	Max ~136
Outlet Stream (lotic zone)	-	Max ~118

5.4 Contaminant Flux and Epibenthic Exposure

5.4.1 Calculated Fluxes Along Transect E-W

The contaminant mass flux was calculated for saccharin, total PFAS, and ammonium at 11 locations along Transect E-W. The contaminant mass flux was calculated using the average groundwater flux from FLUX-LM and the contaminant concentrations from the semi-permanent solution samplers, both from summer 2019. The temperature rods TR-T3, TR-T13, TR-T31, TR-T43, and TR-T66 were used, and the solution samplers along Transect E-W ranged from 14 cm to 39 cm in depth. It was assumed that there were no degradation processes occurring across the sediment interface (noting PFAS is not known to degrade and SAC and NH_4 are more recalcitrant under reducing conditions), or substantial plant uptake. In addition, it was assumed that sorption was at equilibrium (sorption sites were saturated) based on the age of the leachate plume (historical). Essentially, all contaminants measured in the shallow groundwater were assumed to

discharge into the pond. Elevated contaminant fluxes entering the pond from 3 m to 21 m (Figure 5.19) indicated likely exposure from leachate-plume contaminants to the epibenthic organisms. Note that the contaminant flux was calculated at singular points and the conditions in-between can vary. Overall, the pattern of contaminant flux suggested internal spatial variations reflecting those of the concentrations in the plume, as there were peaks found at 8 m and 21 m across Transect E-W. An even greater contaminant flux may occur beyond 21 m as there was a zone of high interpolated groundwater flux (73 m/s at 25m) (Figure 5.11) and therefore the plume footprint likely extended to 25 m. Although the contaminant data showed that the plume does not reach that area of highest groundwater flux (~ 30 m) in the sampling periods, they were areas of concern as they could potentially become contaminant hot spots with a change in the extent of the plume. These hot spots may occur at other areas in the pond (that were not measured) and at other sites due to heterogeneous geology. The contaminant mass flux was important as it indicated exposure conditions for epibenthic organisms while the contaminant concentration in the groundwater alone described exposure conditions for the endobenthic community. Since the site was a non-flowing water body, this means that contaminants entering the pond at the sediment surface were not being carried away/mixed/diluted like in a stream and therefore the epibenthic community was more likely affected. These observations also have implications for monitoring as it was important to account for heterogeneities to see all possible impacted zones.

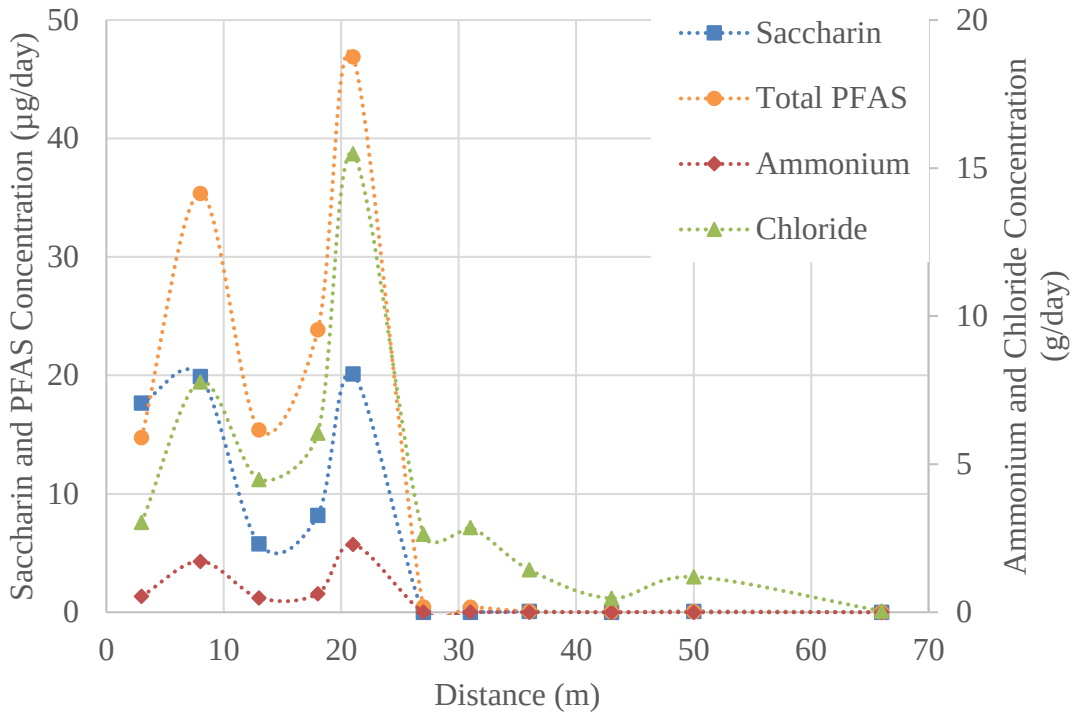

Figure 5.19. Calculated saccharin, ammonium-N, chloride, and total PFAS flux into the pond across Transect E-W (0 m represents the east shore).

5.4.2 Electrical Conductivity at Sediment Interface

Hydrologic observations suggested that the epibenthic community may experience worse conditions after precipitation events, at night, and in the winter season, given potential increases in the groundwater flow to the pond. To validate this, three electrical conductivity (EC) loggers were deployed at ~1 cm above the sediment surface in a line north of Transect E-W (Figure 4.1), using EC as a tracer for discharging leachate-impacted groundwater. The EC (corrected to 25℃) was plotted with precipitation, wind, and daily temperature data from a nearby weather station (Delhi; ~ 22 km from site) in Figure 5.20. It is important to note that the EC sensors were measuring just above the groundwater and surface water interface and could either be reading more of the surface water or more of the groundwater influence. Most likely the groundwater influence was a

change in groundwater flux. Surface water influence may include mixing of the pond by wind and temperature gradients. Therefore, some inconsistency was likely due to external factors such as mixing of the pond by wind and temperature gradients.

The EC sensors show temporal variability over the study period (Figure 5.21), especially for the two data loggers nearest the east bank. Some changes might be associated with times of sampling or measurement activity (human disturbance; < monthly) or the sensor being redeployed at a slightly different distance from the pond bed (following downloading). However, the vast majority reflected changes occurring with the pond - groundwater system. The east sensor was located at around 10 m from the east shore while the middle sensor was located at around 20 m. Judging from the contaminant data for nearby Transect E-W, the plume ended around 25m, and therefore the two EC sensors were likely within the plume footprint. Both sensors had typical or base values within the EC range measured for groundwater in the plume (Figure 5.20), indicating the epibenthic organisms (organisms right above the sediment interface) here may be experiencing harmful leachate affected groundwater discharging into the pond.

There was a diurnal pattern in the EC data that was strongest from the east sensor and differed in its timing between the three sensors (Figure 5.21). For example, the EC for the middle and east sensors increased at different rates, which was also shown by the water level piezometers at similar locations. The east sensor peaked at night and matched the timing for the east piezometer which fit with reduced evapotranspiration on land, and since plants were no longer taking up soil water and groundwater at night this led to greater groundwater discharge at night. Meanwhile, the west sensor showed the smallest

changes and peaked during the day. The west sensor pattern fit with patterns found in the west piezometer in which the evaporation from the pond lowered the pond head during the day, leading to greater groundwater flux then. The low range (700 µS/cm to 750 µS/cm) in EC likely reflected similar EC between uncontaminated background groundwater and the pond. The middle EC sensor had broader peaks that extended from night into early day which might be a mix of the two influences, both evapotranspiration reduction at night and pond evaporation during the day. Additionally, the diurnal fluctuations in groundwater levels disappeared during the fall season, likely because of the lack of evapotranspiration and evaporation in the cooler seasons. All together, these findings suggest the diurnal EC signal was being driven by fluctuations in groundwater flux.

There were also bigger spikes in EC above the sediment mainly seen in the east EC sensor but periodically in the middle and west. These large spikes were not a part of the diurnal patterns and showed a ~1000-2000 µS/cm change (Figure 5.21). Some at least were likely associated with increased recharge from rain or snowmelt events, though internal mixing or circulation changes in the pond could also be a cause, especially for the west sensor outside the plume footprint. For example, a known large rain event on August 18, 2019 exhibited ~800 µS/cm increase (Figure 5.21). However, precipitation events did not directly impact the EC, as it was the hydraulic gradient that drove the contaminant groundwater flux into the pond. For example, rainfall on unsaturated soils during the dry season will recharge the subsurface first before contributing to the leachate

plume. Therefore, some rainfalls will contribute/dilute the pond directly more than the contaminant plume.

Finally, there also appeared to be a seasonal influence that has affected the two EC sensors in the plume footprint (Figure 5.20). The EC data followed the same seasonal trend as the surrounding water level data with a large increase in EC during the winter months. This too then likely reflects greater groundwater discharge due to more recharge (less evapotranspiration) in this season. This means prolonged exposure over months for the epibenthic organisms within the plume footprint.

To summarize, the electrical conductivity increased at night, after rain events, and in the winter and appeared to be largely controlled by the groundwater flux into the pond. The temporal pattern was likely influenced by evapotranspiration from the surrounding land and evaporation from the pond. Determining which other factors, such as internal pond mixing patterns, were contributing is outside the scope of this study. This has implications to the epibenthic zone experiencing exposure to harmful contaminants from groundwater. For example, the EC for the east sensor ranged from 850-1050 µS/cm and 1000-1090 µS/cm for the middle sensor over a 24-hour period in August 2019 (Figure 5.21). This is about a 20% increase in EC over a short period of time (24 hours) and suggests that contaminant concentrations were also drastically changing currently. However, it is important to note that these concentrations were found within the groundwater at a depth of 14 to 44 cm, and some contaminants may be attenuated in the shallow sediment before reaching the pond surface water.

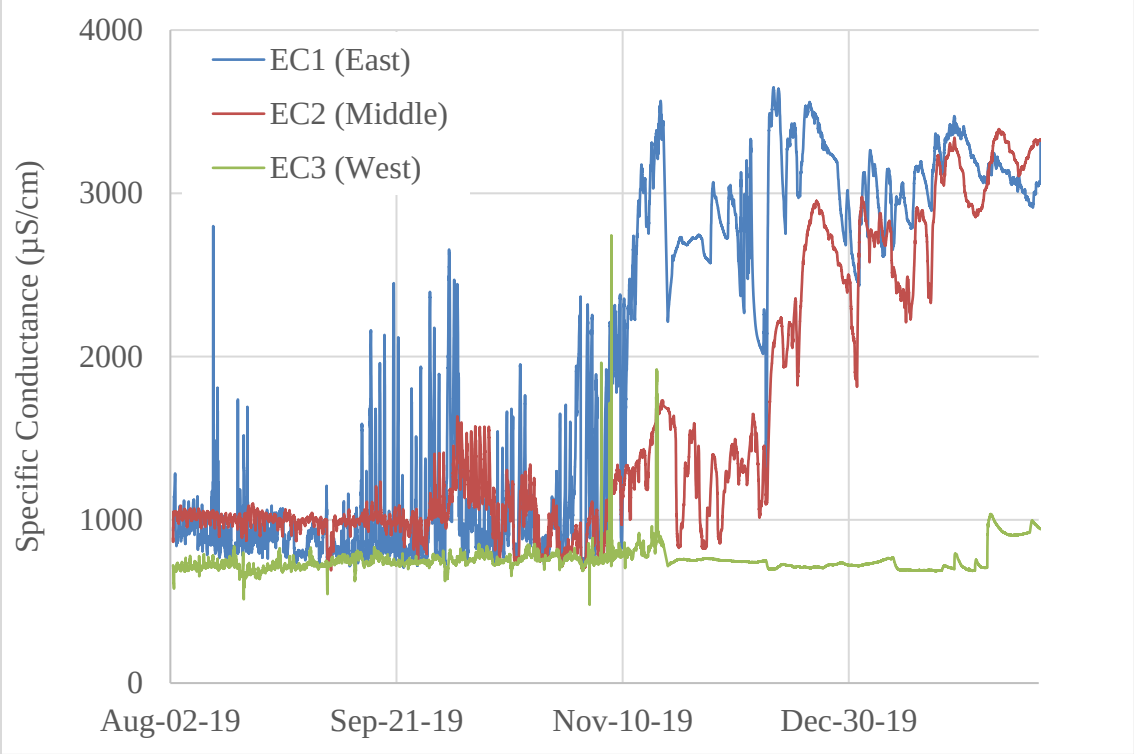

Figure 5.20. Specific conductance standardized to 25°C measured ~1cm above sediment bed at locations 10 m, 20 m, and 40 m from the east shore (Figure 4.1) at intervals of 15 minutes.

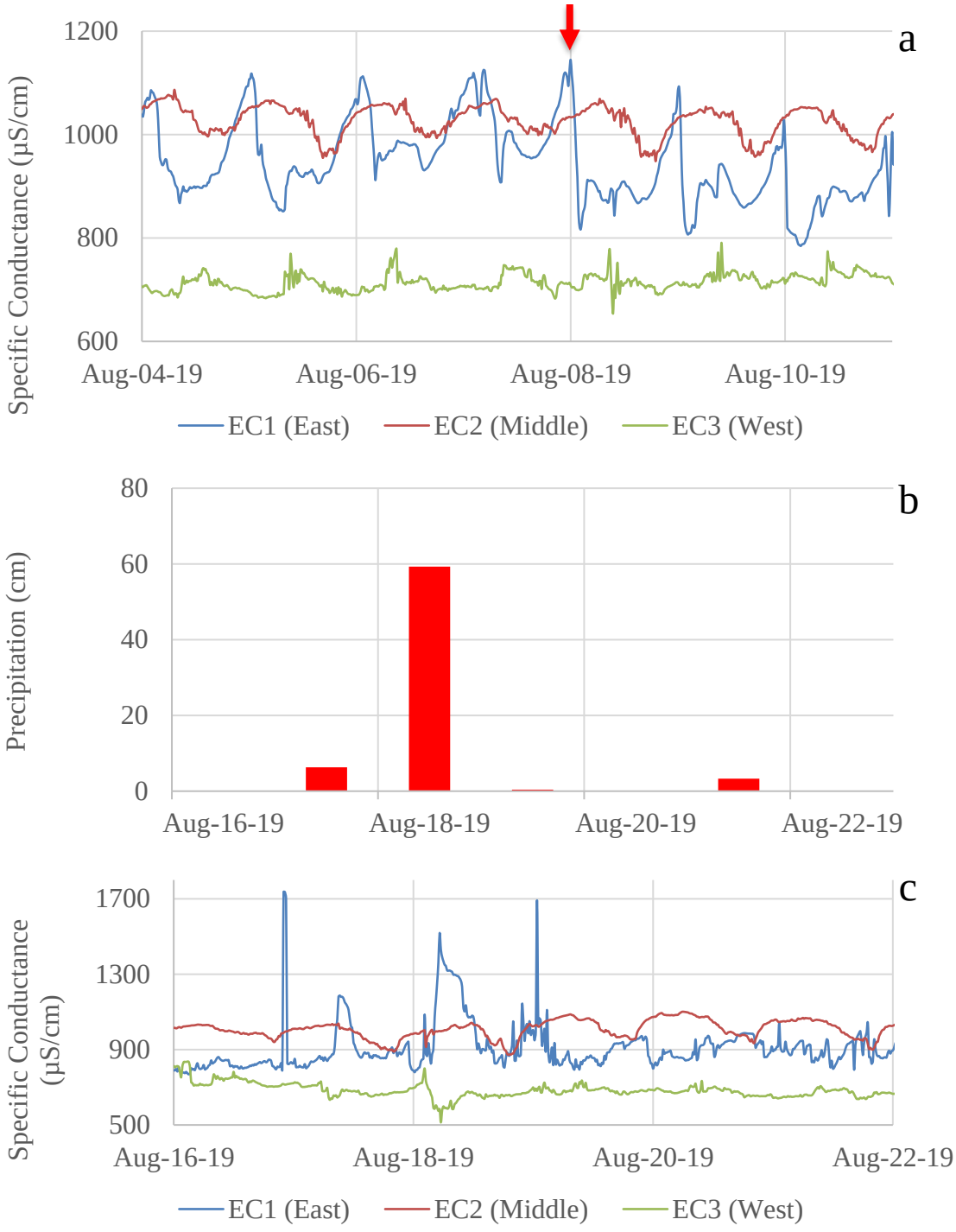

Figure 5.21. a) Diurnal patterns in electrical conductivity (25°C) (August 4-10, 2019) c) Precipitation (cm) for August 16-21, 2019 d) electrical conductivity during a rain event (August 16-21, 2019). Precipitation event (5.6 cm) denoted by red arrow for August 8, 2019.

5.5 Contaminant Concentrations in the Pond and Pelagic Exposure

The concentrations of various leachate contaminants were measured at the pond outlet and WS1 periodically throughout the field season. Those for saccharin and ammonium (every 2-3 weeks) and chloride and nitrate (less often) are shown in Figure 5.22 for the pond outlet. The concentrations are generally similar for the pond edge samples (Figure A7) but show more variability. The pond edge concentration variability was not unexpected because the pond edge was within the landfill plume footprint as well as down flow from the landfill, and likely less fully mixed compared to the outlet.

Concentrations measured in the pond were largely affected by the volume in the pond and the mass of contaminants entering and interacting with the pond. The factors controlling the volume of the pond were the groundwater discharge into the pond, evaporation, evapotranspiration, and precipitation. The factors controlling the mass in the pond was the total mass entering the pond, attenuation processes such as transformations (degradation, redox, microbial activity), uptake by organisms (ex. plants), and sorption. Although with sorption, the age of the plume suggests the areas for potential sorption were taken up over the years, and therefore not a big factor now. Other factors include, photodegradation, volatilization (ex. VOCs). Turnover rate determined the residence time in the pond and thereby the time of which reactions could occur. The plant's uptake rate would also depend on temperature and light availability. In summary, these factors were considered when assessing the concentrations of ammonium, saccharin, and chloride at the two pond locations.

To start off, chloride was affected the least as the concentrations do not change temporally. Chloride is a conservative tracer and has elevated concentrations within the plume footprint. The concentration of chloride within the plume footprint was an order of magnitude greater than the background groundwater. For example, in the August sampling campaign the chloride concentrations in the plume were >400 mg/L and the background concentrations were around 40 mg/L, while the surface water concentrations were around 60 mg/L, suggesting mixing of the plume and background groundwaters were occurring. There could be other sources of chloride contributing to the slightly higher concentration at the outlet compared to background groundwater, such as agricultural inputs from the inorganic fertilizer or manure used in the surrounding farms. However, it was not likely road salting, although common, because there were no major roads near the site that would have salting during the snow season.

Saccharin was analyzed more frequently than chloride in surface water samples, therefore provided a more complete temporal data set. However, unlike chloride, saccharin can degrade in aerobic conditions (Luo et al., 2019). Similar to chloride, the saccharin concentrations stayed consistent across the study season, which suggests saccharin was not significantly degraded in the pond. This pattern also suggests a steady balance between inputs of contaminated groundwater and other inputs (precipitation, background groundwater). These data also indicate persistent exposure of saccharin and potentially other non-reactive contaminants to the pelagic organisms within the pond (Figure 5.22).

Ammonium was also being added at high concentrations with the discharging plume but did not show this consistent trend over the study period, with lower concentrations in the summer and increasing concentrations into the winter (Figure 5.22). Nitrate, which was at negligible concentrations in the plume, increased in concentration along with ammonium. Its source could be background groundwater as there was high nitrate at a high discharge zone along Transect E-W and could be created from the ammonium by nitrification within the oxic pond water. Nitrate can further transform into nitrogen gas, which is quickly volatilized, by microorganisms in the sediments and slow in colder conditions. The aquatic plants *Chara* was potentially active throughout the winter, although less so because of the lower light levels and cooler temperatures (Pukacz et al., 2016), and since both species of nitrogen are taken up by plants, the observed trend for these N species could be due to reduced losses to aquatic plants and microbial transformations.

Concentration data for PFAS from the pond outlet and edge locations were only available for July and August 2019 and show similar concentrations for those dates (Figure 5.23). The concentration decreased slightly between the pond and the outlet because of the influx of clean groundwater causing dilution before reaching the outlet stream. The PFAS composition was similar between the two locations suggesting no major losses of individual PFAS compounds during transport in pond water to the outlet. Although sorption is preferential to longer chained PFAS, there was not a decrease in them, likely because the sorption areas were filled up due to the long-time exposure. The differences between the times were not significant enough to identify the main factor

causing a slight change in concentration between July and August. These concentrations represent exposure to pond pelagic organisms.

Since PFAS in the surface water was only measured twice over the year, to predict future possible trends, a proxy such as saccharin or chloride can be used. All three compounds (PFAS, saccharin, chloride) are non-transformative (seems so for saccharin here), less likely to volatilize, and be taken up by plants. Additionally, saccharin and PFAS will likely sorb somewhat, some PFAS compounds more than others, but given the age of the leachate plume, the system may be near steady state, in other words, possible areas for sorption are filled. Similarly, all three compounds saw slight decreases in concentration from July and August. Therefore, the trend for PFAS was likely observed for both saccharin and chloride, meaning steady concentrations over the study period.

Based on the water level data, contaminant flux, and electrical conductivity data of the study, there was more leachate affected groundwater entering the plume in the winter. This led to speculation for the snowmelt season, as due to the pandemic, it was not possible to obtain data for any of the parameters during the snowmelt period (mentioned before). Depending on the speed of the snow melt, the effect on the concentration levels in the pond will change. For example, if the snow melts fast, the runoff will dilute concentrations in the pond. Conversely, low snowmelt can also become runoff if the ground is still frozen. There would be less change in the concentration in the pond if the snow melts and infiltrates the subsurface and potentially increases the influx of both contaminated and uncontaminated groundwater, as suggested by the steady pond concentrations of chloride and saccharin. Alternately, if recharge timing or amount is

higher for the landfill area, the contaminant flux might be relatively greater. Measurements would be required to see what happens, though the results might be different from year to year.

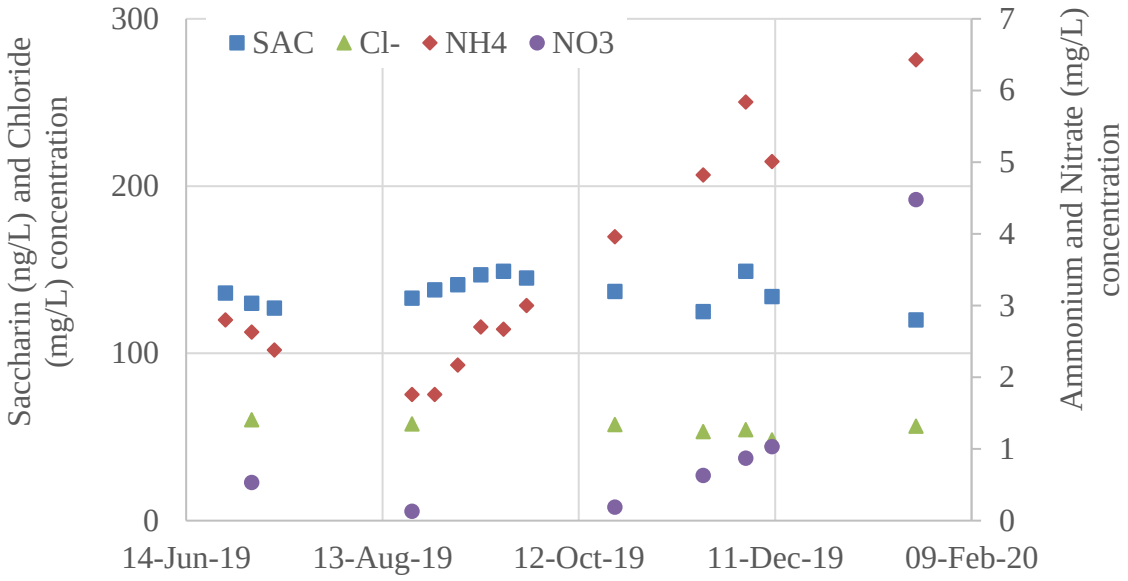

Figure 5.22. Contaminant concentrations in outlet stream surface water samples.

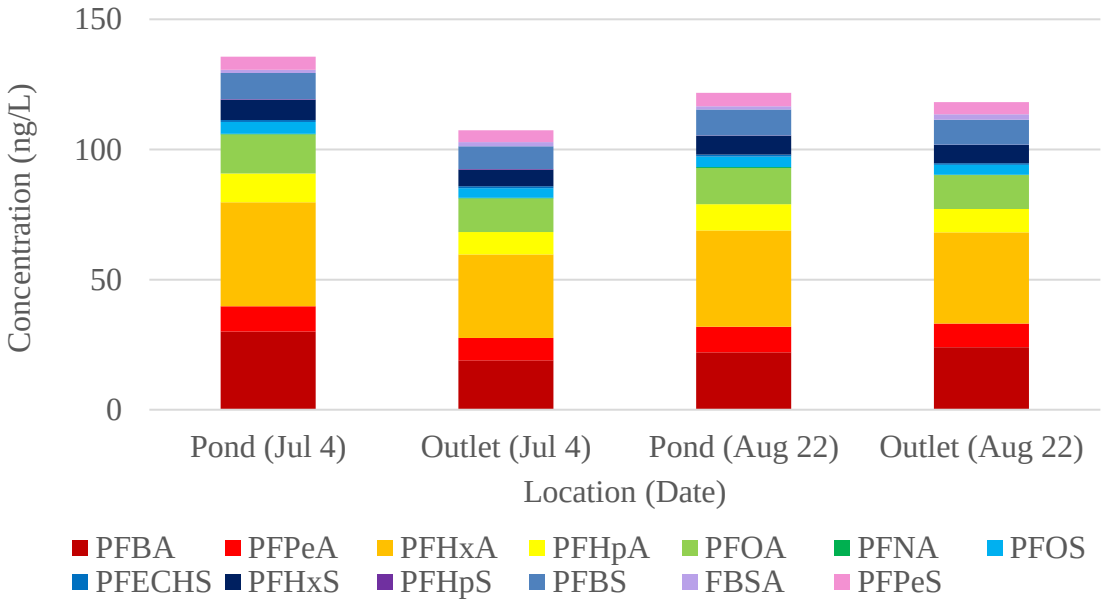

Figure 5.23. PFAS concentrations in surface water samples from July 4 and August 22 at the pond edge and outlet.

5.6 Contaminant Mass Discharge from Pond Outlet and Exposure Downstream

The surface water concentration data provided insights into conditions experienced by the pelagic community (organisms residing in open waters) in the pond. Meanwhile, the mass discharge was important for organisms and other receptors downstream. The mass discharge was calculated by multiplying the stream discharge and the associated surface water contaminant concentration measured at the pond outlet. As mentioned before, there was also a higher percent error, likely 2-20% (Turnipseed and Sauer, 2010) with the mass discharge because of the uncertainty in the outlet discharge values.

From the graphs, the mass discharge first dipped in August and increased over time from September to January (Figure 5.24 and Figure 5.24). The ammonium mass discharge was approximately 7 times greater in winter than summer. Meanwhile for saccharin and chloride it was only approximately 3 times greater. PFAS mass discharge was expected to show similar trends shown by saccharin and chloride. The large increase in ammonium compared to saccharin and chloride was likely due to the lack of plant uptake in the wintertime. Meanwhile the nitrate mass discharge also showed a large range, likely due to nitrification of ammonium. For the snowmelt period, an increase in contaminant mass discharge may also be expected. Also, given the temporal patterns in pond level continuous data (Figure 5.1), mass discharge may also increase somewhat following precipitation events, and be slightly higher at night than during the day.

The contaminant mass discharge from the pond outlet can provide insights to potential impacts on the pelagic community in the stream fed by the outlet. Much like the endobenthic and epibenthic zone, the pelagic zone downstream was also experiencing

worse conditions during the winter season. Additionally, the outlet may be losing volume from infiltrations to the subsurface which may end up in Branch Creek nearby (Townley & Trefry, 2000). Therefore, the results of the study may be underestimating the mass discharge from the pond. Downstream inputs from surface water or groundwater will dilute the contaminant mass in the receiving stream.

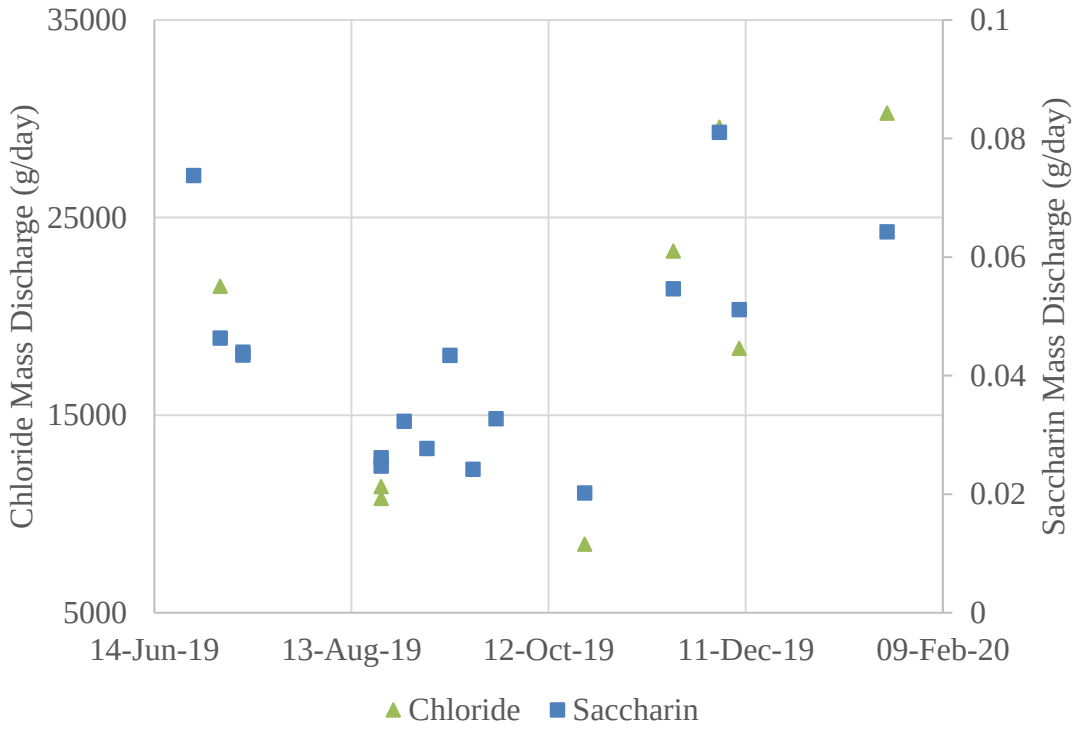

Figure 5.24. Chloride and saccharin mass discharge from pond outlet from summer 2019 to winter 2020.

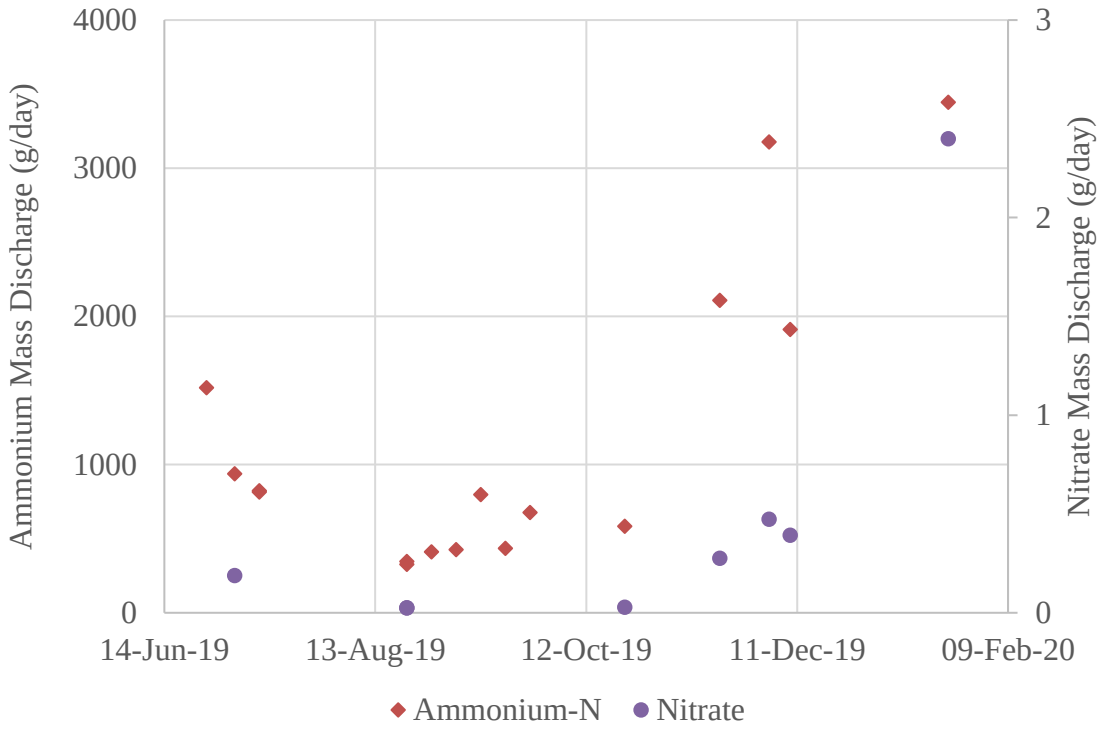

Figure 5.25. Ammonium-N and nitrate mass discharge at the pond outlet from summer 2019 to winter 2020.

6.0 Conclusions

6.1 Key Findings

This study has shown that the multi-method approach using targeted data can provide insights to exposure in ecological zones, spatially and temporally, particularly for the endobenthic and epibenthic communities, which are not typically monitored. Hydrological data using water level piezometers, temperature rods, sediment temperature mapping, and outlet discharge measurements provided insights to the groundwater flow regime, and revealed temporal and spatial patterns, further discussed below. Contaminant data from shallow groundwater sampling campaigns (for leachate indicators, and contaminants of emerging concern), surface water sampling, and electrical conductivity at the pond sediment interface provided insight to the contaminant exposure patterns and contaminant mass entering the pond. The data combined showed that there was a leachate-affected groundwater plume impacting a larger area than previously anticipated. The shallow leachate plume extended about half the length of the pond and a third across showing that the leachate plume can extend further than expected. More specifically, the plume likely spanned 120 m along the Transect N-S and extended 25 m along Transect E-W starting from the east shore.

The landfill leachate plume had spatial heterogeneities as there were zones of elevated concentrations along with areas of high groundwater flux into the pond. For example, there were concentration peaks at 8 m and 21 m (for ammonium, chloride, PFAS) but peaks varied with saccharin (peaked at 3 m). Temperature-depth profiles from the temperature rods were used to calculate the groundwater flux entering the pond and

showed a high groundwater flux in the middle of the pond (31 m) and decreased towards the shores (east and west). The patterns of contaminant concentration and groundwater flux did not match up thereby demonstrating that exposure to endobenthic and epibenthic organisms can be different. However, if the peaks in concentrations and flux were to match up, it would result in contaminant hot spots affecting both benthic zones and this could be applicable to areas not monitored at the site and at other sites.

The contaminant data measured from the groundwater and surface water indicated that the plume entering the pond from the east shore is contaminated by landfill leachate, with the presence of elevated concentrations of many legacy contaminants (e.g., ammonium), but also emerging contaminants, including PFAS. This study provides more information on PFAS inputs with leachate-affected groundwater plumes discharging to a non-flowing surface water body. Notably, there was variation in the composition across the plume (Transect N-S) demonstrating variability within the plume itself. Measured electrical conductivity at the sediment interface corroborated that there were contaminants passing through the sediment interface into the pond. Furthermore, elevated concentrations measured in the pond surface water and at the outlet indicate impacts to the pond as well as downstream. These impacts vary seasonally, for instance nitrate and ammonium increased through the fall season into the winter while saccharin and chloride concentrations were consistent into the winter season.

Factors impacting groundwater to surface water interactions can influence the contaminant exposure and mass discharge patterns. The results of this study suggest that evapotranspiration may be important in creating diurnal and seasonal patterns in

contaminant flux. This process is broadly applicable at similar sites, and at sites with strong seasons. The contaminants appeared to persist in each ecological zone all year round however hydrological data suggested higher discharge into the pond at night, after precipitation events, and during the winter season, which can result in worse conditions at times not typically sampled. There was a strong diurnal signal in the water level data during the summer months likely due to evapotranspiration, and evaporation from the pond. The diurnal signal decreased through the fall and dissipated in the winter as the plants died or became dormant and no longer affected groundwater levels. In conclusion, contaminant data combined with hydrologic data provided quantitative evidence that this leachate plume impacted many areas in and around the pond, and temporally, the exposure was worse at night, after rain events, and during the winter season. This study demonstrates that historic landfill can be a contamination source to surface water bodies nearby.

6.2 Ecological Risks

The various datasets collected can provide insights to different parts of the ecosystem. First, shallow groundwater concentrations provide insight to the impacts on the endobenthic community. Next, the groundwater flux calculated using temperature depth data, as well as electrical conductivity above the sediment interface provide insights to impacts on the epibenthic community. Finally, the contaminant mass discharge measured at the pond outlet, and pond surface water concentrations give indications to the impacts on the pelagic community within the pond and downstream ecosystems. Based on the study's results, epibenthic zones generally experience worse conditions at night,

following rain events, and in the wintertime. The zone with greatest risk would be the endobenthic zone as they are experiencing contaminants not yet diluted by surface waters.

The aquatic plants could also potentially be negatively impacted by the leachate plume. Evidence of potential impacts are the bare patches on the pond floor, largely located at the northern side. There was also potential iron staining on the plants creating more orange-coloured leaves compared to the dark green leaves found at the southern side of the pond. The reduced coverage at the pond bottom could be linked to the leachate plume, but no data on this was collected in this study. Notably, there was a large bare patch seen at the north west side of the pond, where clean groundwater is likely discharging. However, the large empty patches on the west are potentially from vehicles driving along the pond as mentioned by the neighbouring residents.

6.3 Implications for Monitoring

Monitoring potentially contaminated groundwater discharging into a surface water body such as a pond can be challenging due to the heterogeneous nature of the groundwater flow regime and the contaminant fate and transport. Typical monitoring protocols (i.e., annual surface water/well sampling, generally in the summertime) could potentially miss impacted ecological zones (i.e., endobenthic/epibenthic zones) in ponds receiving leachate-affected groundwater. However, this study provides insight into these ecological zones and additional times in which monitoring programs would be more effective and capture more of the heterogeneity using targeted data. Sampling cost efficiency is important since higher resolution data require more time and resources. Based on the

results of this study, it is important to assess potential changes in impacts at night, following rain events, and during the wintertime because ecological zones are most likely experiencing worse conditions. It is also important to measure the endobenthic and epibenthic zones in the event of monitoring groundwater entering a surface water body because surface water samples will only indicate conditions the pelagic community is experiencing. Pelagic zone exposure can change over time from in-pond transformations (i.e., nitrification), and therefore annual surface water sampling in the summertime may not properly represent the landfill impacts. Finally, this study's results inform operators of historic landfills to also monitor contaminants of emerging concern such as PFAS as elevated concentrations pose health risk to humans and the surrounding ecosystem. However, analysis of PFAS is expensive and therefore not currently viable for regular sampling. Targeted sampling is useful to limit the number of samples needed, and this study provides insights to locations and times that will optimize the information that can be obtained (i.e., areas of high groundwater flux in the winter). As mentioned before, older landfills have greater possibility of leaking due to lack of infrastructure and can affect nearby surface water. Multiple locations should be sampled as one leachate well may not be representative of the concentrations found in the landfill leachate plume, especially because of various factors causing spatial and temporal variability.

6.4 Research Recommendations

A second step to this study would be to assess the impact of the contamination on aquatic communities within and around the pond. This is important because this study was able to determine the locations and times of high contaminant exposure but not the result of

said exposure. Ecotoxicity is currently being explored at this site to assess the impact on the aquatic organisms. To test, aquatic organisms are caged and placed on the pond bottom and observed over a month to compare survival rates. Additionally, pond sediment was sampled to compare the number and different types of endobenthic organisms within and outside the plume footprint. Locations were chosen based on this study's results to capture different exposure levels.

Furthermore, a preliminary investigation into phytoscreening was conducted this past year, though it was impeded by the pandemic. The uptake of saccharin in the cattails surrounding the pond may provide another important mechanism to determine impact on terrestrial organisms, and another possible pathway for emerging contaminants. Phytoscreening is useful for monitoring as well because it is easier and faster compared to groundwater sampling and can provide insights to potential contaminants in the groundwater within the extent of the plant's root system.

Data from the snowmelt period were not obtained due to the pandemic, as many of the data loggers, such as the iButtons and EC sensors, were overwritten or filled resulting in missing data from April and March. A final sampling campaign planned during that time was also not possible. Therefore, additional data during this period could potentially provide more insights into how snowmelt might affect groundwater to surface water interactions, and contaminant fluxes. Snowmelt data can provide insights to exposure levels to the ecosystem, especially during a time when organisms and plants become more active.

On a broader scale, it is recommended to continue to monitor PFAS in groundwater, particularly at older landfills, because it is a contaminant of emerging concern. There needs to be more data on the transport and fate of PFAS in different scenarios and the analyses should become more accessible (i.e., standardized sampling protocols, cheaper analysis methods). The multi-method study provides insights to other possible research designs that encompass more ecological zones and time scales. Additionally, this method can be applied to other contaminant plumes affecting a non-flowing surface water body, such as a pond.

7.0 References

Ančić, M., Huđek, A., Rihtarić, I., Cazar, M., Bačun-Družina, V., Kopjar, N., & Durgo, K. (2020). PHYSICO chemical properties and toxicological effect of landfill groundwaters and leachates. *Chemosphere*, *238*, 124574. https://doi.org/10.1016/j.chemosphere.2019.124574

Atekwana, E. A., & Krishnamurthy, R. V. (2004). Investigating landfill-impacted groundwater seepage into headwater streams using stable carbon isotopes. *Hydrological Processes*, *18*(10), 1915–1926. https://doi.org/10.1002/hyp.1457

Barker, J. (1987). Volatile Aromatic and Chlorinated Organic Contaminants in Groundwater at Six Ontario Landfills. *Water Quality Research Journal*, *22*(1), 33–48.

Baun, D. L., & Christensen, T. H. (2004). Speciation of Heavy Metals in Landfill Leachate: A Review. *Waste Management & Research*, *22*(1), 3–23. https://doi.org/10.1177/0734242X04042146

Bjerg, P. L., Tuxen, N., Reitzel, L. A., Albrechtsen, H.-J., & Kjeldsen, P. (2011). Natural Attenuation Processes in Landfill Leachate Plumes at Three Danish Sites. *Ground Water*, *49*(5), 688–705. https://doi.org/10.1111/j.1745-6584.2009.00613.x

Björnsdotter, M. K., Yeung, L. W. Y., Kärrman, A., & Jogsten, I. E. (2019). Ultra-Short-Chain Perfluoroalkyl Acids Including Trifluoromethane Sulfonic Acid in Water Connected to Known and Suspected Point Sources in Sweden. *Environmental Science & Technology*, *53*(19), 11093–11101. https://doi.org/10.1021/acs.est.9b02211

Borden, R. C., & Yanoschak, T. M. (1990). GROUND AND SURFACE WATER QUALITY IMPACTS OF NORTH CAROLINA SANITARY LANDFILLS1. *JAWRA Journal of the American Water Resources Association*, *26*(2), 269–277. https://doi.org/10.1111/j.1752-1688.1990.tb01370.x

Brandsma, S. H., Koekkoek, J. C., van Velzen, M. J. M., & de Boer, J. (2019). The PFOA substitute GenX detected in the environment near a fluoropolymer manufacturing plant in the Netherlands. *Chemosphere*, *220*, 493–500. https://doi.org/10.1016/j.chemosphere.2018.12.135

Bredehoeft, J. D., and Papaopulos, I. S. (1965), Rates of vertical groundwater movement estimated from the Earth's thermal profile, Water Resour. Res., 1(2), 325– 328, doi:10.1029/WR001i002p00325.

Brett, J. R. (1974). Tank experiments on the culture of pan-size sockeye (Oncorhynchus nerka) and pink salmon (O. gorbuscha) using environmental control. *Aquaculture*, *4*, 341–352. https://doi.org/10.1016/0044-8486(74)90063-5

Briggs, M. A., & Hare, D. K. (2018). Explicit consideration of preferential groundwater discharges as surface water ecosystem control points. *Hydrological Processes*, *32*(15), 2435–2440. https://doi.org/10.1002/hyp.13178

Buszka, P. M., Yeskis, D. J., Kolpin, D. W., Furlong, E. T., Zaugg, S. D., & Meyer, M. T. (2009). Waste-Indicator and Pharmaceutical Compounds in Landfill-Leachate-Affected Ground Water near Elkhart, Indiana, 2000–2002. *Bulletin of Environmental Contamination and Toxicology*, *82*(6), 653–659. https://doi.org/10.1007/s00128-009-9702-z

Canadian Council of Ministers of the Environment (CCME). (2001). Canadian water quality guidelines for the protection of aquatic life: Ammonia. In: Canadian environmental quality guidelines, 2001, Canadian Council of Ministers of the Environment, Winnipeg, MB.

Canadian Council of Ministers of the Environment (CCME). (2011). Canadian water quality guidelines for the protection of aquatic life: Chloride. In: Canadian environmental quality guidelines, 2011, Canadian Council of Ministers of the Environment, Winnipeg, MB.

Cejudo, E., Taylor, W., & Schiff, S. (2020). Epilithic algae from an urban river preferentially use ammonium over nitrate. *International Aquatic Research*, *Online First*. https://doi.org/10.22034/iar(20).2020.671068

Christensen, T. H., Kjeldsen, P., Bjerg, P. L., Jensen, D. L., Christensen, J. B., Baun, A., Albrechtsen, H.-J., & Heron, G. (2001). Biogeochemistry of landfill leachate plumes. *Applied Geochemistry*, 60.

Coakley, J. P. (1989). Contamination Hazard from Waste Disposal Sites near Receding Great Lakes Shorelines. *Water Quality Research Journal*, *24*(1), 81–100. https://doi.org/10.2166/wqrj.1989.005

Conant, B. (2004). Delineating and Quantifying Ground Water Discharge Zones Using Streambed Temperatures. *National Ground Water Association*, *42*(2), 243–257. https://doi.org/10.1111/j.1745-6584.2004.tb02671.x

Conant, B., Robinson, C. E., Hinton, M. J., & Russell, H. A. J. (2019). A framework for conceptualizing groundwater-surface water interactions and identifying

potential impacts on water quality, water quantity, and ecosystems. *Journal of Hydrology*, *574*, 609–627. https://doi.org/10.1016/j.jhydrol.2019.04.050

Cousins, I. T., Vestergren, R., Wang, Z., Scheringer, M., & McLachlan, M. S. (2016). The precautionary principle and chemicals management: The example of perfluoroalkyl acids in groundwater. *Environment International*, *94*, 331–340. https://doi.org/10.1016/j.envint.2016.04.044

Cozzarelli, I. M., Böhlke, J. K., Masoner, J., Breit, G. N., Lorah, M. M., Tuttle, M. L. W., & Jaeschke, J. B. (2011). Biogeochemical Evolution of a Landfill Leachate Plume, Norman, Oklahoma. *Ground Water*, *49*(5), 663–687. https://doi.org/10.1111/j.1745-6584.2010.00792.x

D'Agostino, L. A., & Mabury, S. A. (2017). Certain Perfluoroalkyl and Polyfluoroalkyl Substances Associated with Aqueous Film Forming Foam Are Widespread in Canadian Surface Waters. *Environmental Science & Technology*, *51*(23), 13603–13613. https://doi.org/10.1021/acs.est.7b03994

Dickman, M., & Rygiel, G. (1998). Municipal landfill impacts on a natural stream located in an urban wetland in regional Niagara, Ontario. *Canadian Field Naturalist*, *112*, 619–630.

Directive 2013/39/EU of the European Parliament and of the Council of 12 August 2013 amending Directives 2000/60/EC and 2008/105/EC as regards priority substances in the field of water policy. Official Journal of the European Union L226/1-L226/17 [online]. http://eur-lex.europa.eu/legal-content/EN/TXT/PDF/?uri=CELEX:32013L0039&from=EN (accessed March 11, 2021).

Douglass, J. L., & Borden, R. C. (1992). The Impact of a Piedmont Sanitary Landfill on Surface and Ground Water Quality. *Water Resources Research Institute, 226*.

Environment and Climate Change Canada (ECCC). (2018a). Federal Environmental Quality Guidelines: Perfluorooctane Sulfonate (PFOS). https://www.canada.ca/en/health-canada/services/chemical-substances/fact-sheets/federal-environmental-quality-guidelines.html#a8 (accessed March 11, 2021)

Fitzgerald, A., Roy, J. W., & Smith, J. E. (2015). Calculating discharge of phosphorus and nitrogen with groundwater base flow to a small urban stream reach. *Journal of Hydrology*, *528*, 138–151. https://doi.org/10.1016/j.jhydrol.2015.06.038

Ford, R. G., Acree, S. D., Lien, B. K., Scheckel, K. G., Luxton, T. P., Ross, R. R., Williams, A. G., & Clark, P. (2011). Delineating landfill leachate discharge to an arsenic contaminated waterway. *Chemosphere*, *85*(9), 1525–1537. https://doi.org/10.1016/j.chemosphere.2011.09.046

Gewurtz, S. B., Bradley, L. E., Backus, S., Dove, A., McGoldrick, D., Hung, H., & Dryfhout-Clark, H. (2019). Perfluoroalkyl Acids in Great Lakes Precipitation and Surface Water (2006–2018) Indicate Response to Phase-outs, Regulatory Action, and Variability in Fate and Transport Processes. *Environmental Science & Technology*, *53*(15), 8543–8552. https://doi.org/10.1021/acs.est.9b01337

Gooddy, D. C., Macdonald, D. M. J., Lapworth, D. J., Bennett, S. A., & Griffiths, K. J. (2014). Nitrogen sources, transport and processing in peri-urban floodplains. *Science of The Total Environment*, *494–495*, 28–38. https://doi.org/10.1016/j.scitotenv.2014.06.123

Gyllenhammar, I., Benskin, J. P., Sandblom, O., Berger, U., Ahrens, L., Lignell, S., Wiberg, K., & Glynn, A. (2019). Perfluoroalkyl Acids (PFAAs) in Children's Serum and Contribution from PFAA-Contaminated Drinking Water. *Environmental Science & Technology*, *53*(19), 11447–11457. https://doi.org/10.1021/acs.est.9b01746

Hamid, H., Li, L. Y., & Grace, J. R. (2018). Review of the fate and transformation of per- and polyfluoroalkyl substances (PFASs) in landfills. *Environmental Pollution*, *235*, 74–84. https://doi.org/10.1016/j.envpol.2017.12.030

Harrad, S., Drage, D. S., Sharkey, M., & Berresheim, H. (2019). Brominated flame retardants and perfluoroalkyl substances in landfill leachate from Ireland. *Science of The Total Environment*, *695*, 133810. https://doi.org/10.1016/j.scitotenv.2019.133810

Hayashi, M. (2004). Temperature-Electrical Conductivity Relation of Water for Environmental Monitoring and Geophysical Data Inversion. *Environmental Monitoring and Assessment*, *96*(1–3), 119–128. https://doi.org/10.1023/B:EMAS.0000031719.83065.68

Hepburn, E., Madden, C., Szabo, D., Coggan, T. L., Clarke, B., & Currell, M. (2019). Contamination of groundwater with per- and polyfluoroalkyl substances (PFAS) from legacy landfills in an urban re-development precinct. *Environmental Pollution*, *248*, 101–113. https://doi.org/10.1016/j.envpol.2019.02.018

Howard, K. W. F., Eyles, N., & Livingstone, S. (1996). Municipal Landfilling Practice And Its Impact On Groundwater Resources In And Around Urban

Toronto, Canada. *Hydrogeology Journal*, *4*(1), 64–79. https://doi.org/10.1007/s100400050092

Kidmose, J., Nilsson, B., Engesgaard, P., Frandsen, M., Karan, S., Landkildehus, F., Søndergaard, M., & Jeppesen, E. (2013). Focused groundwater discharge of phosphorus to a eutrophic seepage lake (Lake Væng, Denmark): Implications for lake ecological state and restoration. *Hydrogeology Journal*, *21*(8), 1787–1802. https://doi.org/10.1007/s10040-013-1043-7

Kjeldsen, P., Barlaz, M. A., Rooker, A. P., Baun, A., Ledin, A., & Christensen, T. H. (2002). Present and Long-Term Composition of MSW Landfill Leachate: A Review. *Critical Reviews in Environmental Science and Technology*, *32*(4), 297–336. https://doi.org/10.1080/10643380290813462

Kjeldsen, P., & Christophersen, M. (2001). Composition of leachate from old landfills in Denmark. *Waste Management & Research*, *19*(3), 249–256. https://doi.org/10.1177/0734242X0101900306

Kurylyk, B. L., Irvine, D. J., & Bense, V. F. (2019). Theory, tools, and multidisciplinary applications for tracing groundwater fluxes from temperature profiles. *Wiley Interdisciplinary Reviews: Water*, *6*(1), e1329. https://doi.org/10.1002/wat2.1329

Kurylyk, B. L., Irvine, D. J., Carey, S. K., Briggs, M. A., Werkema, D. D., & Bonham, M. (2017). Heat as a groundwater tracer in shallow and deep heterogeneous media: Analytical solution, spreadsheet tool, and field applications. *Hydrological Processes*, *31*(14), 2648–2661. https://doi.org/10.1002/hyp.11216

Lapham, W. W. (1989). *Use of temperature profiles beneath streams to determine rates of vertical ground-water flow and vertical hydraulic conductivity* (Report No. 2337; Water Supply Paper). USGS Publications Warehouse. https://doi.org/10.3133/wsp2337

Li, B., Danon-Schaffer, M. N., Li, L. Y., Ikonomou, M. G., & Grace, J. R. (2012). Occurrence of PFCs and PBDEs in Landfill Leachates from Across Canada. *Water, Air, & Soil Pollution*, *223*(6), 3365–3372. https://doi.org/10.1007/s11270-012-1115-7

Lisk, D. J. (1991). Environmental effects of landfills. *Science of The Total Environment*, *100*, 415–468. https://doi.org/10.1016/0048-9697(91)90387-T

Liu, S., Yang, R., Yin, N., & Faiola, F. (2020). The short-chain perfluorinated compounds PFBS, PFHxS, PFBA and PFHxA, disrupt human mesenchymal

stem cell self-renewal and adipogenic differentiation. *Journal of Environmental Sciences*, *88*, 187–199. https://doi.org/10.1016/j.jes.2019.08.016

Lorah, M. M., Cozzarelli, I. M., & Böhlke, J. K. (2009). Biogeochemistry at a wetland sediment–alluvial aquifer interface in a landfill leachate plume. *Journal of Contaminant Hydrology*, *105*(3–4), 99–117. https://doi.org/10.1016/j.jconhyd.2008.11.008

Luo, J., Wu, L., Zhang, Q., Wu, Y., Fang, F., Feng, Q., Li, C., Xue, Z., & Cao, J. (2019). Review on the determination and distribution patterns of a widespread contaminant artificial sweetener in the environment. *Environmental Science and Pollution Research*, *26*(19), 19078–19096. https://doi.org/10.1007/s11356-019-05261-4

Maqbool, F., Bhatti, Bhatti, Z., Malik, Pervez, & Mahmood, Q. (2011). Effect of Landfill Leachate on the Water Quality of the Salhad Stream in Abbottabad, Pakistan. *International Journal of Environmental Research*, *5*, 491–500.

Masoner, J. R., Kolpin, D. W., Cozzarelli, I. M., Barber, L. B., Burden, D. S., Foreman, W. T., Forshay, K. J., Furlong, E. T., Groves, J. F., Hladik, M. L., Hopton, M. E., Jaeschke, J. B., Keefe, S. H., Krabbenhoft, D. P., Lowrance, R., Romanok, K. M., Rus, D. L., Selbig, W. R., Williams, B. H., & Bradley, P. M. (2019). Urban Stormwater: An Overlooked Pathway of Extensive Mixed Contaminants to Surface and Groundwaters in the United States. *Environmental Science & Technology*, *53*(17), 10070–10081. https://doi.org/10.1021/acs.est.9b02867

Masoner, J. R., Kolpin, D. W., Cozzarelli, I. M., Smalling, K. L., Bolyard, S. C., Field, J. A., Furlong, E. T., Gray, J. L., Lozinski, D., Reinhart, D., Rodowa, A., & Bradley, P. M. (2020). Landfill leachate contributes per-/poly-fluoroalkyl substances (PFAS) and pharmaceuticals to municipal wastewater. *Environmental Science: Water Research & Technology*, *6*(5), 1300–1311. https://doi.org/10.1039/D0EW00045K

McMahon, P. B., & Chapelle, F. H. (2008). Redox Processes and Water Quality of Selected Principal Aquifer Systems. *Ground Water*, *46*(2), 259–271. https://doi.org/10.1111/j.1745-6584.2007.00385.x

Milley, S. A., Koch, I., Fortin, P., Archer, J., Reynolds, D., & Weber, K. P. (2018). Estimating the number of airports potentially contaminated with perfluoroalkyl and polyfluoroalkyl substances from aqueous film forming foam: A Canadian example. *Journal of Environmental Management*, *222*, 122–131. https://doi.org/10.1016/j.jenvman.2018.05.028

Milosevic, N., Thomsen, N. I., Juhler, R. K., Albrechtsen, H.-J., & Bjerg, P. L. (2012a). Identification of discharge zones and quantification of contaminant mass discharges into a local stream from a landfill in a heterogeneous geologic setting. *Journal of Hydrology*, *446–447*, 13–23. https://doi.org/10.1016/j.jhydrol.2012.04.012

Milosevic, N., Thomsen, N. I., Juhler, R. K., Albrechtsen, H.-J., & Bjerg, P. L. (2012b). Identification of discharge zones and quantification of contaminant mass discharges into a local stream from a landfill in a heterogeneous geologic setting. *Journal of Hydrology*, *446–447*, 13–23. https://doi.org/10.1016/j.jhydrol.2012.04.012

Mullaney, J. R., Lorenz, D. L., & Arntson, A. D. (2009). *Chloride in Groundwater and Surface Water in Areas Underlain by the Glacial Aquifer System, Northern United States* (Report No. 2009–5086; Scientific Investigations Report). USGS Publications Warehouse. https://doi.org/10.3133/sir20095086

Musolff, A., Leschik, S., Reinstorf, F., Strauch, G., & Schirmer, M. (2010). Micropollutant Loads in the Urban Water Cycle. *Environmental Science & Technology*, *44*(13), 4877–4883. https://doi.org/10.1021/es903823a

Parisio, S., Keimowitz, A. R., Simpson, H. J., Lent, A., & Blackman, V. (2006). Arsenic-Rich Iron Floc Deposits in Seeps Downgradient of Solid Waste Landfills. *Soil and Sediment Contamination: An International Journal*, *15*(5), 443–453. https://doi.org/10.1080/15320380600846775

Propp, V. R., De Silva, A. O., Spencer, C., Brown, S. J., Catingan, S. D., Smith, J. E., & Roy, J. W. (2021). Organic contaminants of emerging concern in leachate of historic municipal landfills. *Environmental Pollution*, *276*, 116474. https://doi.org/10.1016/j.envpol.2021.116474

Pukacz, A., Pełechaty, M., & Frankowski, M. (2016). Depth-dependence and monthly variability of charophyte biomass production: Consequences for the precipitation of calcium carbonate in a shallow Chara-lake. *Environmental Science and Pollution Research*, *23*(22), 22433–22442. https://doi.org/10.1007/s11356-016-7420-8

Rodowa, A. E., Christie, E., Sedlak, J., Peaslee, G. F., Bogdan, D., DiGuiseppi, B., & Field, J. A. (2020). Field Sampling Materials Unlikely Source of Contamination for Perfluoroalkyl and Polyfluoroalkyl Substances in Field Samples. *Environmental Science & Technology Letters*, *7*(3), 156–163. https://doi.org/10.1021/acs.estlett.0c00036

Rosenberry, D. O., Bukaveckas, P. A., Buso, D. C., & Likens, G. E. (1999). Movement of Road Salt to a Small New Hampshire Lake. *Water, Air, & Soil Pollution*, *109*(1–4), 179–206. https://doi.org/10.1023/A:1005041632056

Roy, James W. (2019). Endobenthic Organisms Exposed to Chronically High Chloride from Groundwater Discharging along Freshwater Urban Streams and Lakeshores. *Environmental Science & Technology*, *53*(16), 9389–9397. https://doi.org/10.1021/acs.est.9b02288

Roy, James W., & Bickerton, G. (2010). Proactive Screening Approach for Detecting Groundwater Contaminants along Urban Streams at the Reach-Scale. *Environmental Science & Technology*, *44*(16), 6088–6094. https://doi.org/10.1021/es101492x

Roy, James W., Van Stempvoort, D. R., & Bickerton, G. (2014). Artificial sweeteners as potential tracers of municipal landfill leachate. *Environmental Pollution*, *184*, 89–93. https://doi.org/10.1016/j.envpol.2013.08.021

Roy, J.W., Grapentine, L., & Bickerton, G. (2018). Ecological effects from groundwater contaminated by volatile organic compounds on an urban stream's benthic ecosystem. *Limnologica*, *68*, 115–129. https://doi.org/10.1016/j.limno.2017.01.004

Sabel, G. V., & Clark, T. P. (1984). Volatile organic compounds as indicators of municipal solid waste leachate contamination. *Waste Management & Research*, *2*(2), 119–130. https://doi.org/10.1016/0734-242X(84)90135-6

Sebok, E., Duque, C., Kazmierczak, J., Engesgaard, P., Nilsson, B., Karan, S., & Frandsen, M. (2013). High-resolution distributed temperature sensing to detect seasonal groundwater discharge into Lake Vaeng, Denmark: SEASONAL DISCHARGE INTO LAKE VAENG. *Water Resources Research*, *49*(9), 5355–5368. https://doi.org/10.1002/wrcr.20436

Shan, C., & Bodvarsson, G. (2004). An analytical solution for estimating percolation rate by fitting temperature profiles in the vadose zone. *Journal of Contaminant Hydrology*, *68*(1–2), 83–95. https://doi.org/10.1016/S0169-7722(03)00126-8

South Australia EPA. (2019). *EPA Guidelines for environmental management of landfill facilities (municipal solid waste and commercial and industrial general waste).* Environment Protection Authority. http://www.epa.sa.gov.au/pdfs/guide_landfill.pdf

Stallman, R.W. (1963). Computation of groundwater velocity from temperature data. In: Bentall, R. (Ed.), Methods of Collecting and Interpreting Ground-Water Data, Water Supply Paper 1544-H, USGS, Washington, DC, pp. 36–46

Stefania, G. A., Rotiroti, M., Buerge, I. J., Zanotti, C., Nava, V., Leoni, B., Fumagalli, L., & Bonomi, T. (2019). Identification of groundwater pollution sources in a landfill site using artificial sweeteners, multivariate analysis and transport modeling. *Waste Management*, *95*, 116–128. https://doi.org/10.1016/j.wasman.2019.06.010

Stolte, S., Steudte, S., Schebb, N. H., Willenberg, I., & Stepnowski, P. (2013). Ecotoxicity of artificial sweeteners and stevioside. *Environment International*, *60*, 123–127. https://doi.org/10.1016/j.envint.2013.08.010

Stuart, M., Lapworth, D., Crane, E., & Hart, A. (2012). Review of risk from potential emerging contaminants in UK groundwater. *Science of The Total Environment*, *416*, 1–21. https://doi.org/10.1016/j.scitotenv.2011.11.072

Thomsen, N. I., Milosevic, N., & Bjerg, P. L. (2012a). Application of a contaminant mass balance method at an old landfill to assess the impact on water resources. *Waste Management*, *32*(12), 2406–2417. https://doi.org/10.1016/j.wasman.2012.06.014

Thomsen, N. I., Milosevic, N., & Bjerg, P. L. (2012b). Application of a contaminant mass balance method at an old landfill to assess the impact on water resources. *Waste Management*, *32*(12), 2406–2417. https://doi.org/10.1016/j.wasman.2012.06.014

Toran, L., Nyquist, J., Rosenberry, D., Gagliano, M., Mitchell, N., & Mikochik, J. (2015). Geophysical and Hydrologic Studies of Lake Seepage Variability. *Groundwater*, *53*(6), 841–850. https://doi.org/10.1111/gwat.12309

Townley, L. R., & Trefry, M. G. (2000). Surface water-groundwater interaction near shallow circular lakes: Flow geometry in three dimensions. *Water Resources Research*, *36*(4), 935–948. https://doi.org/10.1029/1999WR900304

Turnipseed, D. P., & Sauer, V. B. (2010). Discharge Measurements at Gaging Stations. Chapter 8 of Book 3, Section A. In *U.S. Geological Survey Techniques and Methods* (p. 87). U.S. Geological Survey.

Van Stempvoort, D. R., Roy, J. W., Grabuski, J., Brown, S. J., Bickerton, G., & Sverko, E. (2013). An artificial sweetener and pharmaceutical compounds as co-tracers of urban wastewater in groundwater. *Science of The Total Environment*, *461–462*, 348–359. https://doi.org/10.1016/j.scitotenv.2013.05.001

Van Stempvoort, D. R., Spoelstra, J., Brown, S. J., Robertson, W. D., Post, R., & Smyth, S. A. (2019). Sulfamate in environmental waters. *Science of The Total Environment*, *695*, 133734. https://doi.org/10.1016/j.scitotenv.2019.133734

Walter, D., Masterson, J. P., & LeBlanc, D. R. (2002). *Simulated pond-aquifer interactions under natural and stressed conditions near Snake Pond, Cape Cod, Massachusetts* (Report No. 99–4174; Water-Resources Investigations Report). USGS Publications Warehouse. https://doi.org/10.3133/wri994174

Winter, T. C., Harvey, J. W., Franke, O. L., & Alley, W. M. (1998). *Ground water and surface water: A single resource* (Report No. 1139; Circular). USGS Publications Warehouse. https://doi.org/10.3133/cir1139

WSP. (2018). *[HB] Landfill—Closed 2018 Water Monitoring Report* (No. 111-53037–09). [full citation available upon request]

Youcai, Z. (2018). *Pollution Control Technology for Leachate from Municipal Solid Waste*. Elsevier. https://doi.org/10.1016/C2017-0-03224-X

Appendix A

Supplemental Figure and Tables

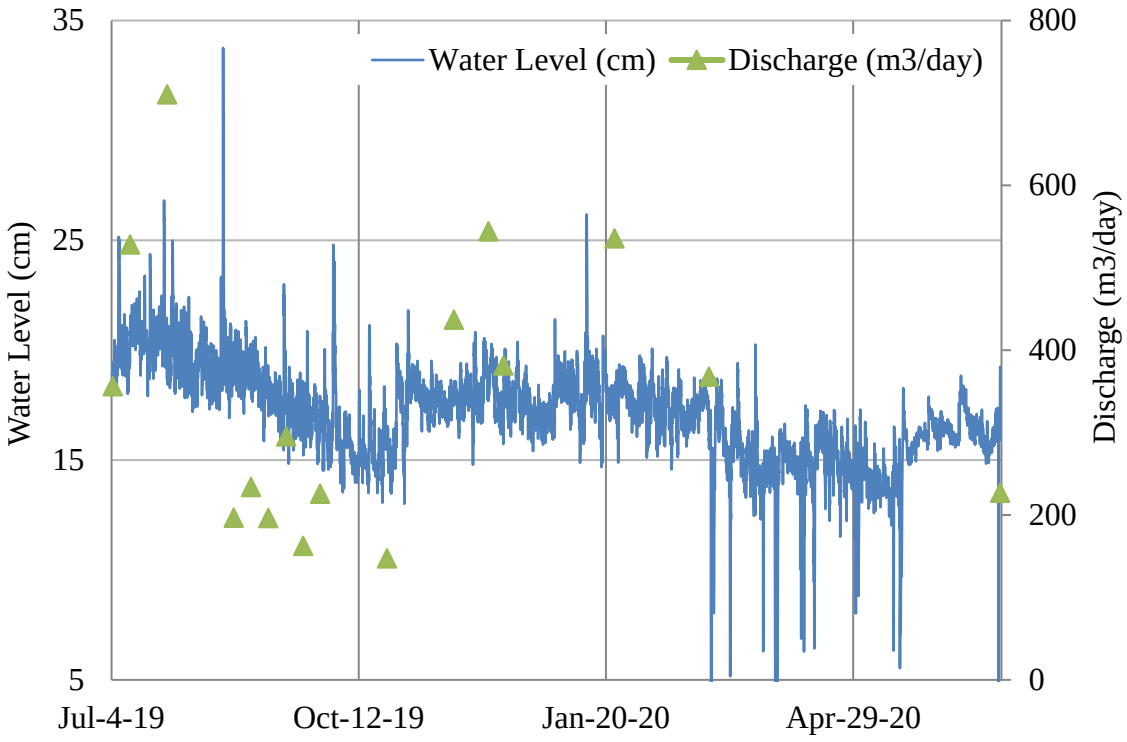

Figure A1: Outlet water level (cm) with discharge measurements over time

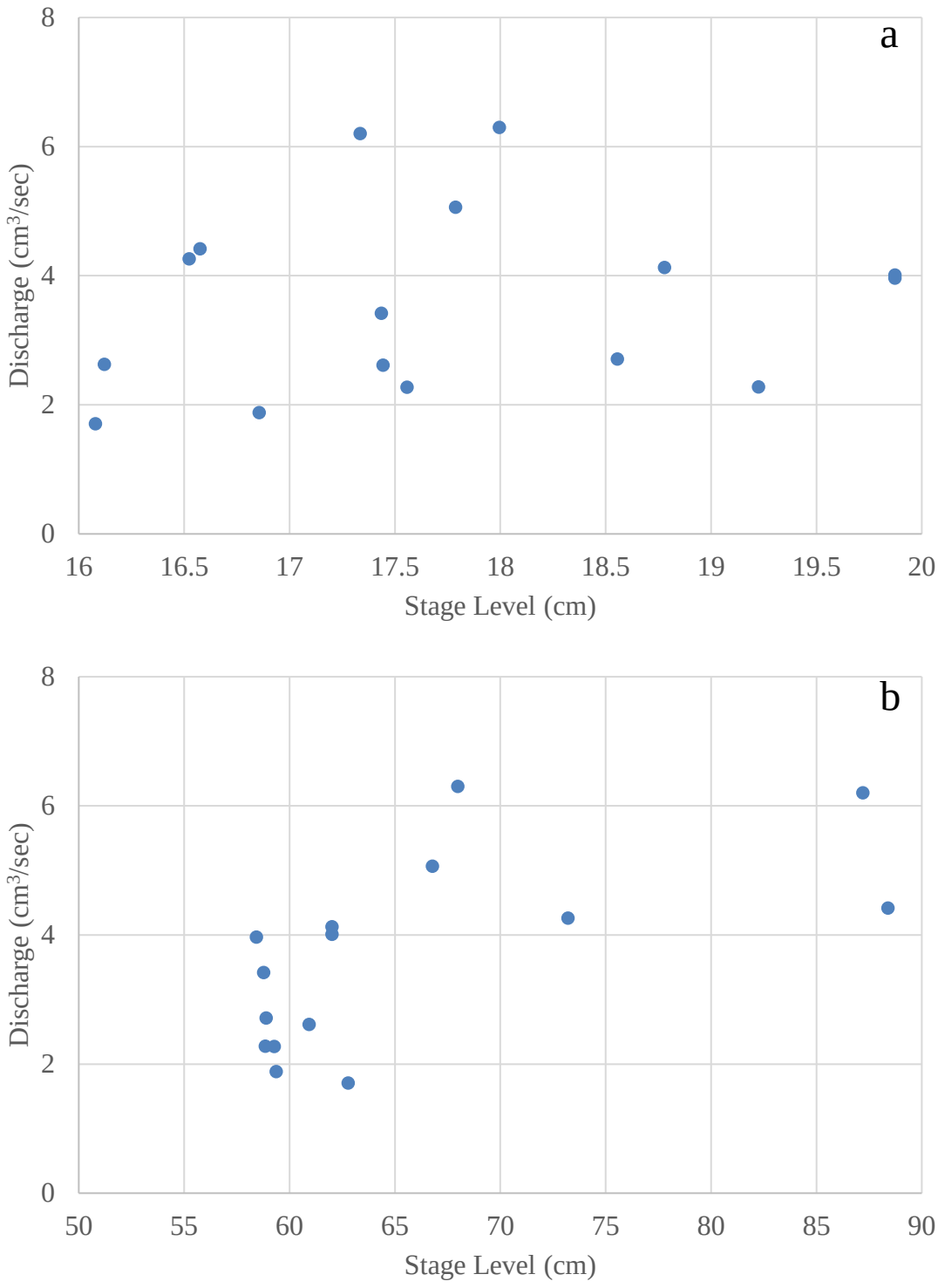

Figure A2: Rating curve for a) stream stage level at the outlet b) pond water level

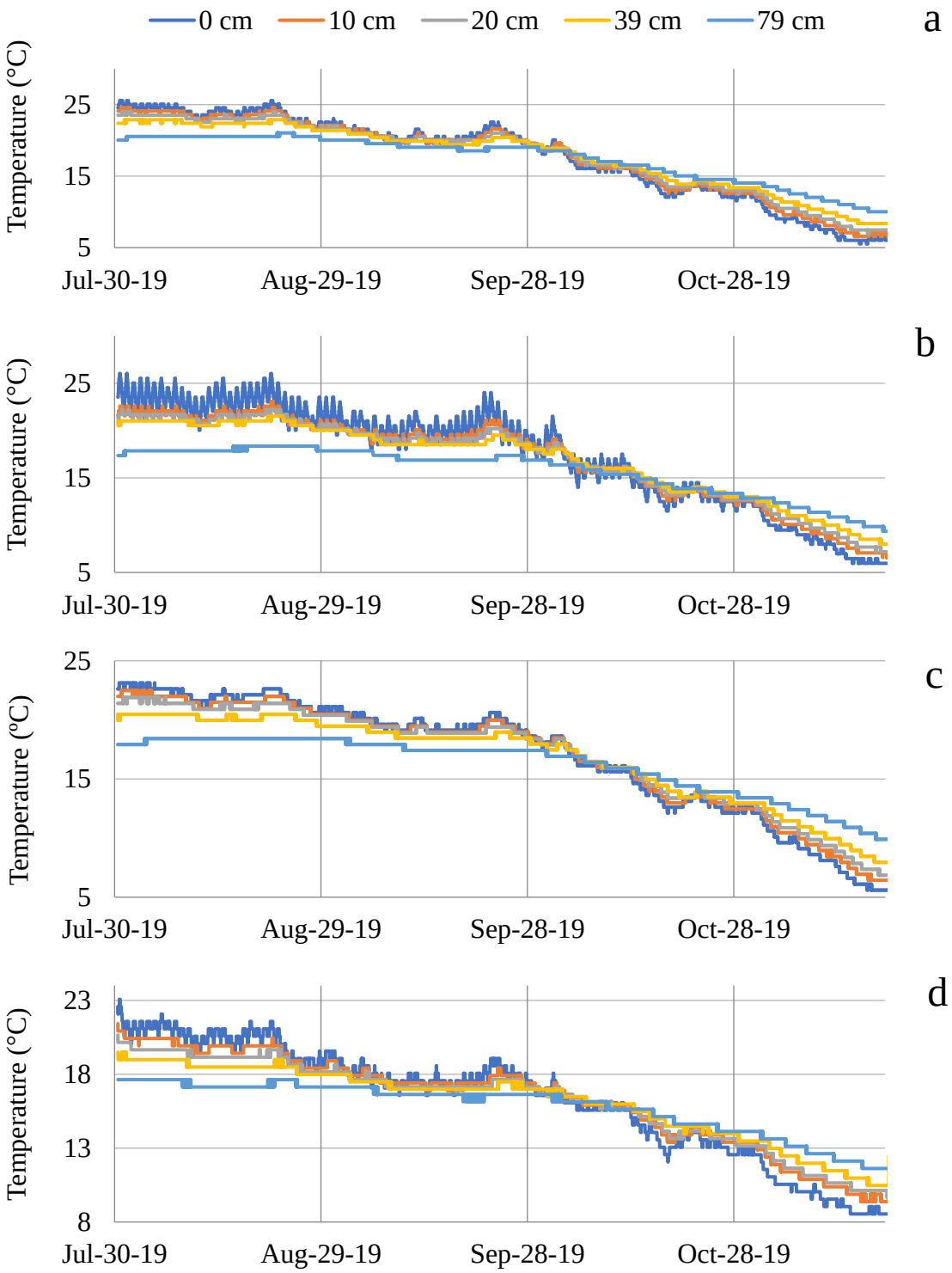

Figure A3a: Temperature data from iButtons within Temperature rods a) TR-WS1 b) TR-WN7 c) TR-T3 d) TR-T13 for July 2019 to November 2019, first period

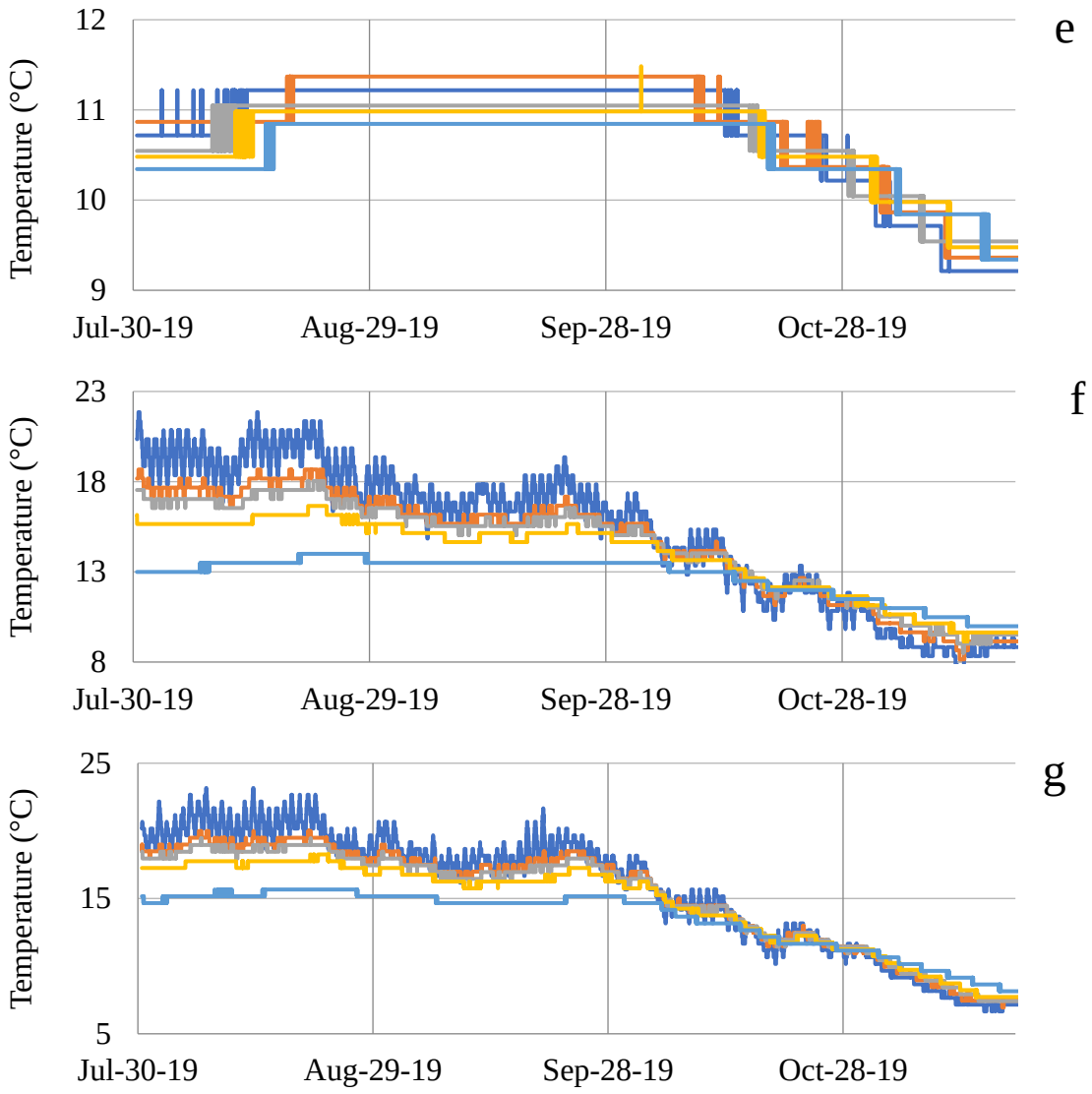

Figure A3b: Temperature data from iButtons within Temperature rods e) TR-T31 f) TR-T43 g) TR-T66 for July 2019 to November 2019, first period

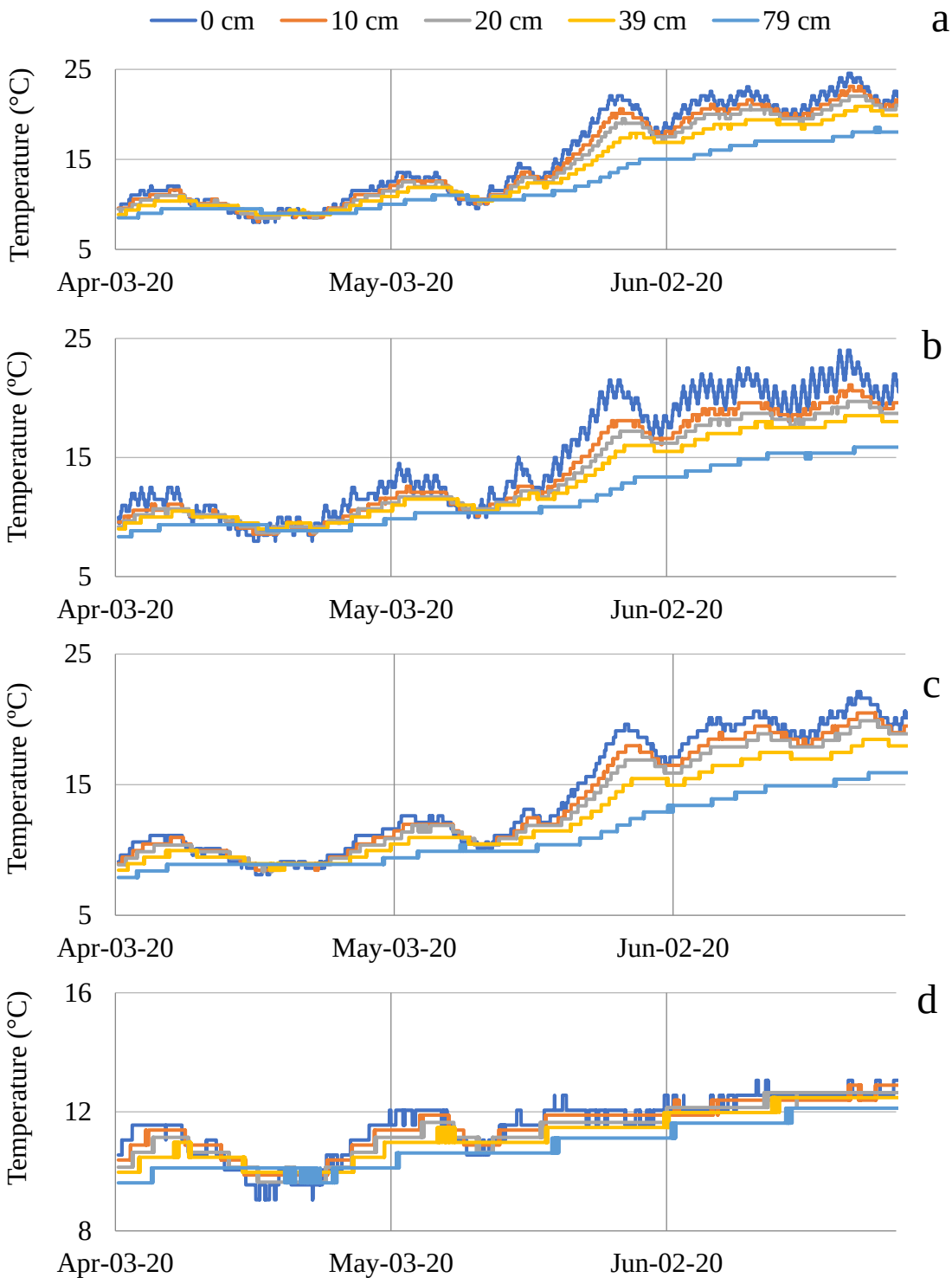

Figure A4a: Temperature data from iButtons within Temperature rods a) TR-WS1 b) TR-WN7 c) TR-T3 d) TR-T13 for April 2020 to June 2020.

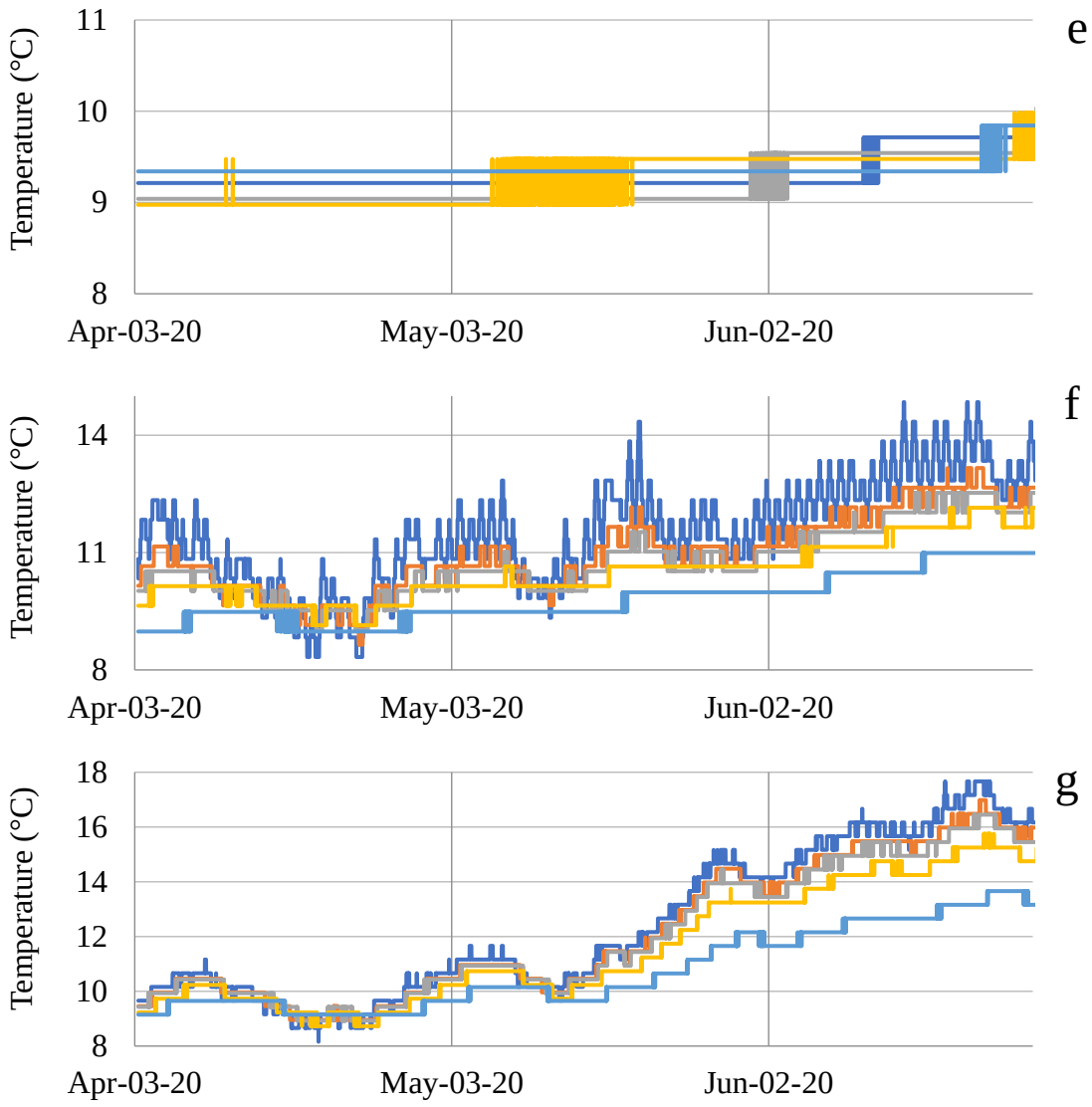

Figure A4b: Temperature data from iButtons within Temperature rods e) TR-T31 f) TR-T43 g) TR-T66 for April 2020 to June 2020.

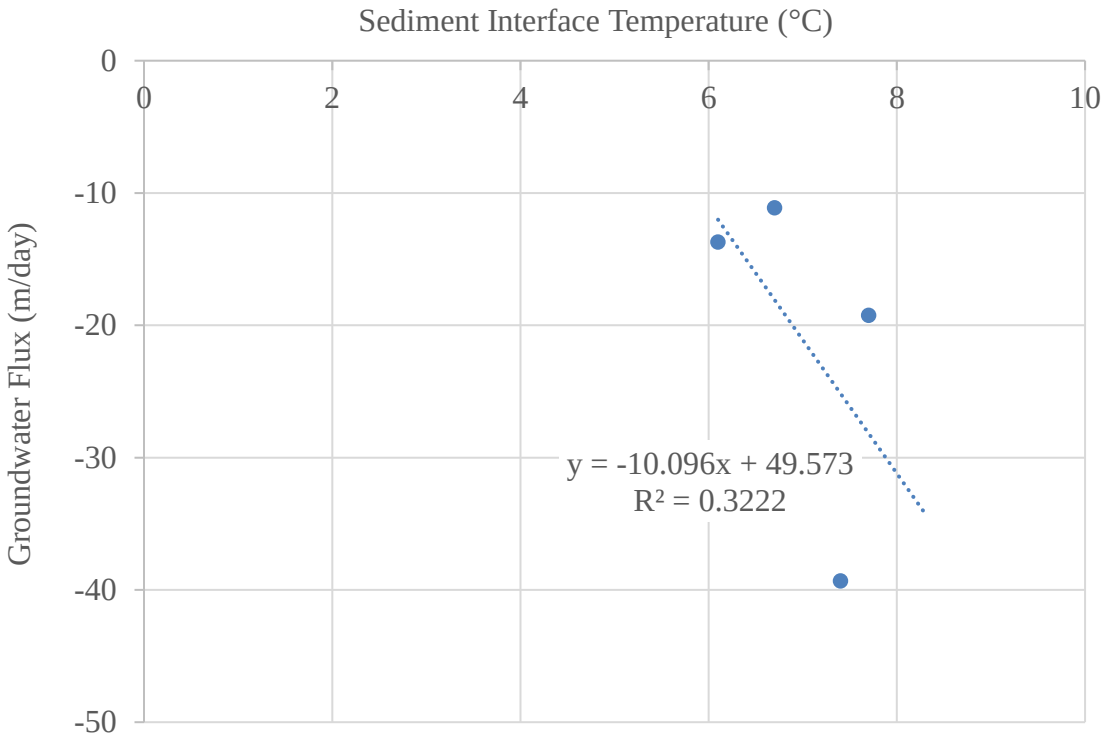

Figure A5: Sediment surface temperature versus groundwater flux along Transect E-W on December 10, 2019. Linear relationship used to calculate interpolated groundwater fluxes. R2 value= 0.3222. Without a measured value at 31 m due to the temperature profile being too vertical, the fit is too poor to be used to interpolate groundwater flux.

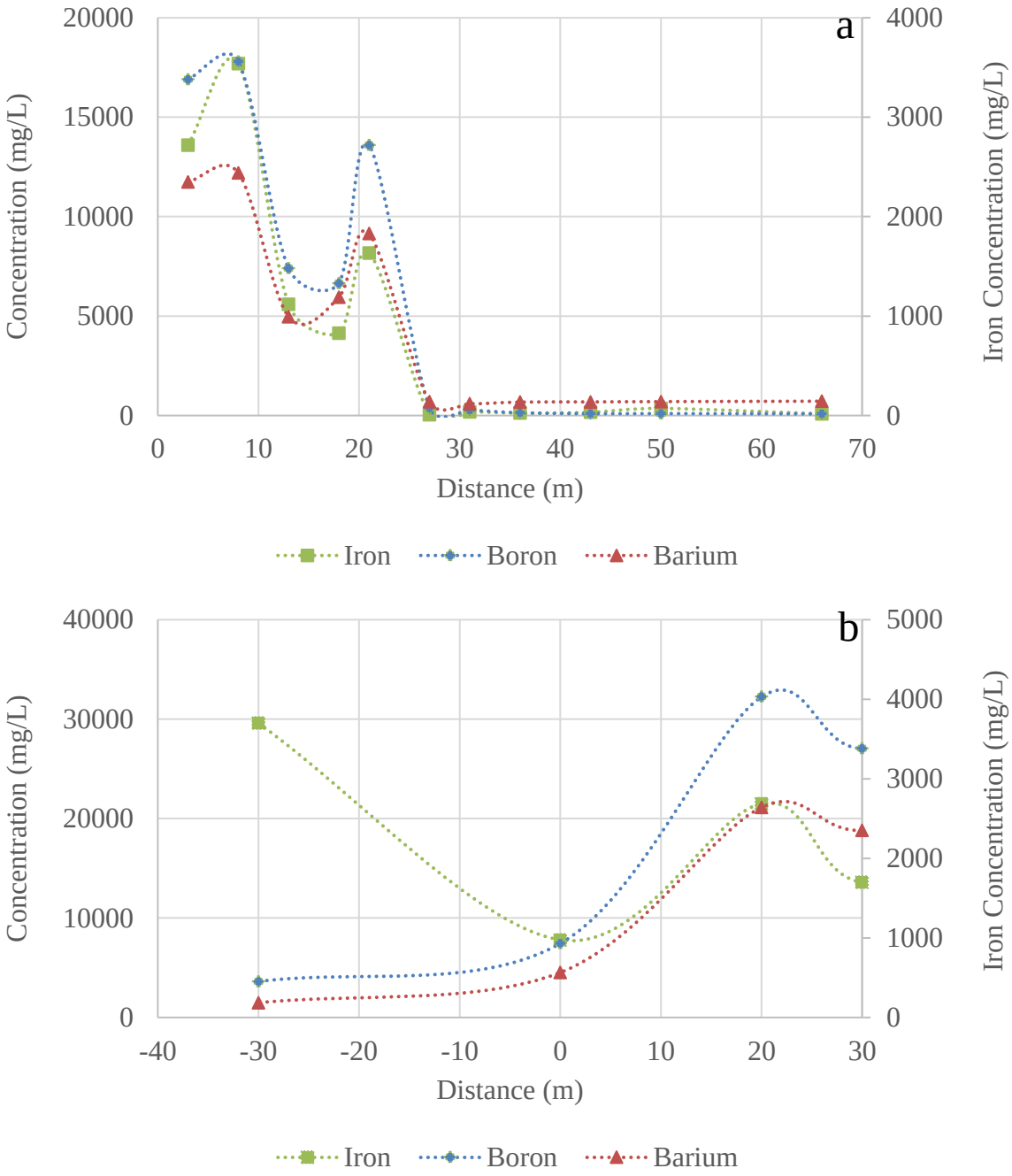

Figure A6a. Other parameters measured such as dissolved metals along a) Transect E-W and b) Transect N-S during the August sampling campaign depicting very similar trends. For the north and south transect plots, WS1 = 0m, and north is to the right of the graph

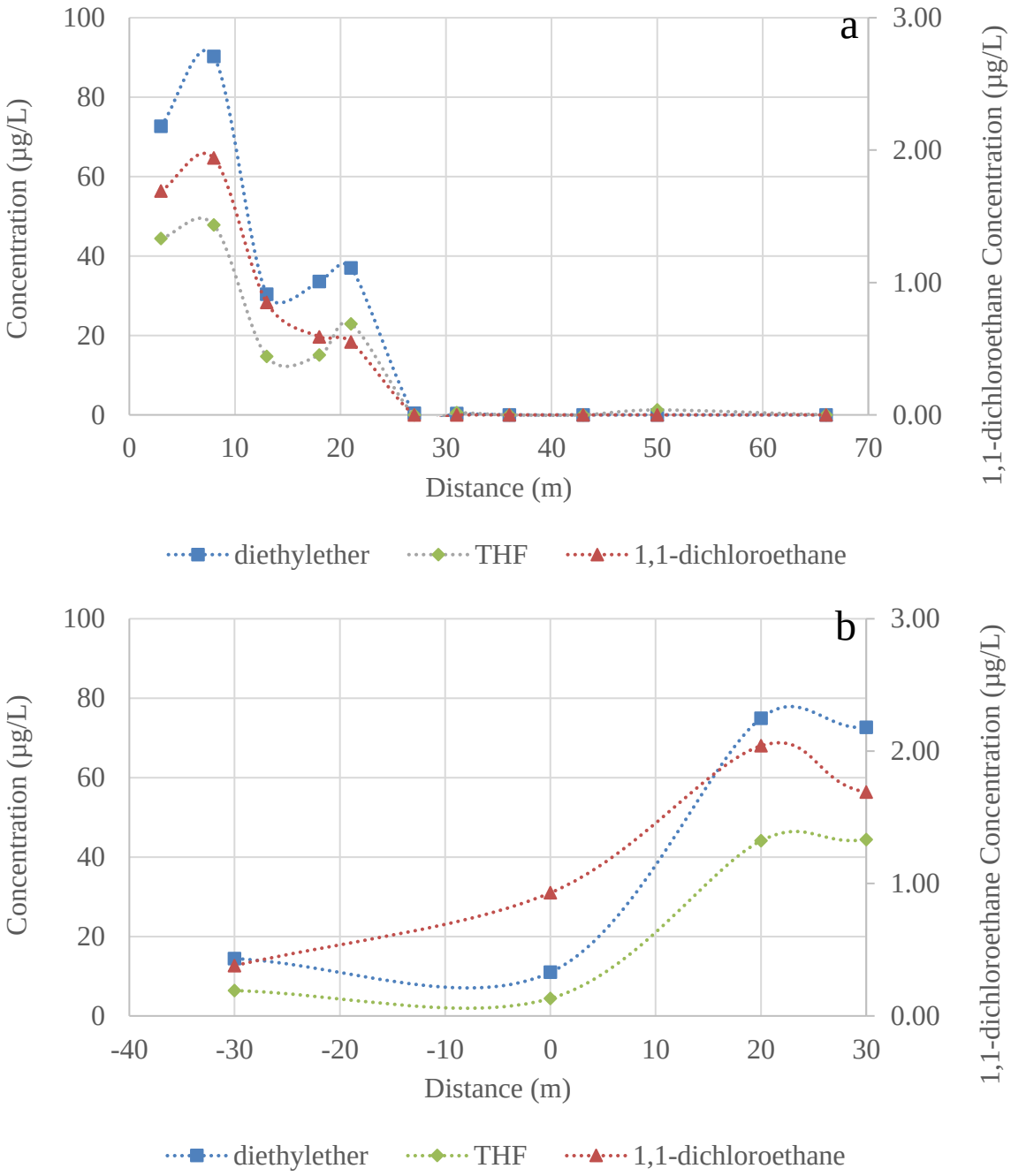

Figure A6b. Other parameters measured such as VOCs along a) Transect E-W and b) Transect N-S during the August sampling campaign depicting very similar trends. For the north and south transect plots, WS1 = 0m, and north is to the right of the graph

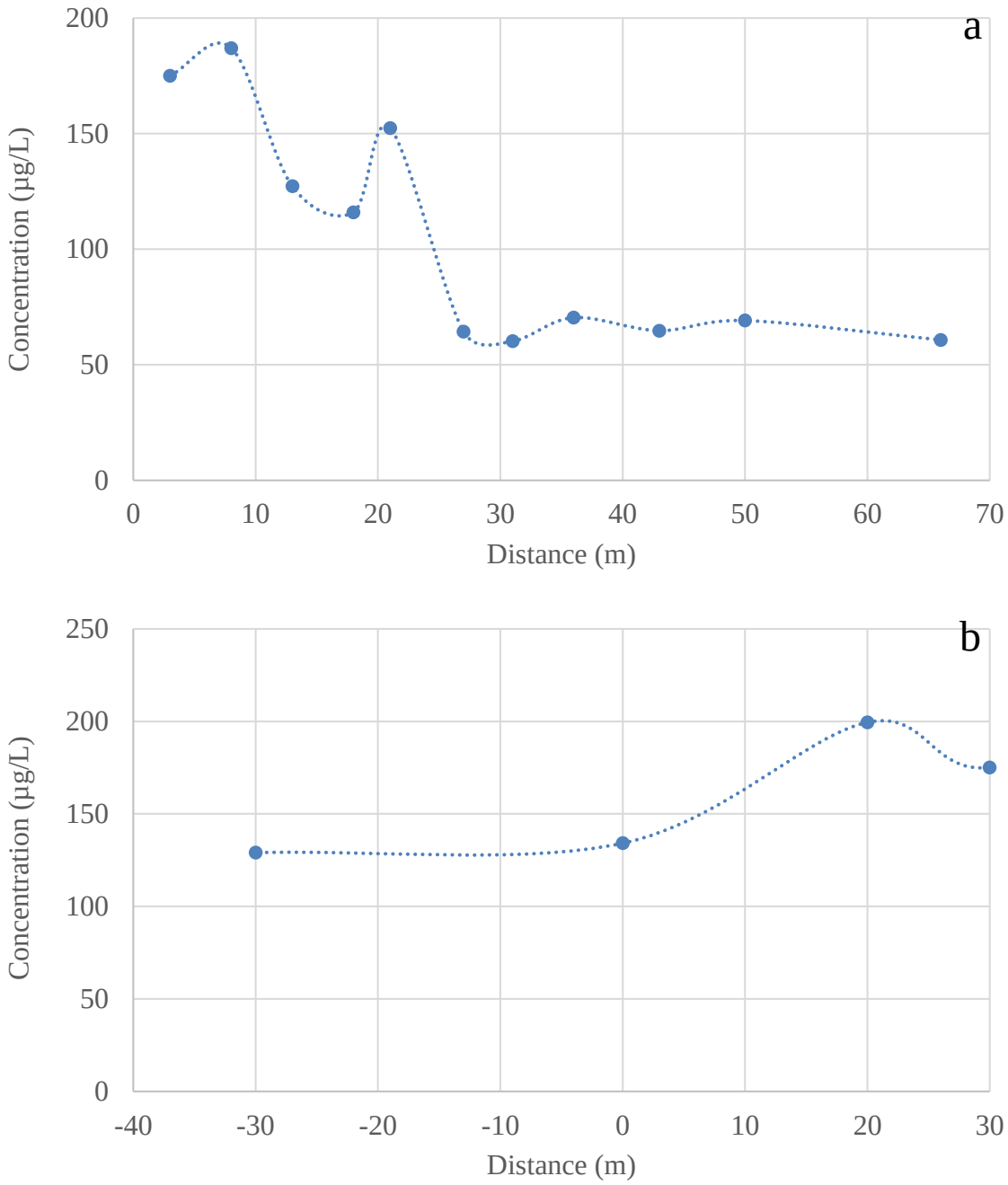

Figure A6c. Other parameters measured such as SRP along a) Transect E-W and b) Transect N-S during the August sampling campaign depicting very similar trends. For the north and south transect plots, WS1 = 0m, and north is to the right of the graph

Table A1. List of PFAS analyzed with their respective acronym

Perfluorobutanoic acid	PFBA
Perfluoropentanoic acid	PFPeA
Perfluorohexanoic acid	PFHxA
Perfluoroheptanoic acid	PFHpA
Perfluorooctanoic acid	PFOA
Perfluorononanoic acid	PFNA
Perfluorodecanoic acid	PFDA
Perfluoroundecanoic acid	PFUnDA
Perfluorododecanoic acid	PFDoDA
Perfluorotridecanoic acid	PFTrDA
Perfluorotetradecanoic acid	PFTeDA
Perfluorohexadecanoic acid	PFHxDA
Perfluorooctanesulfonate	PFOS
Perfluorodecanesulfonate	PFDS
Perfloroethylcyclohexane sulfonate	PFECHS
Perfluorohexanesulfonate	PFHxS
Perfluoroheptanesulfonic acid	PFHpS
Perfluorobutanesulfonate	PFBS
Perfluorooctanesulfonamide	FOSA
Perfluorobutane sulfonamide	FBSA
4,8-dioxa-3H-perfluorononanoate	ADONA
Sodium 8-chloroperfluoro-1-octanesulfonate	8ClPFOS (C8F16ClSO3)
9-chlorohexadecafluoro-3-oxanone-1- sulfonic acid	9 Cl-PF3ONS, F53B (C8F16ClSO4)
11-chloroeicosafluoro-3-oxaundecane-1-sulfonic acid	11Cl-PF3OUdS, F53B(C10F20ClSO4)
Perfluoropolyethers	PFPeS
Perfluorododecane sulfonic acid	PFDoDS
Hexafluoropropylene oxide dimer acid	HFPO-DA

Table A2. List of compounds analyzed

Artificial Sweeteners	Acesulfame, Saccharin, Cyclamate, Sucralose, Perchlorate, Glyphosate, 2,4-D, Fosamine, MCPA, Picloram, Sulfamic Acid
Anions	Fluoride, Chloride, Nitrite, Bromide, Sulfate, Nitrate, Phosphate
Cations	Calcium, Magnesium, Potassium, Silica, Sodium
Dissolved Metals	Antimony, Arsenic, Barium, Beryllium, Bismuth, Boron, Cadmium, Cerium, Cesium, Chromium, Cobalt, Copper, Gallium, Iron, Lanthanum, Lead, Lithium, Manganese, Molybdenum, Nickel, Niobium, Platinum, Rubidium, Selenium, Silver, Strontium, Thallium, Tin, Titanium, Tungsten, Uranium, Vanadium, Yttrium, Zinc
Volatile Organic Compounds	Chloromethane, vinyl chloride, bromomethane, chloroethane, diethylether, carbon disulfide, CFC-113, iodomethane, alyl chloride, methylene chloride, trans-1,2-dce, acetonitrile, chloropropene, 1,1-dichloroethane, acrylonitrile, cis-1,2-dce, dichloropropan, chloroform, caron tetrachloride, 1,1,1-trichloroethane, THF, 1,1-dichloropropene, benzene, methylacrylonitrile, 1,2-dichloroethane, trichloroethene, dibromomethane, 1,2-dichlropropane, bromodichloromethane, methyl methacrylate, cis-1,3 dichloropropene, toluene, nitropropane, tetrachloroethene, trans-1,3-dichloropropene, 1,1,2--trichloroethane, ethyl methacrylate, dibromochloromethane, 1,3-dichlropropane, 1,2-dibromomethane, chlorobenzene, ethyl benzene, 1,1,1,2-tetrachloroethane, m+p-xylene, o-xylene, styrene, bromoform, isopropyl benzene, bromobenzene, polypropylbenzene, 1,1,2,2-tetrachloroethane, 2-chlorotoluene, 1,3,5-trimethylbenzene, 1,2,3-trichlropropane, trans-1,4-dichloro-2-butene, 4-chlorotoluene, tert-butylbenzene, pentachloroethane, 1,2,4-trimethylbenzene, sec-butylbenzene, p-cymene, 1,3-dichlorobenzene, 1,4-dichlorobenzene, n-butylbenzene, 1,2-dichlorobenzene, 1,2-dibromo-3-chloropropane, nitrobenzene, hexachlorobutadiene, 1,2,4-trichlorobenzene, naphthalene, 1,2,3-trichlorobenzene,

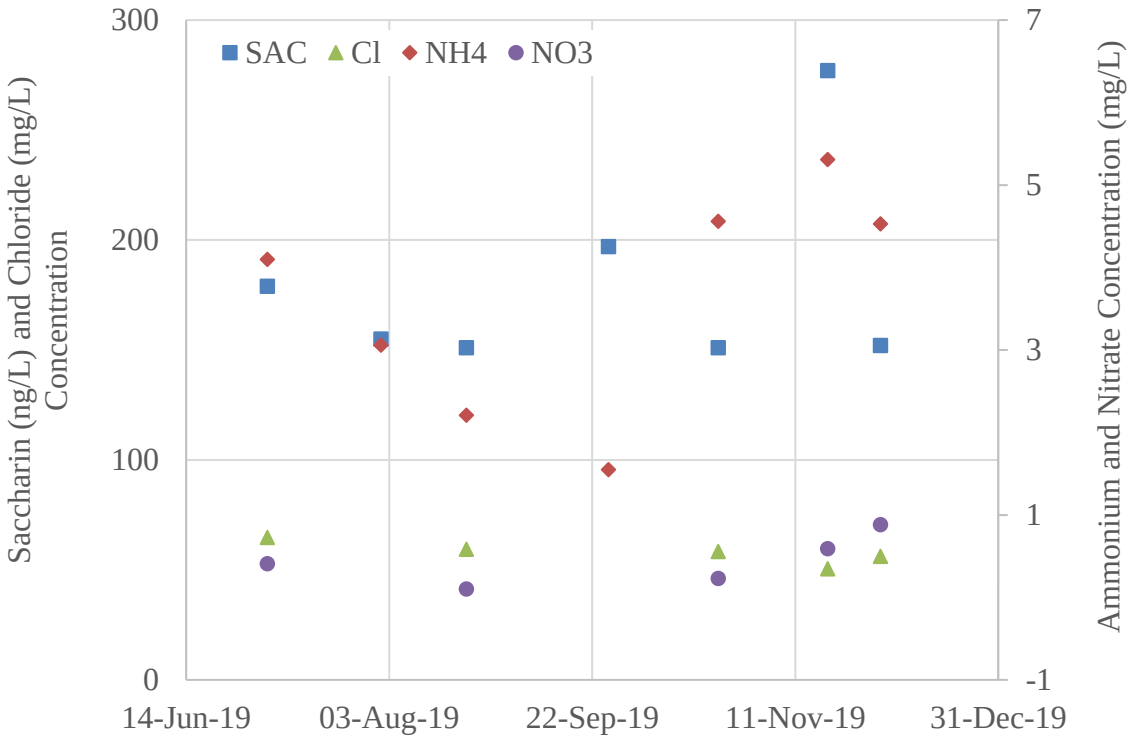

Figure A7: Contaminant concentrations in pond edge surface water samples